

DISS. ETH NO. 24380

**ORIGIN AND REGULATION OF INTRAMUSCULAR
BROWN-LIKE ADIPOCYTES**

A thesis submitted to attain the degree of

DOCTOR OF SCIENCES of ETH ZURICH

(Dr. sc. ETH Zurich)

presented by

TATIANE GORSKI

Master of Science in Sport Science, Universität Bern

born on 15.09.1987

citizen of Brazil

accepted on the recommendation of

Prof. Dr. Christian Wolfrum

Prof. Dr. Jan Krütfeldt

Prof. Dr. Michael Ristow

2017

Acknowledgements

A doctoral thesis is meant to be built on independent scientific work. Ironically, though, it would have been certainly impossible to accomplish it without the help of many people who provided me with scientific, technical, professional and personal support during these more than four years, to whom I would like to say “thank you”.

To Prof. Dr. Jan Krützfeldt, for giving me the opportunity to work on a very exciting project and learning so much in his lab. For his guidance and for always having the door open to discuss technical and scientific matters, to think about results and how to move forward.

To Prof. Dr. Christian Wolfrum and Prof. Dr. Michael Ristow for giving up so much of their time to share their expertise (and even equipment and protocols!) and improve my project. It was a privilege to have you in my doctoral thesis committee.

To the former and current members of the Krützfeldt lab. To Katarina, Amir and Artur for welcoming me to the group, for teaching me techniques I was not familiar with, for our productive discussions and ice-cream pauses at USZ. To Angelika and Edlira for the scientific, technical and emotional support, for making me laugh after never-ending days when things did not go so well in the lab. To Sebastian for contributing already so much to a good working environment in these few months we worked together.

To my colleagues from the Endocrinology Department. To Richard, Maren, Diri, Stephan, Michael, Fabrizio, Hawi, Mara, Marcela, “Claudias” (G. and B.), Heidi, Cornelia, Bettina and Maria, for being always ready to help with last-minute problems; for scientific, cultural, touristic and gastronomic exchange during our lunch pauses, dinners and tours. For making life in the lab more fun!

To people from the Wolfrum group, especially Salvatore and Arionas, for sharing their expertise in adipocyte research and for always welcoming me with a smile when I invaded their lab to run some experiments there.

To all my friends from Zurich and from the other side of the ocean for understanding when I could not meet, or when I suddenly had to leave because of an experiment.

To my family, especially Pai, Mãe, Juli, Vó and Romi. Thanks for always supporting my decisions, for understanding my absence on so many special occasions, for contributing to very nice “recharging” days during my vacations. For always being there for me. Last but not least, for keeping interested in my research findings, even when they were not so easy to follow anymore.

To Fernando... it is difficult to express how grateful I am for the great support I have had during the past 11 years. For the love and friendship, for moving to another country and leaving everything behind because of my doctoral studies, for the cool "out-of-the-box" discussions about our projects, for bringing dinner to the lab when I could not leave at normal times, for understanding my delays, for making me so happy.

Obrigada!

Table of Contents

Acknowledgements	3
Table of Contents	5
Summary	9
Zusammenfassung	11
Abbreviations.....	13
1. Introduction.....	19
1.1. Obesity, adipose tissue and skeletal muscle.....	19
1.2. Adipose tissue	19
1.2.1. White adipose tissue	19
1.2.3. Brown adipose tissue	21
1.2.4. UCP1	23
1.2.5. UCP1-expressing adipocytes in WAT	24
1.2.6. Adipocyte precursors in adult tissue	27
1.2.7. Adipocyte differentiation	28
1.3. Skeletal muscle	29
1.3.1. Skeletal muscle anatomy and function.....	29
1.3.2. Satellite cells.....	31
1.3.3. Fibro/adipogenic progenitors (FAPs)	34
1.3. Intramuscular fatty infiltration.....	36
1.3.1. Impact of intramuscular fatty infiltration on skeletal muscle function.....	36
1.3.2. Origin of brown-like intramuscular adipocytes.....	37
2. Research Aims	39
3. Material and Methods	41
3.1. Chemicals	41
3.2. Antibodies	43
3.3. Animal Procedures.....	45
3.3.1. Animal Husbandry	45

3.3.2. Glycerol and cardiotoxin intramuscular injections.....	45
3.3.3. CL316 treatment.....	45
3.3.4. High-fat diet-feeding	45
3.3.5. Exercise training protocol.....	45
3.4. Physiological Analysis.....	46
3.4.1. Blood Parameters.....	46
3.4.2. Body mass and TA mass.....	47
3.5. Tissue sections	47
3.6. Isolation of primary cells.....	47
3.6.1. Isolation of skeletal muscle FAPs and MPs.....	47
3.6.2. Isolation of cells from WAT SVF	48
3.7. Tissue Culture	48
3.7.1. Immortalized Cell Lines.....	48
3.7.2. Primary Cell Lines.....	48
3.7.3. Differentiation and Stimulation	49
3.7.4. Staining of Cultured Cells	49
3.8. Gene Expression Analysis.....	49
3.8.1. RNA Extraction and Purification.....	49
3.8.2. Reverse transcription and quantitative polymerase chain reaction (qPCR)	50
3.9. Protein Expression Analysis.....	50
3.9.1. Protein Extraction	50
3.9.2. SDS polyacrylamide gel electrophoresis (SDS-PAGE) and Western Blotting...51	
3.9.3. Immunohistochemistry on Tissue Sections	51
3.9.4. Immunofluorescence of Cell Cultures	52
3.10. Statistical Analysis.....	52
4. FAPs differentiate into brown-like adipocytes.....	55
4.1. Expression of UCP1 and other brown-adipocyte markers in skeletal muscle is nearly negligible and does not respond to cold exposure.....	55
4.2. Intramuscular adipocytes express UCP1 and respond to beta 3-adrenergic stimulus	56
4.3. FAPs, but not MPs, differentiate into UCP1-expressing adipocytes.....	57
4.4. UCP1 levels in FAP-derived adipocytes depend on mouse strain	59
4.5. UCP1 expression in FAP-derived adipocytes responds to the thyroid hormone T3	59

4.6. UCP1 expression in FAP-derived adipocytes is sex-dependent	60
4.7. Discussion.....	60
5. Intramuscular Ucp1 expression is not influenced by high-fat diet feeding or exercise-training status in an obesity-resistant mouse strain.....	83
5.1. High-fat diet feeding mildly increases body mass and blood glucose levels of Sv/129 female mice.....	83
5.2. FAPs isolated from Sv/129 female mice fed a high-fat diet maintain their potential to differentiate into brown-like adipocytes <i>in vitro</i>	83
5.3. High-fat diet feeding does not influence intramuscular <i>Ucp1</i> expression following glycerol injection in Sv/129 female mice.....	84
5.4. A four-week exercise training intervention causes only minor changes in gene expression of ingWAT in Sv/129 male mice	85
5.5. FAPs from exercise-trained and from untrained Sv/129 male mice express similar levels of UCP1 following <i>in vitro</i> differentiation	85
5.6. Intramuscular expression of <i>Ucp1</i> after glycerol-induced adipogenesis is similar in exercise-trained and untrained Sv/129 male mice	86
5.7. Discussion.....	86
6. Aging impairs the potential of FAPs to differentiate into brown-like adipocytes in an obesity-resistant mouse strain	105
6.1. Aging or ovariectomy does not impair skeletal muscle regeneration in Sv/129 female mice	105
6.2. Aging decreases the potential of FAPs to differentiate into brown-like adipocytes <i>in vitro</i>	106
6.3. Expression of <i>Ucp1</i> and other brown- and white-adipocyte markers in fatty-degenerated skeletal muscle is not altered in OVX and aged Sv/129 female mice.....	107
6.4. The response of intramuscular <i>Ucp1</i> expression to beta 3-adrenergic stimulus in fatty-infiltrated skeletal muscle is apparently preserved in aged Sv/129 female mice	108
6.5. Discussion.....	109
7. Conclusions and Outlook.....	119
8. References	123
Curriculum vitae.....	139

Summary

Given the rising worldwide prevalence of obesity, there has been growing interest in the development and function of adipose tissue, as well as in mechanisms that could elevate whole-body energy expenditure. While white adipocytes store excess energy intake as triglycerides in intracellular lipid droplets, brown and beige/brite adipocytes dissipate energy as heat in response to cold exposure or a high-fat diet. The latter is only possible due to the activity of uncoupling protein 1 (UCP1), located in the inner mitochondrial membrane of these thermogenic adipocytes. As a result of their high metabolic activity, brown and beige/brite adipocytes act as a sink for excessive glucose in the circulation. In addition to classical white and brown adipose tissue depots, adipose tissue can also accumulate in ectopic locations, including skeletal muscle. Intramuscular fatty infiltration is generally associated with the accumulation of white adipocytes in skeletal muscle, impairing skeletal muscle function and metabolism. In this regard, it is tempting to speculate that the deposition of brown adipocytes instead of white adipocytes in skeletal muscle could improve metabolism of fatty-infiltrated skeletal muscle. Whether such a shift in intramuscular adipocyte phenotype is indeed possible had not yet been elucidated.

Here, we detected intramuscular expression of UCP1 and other brown-adipocyte markers during glycerol-induced fatty infiltration in an obesity-resistant mouse strain and showed that intramuscular adipocytes acquire a brown-like phenotype in response to beta 3-adrenergic stimulus, known to stimulate browning of white adipose tissue (WAT) depots. An extensive comparison of the brown adipogenic potential of myogenic progenitors (MPs) and fibro/adipogenic progenitors (FAPs) residing in skeletal muscle indicates that, while MPs are committed to the myogenic lineage, FAPs undergo brown adipogenesis more readily than previously appreciated. *In vitro*, UCP1 expression in differentiated FAPs was influenced by genetic background, sex and the thyroid hormone triiodothyronine, known as an important regulator of brown adipose tissue (BAT) activity.

The responsiveness of UCP1 expression in fatty-infiltrated skeletal muscle to beta 3-adrenergic stimulation prompted us to study how intramuscular FAPs and adipocytes respond to other factors known to affect UCP1 in other BAT and WAT depots, namely high-fat diet-feeding and exercise training. We observed that fatty-infiltrated skeletal muscle responds to high-fat diet feeding similarly to inguinal WAT (ingWAT), i.e., with an increase in leptin mRNA levels, but with no regulation of *Ucp1* mRNA expression. Importantly, FAPs from high-fat diet-fed animals retained their ability to differentiate into UCP1-positive adipocytes *in vitro*, suggesting that, at least at the early stages of diet-induced metabolic

disturbance, FAPs are still a possible target for interventions aiming at intramuscular-adipocyte browning. Exercise-training status did not influence *Ucp1* expression in skeletal muscle during glycerol-induced fatty infiltration and UCP1 protein levels in FAPs differentiated into brown-like adipocytes *in vitro*. Interestingly, *Ucp1* expression in ingWAT of exercise-trained mice was higher than in untrained mice four weeks after the end of the training period, despite no differences immediately after it, suggesting that the training status-related increase in *Ucp1* expression could result from indirect effects of endurance exercise training.

Finally, we showed that aging, but not ovariectomy, decreases UCP1 protein expression in FAPs following brown adipogenic differentiation *in vitro*, though *Ucp1* mRNA levels in skeletal muscle during glycerol-induced fatty infiltration *in vivo* were not decreased in ovariectomized or aged mice. The results from ovariectomized mice and high-fat diet-fed mice contribute to the notion that, at least in obesity-resistant 129S6/SvEvTac mice, FAPs retain their ability to differentiate into UCP1-positive cells under conditions that are commonly related to impaired skeletal muscle function. The results from the *in vitro* experiments using FAPs from aged mice, on the other hand, show that FAP function and plasticity can be affected by aging, similarly to what has been previously observed in other stem cell populations.

Our results shed light onto the plasticity of intramuscular adipocytes and point to FAPs and intramuscular adipocytes as possible targets for interventions aiming at adipocyte browning. Whether intramuscular brown adipocytes can enhance skeletal muscle metabolism, in contrast to the deleterious effects attributed to intramuscular white adipocytes, remains to be elucidated. The confirmation of the present results in humans could contribute to the development of new therapies to treat obesity and enhance fatty-infiltrated skeletal muscle health.

Zusammenfassung

Aufgrund der weltweit steigenden Prävalenz von Adipositas wächst das Interesse an der Funktion und Entwicklung von Fettgewebe sowie an Mechanismen, die den Energieumsatz erhöhen könnten. Während weisse Adipozyten überschüssige Energie als Triglyzeride in intrazellulären Lipidtröpfchen speichern, setzen braune und «beige»/«brite» Adipozyten Energie, als Reaktion auf Kälte oder während einer fettreichen Diät, in Wärme um. Letzteres ist nur möglich aufgrund der Aktivität von Uncoupling Protein 1 (UCP1), das in der inneren Mitochondrienmembran der thermogenen Adipozyten lokalisiert ist. Infolge ihrer hohen metabolischen Aktivität wirken braune und brite Adipozyten als Senke für übermässig anfallende Glukose im Kreislauf. Neben der Ansammlung von Adipozyten in den klassischen weissen und braunen Fettdepots können sie jedoch auch an ektopischen Orten, wie zum Beispiel in der Skelettmuskulatur, vorkommen. Die intramuskuläre Fettinfiltration ist in der Regel mit der Akkumulation von weissen Adipozyten im Skelettmuskel verbunden, was zur Beeinträchtigung der Skelettmuskelfunktion und des Stoffwechsels führt. In dieser Hinsicht ist es verlockend zu spekulieren, dass die Ablagerung von braunen Adipozyten anstelle von weissen Adipozyten im Skelettmuskel den Stoffwechsel des mit Fett infiltrierten Skelettmuskels verbessern könnte. Ob diese Verschiebung des intramuskulären Adipozyten-Phänotyps in der Tat möglich ist, war bisher noch nicht aufgeklärt.

Wir detektierten die intramuskuläre Expression von UCP1 und anderen Markern von braunen Adipozyten während einer Glycerin-induzierten Fettinfiltration in einem Adipositas-resistenten Mausstamm und zeigten weiterhin, dass intramuskuläre Adipozyten einen braunen Phänotyp als Reaktion auf einen beta 3-adrenergen Stimulus erwerben. Dieser ist bekannt dafür, dass er die Bräunung von weissen Fettgewebe stimuliert. Ein umfangreicher Vergleich des braun-adipogenen Potentials von myogenen Vorläufern des Skelettmuskels (MPs) und fibro/adipogenen Vorläufern (FAPs) zeigte, dass FAPs sich leichter als bisher gedacht, zu braunen Adipozyten differenzieren, während MPs hingegen der myogenen Linie verpflichtet bleiben. *In vitro* konnte es gezeigt werden, dass die UCP1-Expression in differenzierten FAPs durch den genetischen Hintergrund, das Geschlecht und das Schilddrüsenhormon Triiodthyronin, auch bekannt als wichtiger Regulator der Aktivität von braunem Fettgewebe (BAT), beeinflusst wird.

Die Veränderbarkeit der UCP1-Expression im mit Fett infiltrierten Skelettmuskel nach beta 3-adrenerger Stimulation veranlasste uns zu untersuchen, wie intramuskuläre FAPs und Adipozyten auf andere Faktoren reagieren, von denen bekannt ist, dass sie UCP1 in

anderen BAT- und WAT-Depots beeinflussen, wie zum Beispiel eine fettreiche Diät oder Ausdauertraining. Wir beobachteten, dass der mit Fett infiltrierte Skelettmuskel, ähnlich wie das inguinale weiße Fettgewebe (ingWAT), nach einer fettreichen Diät, zu einer Erhöhung der Leptin mRNA-Spiegel, jedoch zu keiner Veränderung der *Ucp1* mRNA-Expression führt. Darüber hinaus behielten FAPs von mit einer fettreichen Diät gefütterte Tieren ihre Fähigkeit, sich *in vitro* in UCP1-positive Adipozyten zu differenzieren. Dies deutet darauf hin, dass FAPs, zumindest in den frühen Stadien der fettreiche Diät-induzierten metabolischen Störung, immer noch ein mögliches Ziel für Interventionen sind, die auf eine intramuskuläre Adipozyten-Bräunung abzielen. Der Trainingsstatus zeigte weder einen Einfluss auf die *Ucp1*-Expression im Skelettmuskel, während der Glycerin-induzierten Fettinfiltration, noch auf die UCP1-Proteinmenge in FAPs, die *in vitro* in braunähnliche Adipozyten differenziert wurden. Interessanterweise jedoch, war vier Wochen nach dem Ende der Trainingszeit die *Ucp1*-Expression im ingWAT von trainierten Mäusen höher als bei Kontrolltieren, obwohl unmittelbar nach dem Training keine Unterschiede feststellbar waren. Dies deutet darauf hin, dass die Trainingsstatus-abhängige Zunahme der *Ucp1*-Expression aus indirekten Effekten des Ausdauertrainings resultieren könnte.

Schlussendlich haben wir gezeigt, dass Alterung, aber nicht Ovariectomie, die UCP1-Proteinmenge in FAPs, nach der braun-adipogenen Differenzierung *in vitro*, verringert, obwohl die *Ucp1* mRNA-Expression im Skelettmuskel, während der Fettinfiltration *in vivo*, bei ovariectomierten oder gealterten Mäusen, nicht verringert wurde. Die Ergebnisse der ovariectomierten und mit einer fettreichen Diät gefütterten Mäuse lassen vermuten, dass FAPs, zumindest bei Adipositas-resistenten 129S6/SvEvTac-Mäusen, ihre Fähigkeit beibehalten, unter verschiedenen Zuständen, die häufig mit einer beeinträchtigten Skelettmuskelfunktion zusammenhängen, in UCP1-positive Zellen zu differenzieren. Die Ergebnisse aus den *in vitro* Experimenten unter Verwendung von FAPs aus gealterten Mäusen zeigen dagegen, dass FAP-Funktion und -Plastizität durch Alterung beeinflusst werden können, ähnlich wie bereits bisherige Untersuchungen in anderen Stammzellpopulationen zeigen konnten.

Unsere Ergebnisse untermauern damit die Plastizität von intramuskulären Adipozyten und zeigen FAPs und intramuskuläre Adipozyten als mögliche Ziele für Interventionen auf, die auf die Bräunung von Adipozyten abzielen. Im Gegensatz zu den negativen Wirkungen, die den intramuskulären weißen Adipozyten zugeschrieben werden, bleibt jedoch zu klären, ob intramuskuläre braune Adipozyten den Skelettmuskelstoffwechsel verbessern können. Die Bestätigung der gegenwärtigen Ergebnisse beim Menschen könnte zu der Entwicklung neuer Therapien zur Behandlung von Adipositas und zur Verbesserung der Gesundheit des mit Fett infiltrierte Skelettmuskels beitragen.

Abbreviations

Abbreviation	Full name
-T3	Lacking addition of T3
+F	Treatment with 10 uM forskolin 4 h before collection
+T3	Supplemented with T3
7AAD	7-Aminoactinomycin D
A-7 integrin	Alpha-7 integrin
ACTB	Actin beta
ACTR2B	Activin receptor type 2 B
ADP	Adenosine diphosphate
AKT1	AKT serine/threonine kinase 1
ANOVA	Analysis of variance
ANP	Atrial natriuretic peptide
APC	Allophycocyanin
ATF2	Activating transcription factor 2
ATGL	Adipose tissue triglyceride lipase
ATP	Adenosine triphosphate
A.U.	Arbitrary units
B3-adrenergic receptor	Beta 3-adrenergic receptor
BAT	Brown adipose tissue
BMI	Body mass index
BMP	Bone morphogenic protein
BSA	Bovine serum albumin
C57Bl/6	C57Bl6/6
cAMP	Cyclic adenosine monophosphate

Abbreviations

CCL2	Chemokine (C-C motif) ligand 2
CEBP	CCAAT/enhancer binding protein
CEBPA	CEBP alpha
CEBPB	CEBP beta
CIDE	Cell death-inducing DANN fragmentation factor 45-like effector
CL316	CL316,243
COL1A1	Collagen type 1, alpha 1
COX7A1	Cytochrome c oxidase subunit 7A1
CREB	cAMP responsive element binding protein
C_t	Cycle threshold
CTRL	Control group
DAB	Diaminobenzidine
DAPI	4',6-diamino-2-phenylindole
ddH₂O	Double-distilled H ₂ O
Dio2	Type 2 iodothyronine deiodinase (gene)
DMEM	Dulbecco's modified Eagle's medium
DMSO	Dimethyl sulfoxide
DNA	Deoxyribonucleic acid
ECM	Extracellular matrix
EDTA	Ethylene diamine tetra acetic acid
ELISA	Enzyme-linked immunosorbent assay
ELOVL3	Elongation of very long chain fatty acids (FEN1/Elo2, SUR4/Elo3, yeast)-like 3
EVA1	Myelin protein zero-like 2
EXE	Exercise group
F10	Ham's F-10 nutrient mix
FABP4	Fatty acid binding protein 4

FACS	Fluorescence-activated cell sorting
FAP	Fibro/adipogenic progenitor
FBS	Fetal bovine serum
FFA	Free fatty acid
FGF	Fibroblast growth factor
FGFB	FGF-Basic
GAPDH	Glyceraldehyde 3-phosphate dehydrogenase
HBSS	Hank's balanced salt solution
H&E	Hematoxylin and eosin
HFD	High-fat diet group
hMADS	Human multipotent adipose-derived stem cells
HOMA-IR	Homeostasis model of insulin resistance index
HSL	Hormone-sensitive lipase
iBAT	Interscapular BAT
IBMX	Isobutylmethylxanthine
IgG	Immunoglobulin G
IL	Interleukin
ingWAT	Inguinal WAT
KLF	Krüppel-like factor
LCFA	Long-chain fatty acids
M	Molecular-weight size marker
MOPS	3-(N-morpholino)propanesulfonic acid
MP	Myogenic progenitor
mRNA	Messenger RNA
MYF5	Myogenic factor 5
MYHC	Myosin heavy chain
MYOD	Myogenic differentiation 1

Abbreviations

OVX	Ovariectomized group
P/S	Penicillin/streptomycin
p38 MAPK	p38 mitogen-activated protein kinase
p70-S6K	Ribosomal protein S6 kinase
PAGE	Polyacrylamide gel electrophoresis
PAX	Paired box
PBS	Phosphate-buffered saline
PDGFRA	Platelet-derived growth factor receptor alpha
PE	Phycoerythrin
PGC1A	PPARg co-activator 1 alpha
PKA	Protein kinase A
PLIN	Perilipin
PPARG	Peroxisome proliferator activated receptor gamma
PRDM16	PR domain containing 16
PREF1	Preadipocyte factor 1
qPCR	Quantitative PCR
RIPA	Radioimmunoprecipitation assay
RNA	Ribonucleic acid
rRNA	Ribosomal RNA
S.E.M.	Standard error of the mean
SCA1	Stem cell antigen-1
SDS	Sodium dodecyl sulfate
SMAD	Small mothers against decapentaplegic
Sv/129	129S6/SvEvTac
SVF	Stromal vascular fraction
T3	Triiodothyronine
T4	Thyroxine

TA	Tibialis anterior
TGFB	Transforming growth factor beta
TNF	Tumor necrosis factor
TNFA	Tumor necrosis factor alpha
TNFR	TNF receptor
TRE	Thyroid responsive element
UCP1	Uncoupling protein 1
VEGF	Vascular endothelial growth factor
WAT	White adipose tissue
WNT7A	Wingless-type MMTV integration site family, member 7A
ZFP423	zinc finger protein 423

Abbreviations

1. Introduction

1.1. Obesity, adipose tissue and skeletal muscle

The prevalence of overweight and obesity has increased worldwide in the past decades, with nearly 37% of men and 38% of women showing a body mass index (BMI) equal or greater than 25 kg/m² in 2013 [1]. If the increasing trend observed after the year 2000 continues, worldwide obesity (defined as a BMI equal or greater than 30 kg/m²) prevalence is expected to reach 18% in men and more than 21% in women by 2025 [2]. This poses an urgent need for the development of methods to prevent and counteract obesity and its associated disorders, such as insulin resistance.

Adipose tissue, which can be classified into brown or white [3], is now recognized as an extremely plastic tissue that has its function and metabolism considerably altered in obese individuals [4, 5]. In obese subjects, adipose tissue can exert a negative impact on other tissues through the secretion of adipokines [6-8] and by promoting chronic systemic low-grade inflammation [9]. On the other hand, the recent studies showing that shifting the phenotype of white adipocytes towards a brown-like adipocyte phenotype can improve metabolic health in rodents [10-12] turned adipose tissues into a possible target for strategies to prevent or treat obesity and associated disorders.

In addition to classical white and brown adipose tissue depots, adipose tissue can also accumulate in ectopic locations, including skeletal muscle, a tissue responsible for most of glucose disposal during the fed state [13, 14]. While many studies have focused on the capacity of adipocytes from classical white adipose tissue (WAT) depots to acquire a brown-like phenotype [10, 15-19], the plasticity of ectopic intramuscular adipocytes – commonly detected in obese [20] and sarcopenic [21] patients, among others – is still much less understood. The classical and intramuscular adipose tissue depots, as well as the impact of intramuscular adipocyte deposition on skeletal muscle health and function, are discussed below.

1.2. Adipose tissue

1.2.1. White adipose tissue

Storing excessive energy intake as triglycerides in adipocytes with single lipid droplets, WAT was considered for a long time to be an inert tissue, responsible only for lipid storage for posterior use [22], mechanical protection of other organs [23] and body insulation [24, 25]. Nowadays, however, it is well known that WAT is a dynamic and metabolically active

Introduction

tissue, expanding through hypertrophy and/or hyperplasia in response to excessive energy intake [26-28], secreting molecules with paracrine and endocrine effects – called adipokines (reviewed in [29]) –, and thereby influencing whole-body metabolism and disease development. WAT is composed by white adipocytes, connective tissue and the stromal vascular fraction (SVF). The SVF contains mesenchymal stem cells, preadipocytes, and endothelial, hematopoietic and immune cells, among others [30].

White adipocytes are large spherical cells (20 μm to 140 μm of diameter) and contain single lipid droplets that occupy almost the entire cell volume [31]. Lipid droplets are formed by triacylglycerol molecules surrounded by a phospholipid monolayer [32] containing perilipin (PLIN)1 – a protein phosphorylated by protein kinase A (PKA) and involved in the mobilization of free-fatty acids from the lipid droplets (lipolysis) [33] – and members of the cell death-inducing DNA fragmentation factor 45-like effector (CIDE) family [34] such as CIDEC [35], among others. Phosphorylation of PLIN1 causes translocation of hormone-sensitive lipase (HSL) to lipid droplets, and regulates accessibility of adipose tissue triglyceride lipase (ATGL) to its co-activator abhydrolase domain containing 5 [36]. The single lipid droplet configuration is optimal for the primary function of white adipocytes – lipid storage –, since it allows for a low surface-to-volume ratio [37]. The cytoplasm of white adipocytes forms a thin rim between the lipid droplet and the cell membrane, where the nucleus and other cellular organelles are found. The few mitochondria residing in white adipocytes are small and elongated, and their cristae are short and randomly organized [38].

Adipocyte activity is under hormonal regulation. During the fed state, insulin promotes the uptake of glucose (via glucose transporter 4) and triglycerides from the circulation and inhibits lipolysis [39, 40]. In fasting conditions, on the other hand, glucagon and catecholamines stimulate lipolysis and the release of fatty acids and glycerol into the circulation, supplying the energy demands of other tissues [41]. WAT, in turn, also influences other tissues via the secretion of adipokines such as leptin, interleukin(IL)6, IL8, adiponectin, chemokine (C-C motif) ligand 2 (CCL2) [6], tumor necrosis factor (TNF)alpha (TNFA) [6, 7] and resistin [8], among others.

In humans, WAT is predominantly located beneath the skin, in the subcutaneous depots. It is also found in visceral depots around the internal organs [42]. In the mouse, the main subcutaneous depots are located in the anterior cervical, subscapular and axillo-thoracic regions, and in the posterior inguinal (ingWAT) and gluteal regions. The main visceral WAT depots are the mediastinal, mesenteric, retroperitoneal and abdominopelvic (which in females comprises the interrenal, periovarian, parametrial and perivesical depots) [43, 44];

males also possess an epididymal depot [45]. WAT depots are heterogeneous: while subcutaneous adipose tissue seems to protect against many undesirable effects of obesity [46, 47], increased size of the visceral WAT depot is associated with impaired glucose metabolism [48]. The different WAT depots also respond differentially to increases in the demand for energy storage: in mice fed a high-fat diet, subcutaneous adipose tissue expands mostly by hyperplasia and visceral adipose tissue by hypertrophy. Accordingly, in mice fed a high-fat diet, average adipocyte size is higher in visceral than in subcutaneous WAT [49]. Furthermore, adipocyte progenitors are more abundant and proliferate at a higher rate in subcutaneous WAT compared to visceral WAT [50].

1.2.3. Brown adipose tissue

In contrast to WAT, the main function of brown adipose tissue (BAT) is non-shivering thermogenesis, the conversion of chemical energy into heat independently of skeletal muscle shivering. Non-shivering thermogenesis is of particular importance in small mammals and hibernators, which rely on this tissue to maintain their body temperatures during exposure to cold. In mice, a model frequently used to study BAT function and metabolism, the main classical BAT depots are the interscapular (iBAT), perirenal, periaortic and intercostal (extensively reviewed in [51]).

In humans, BAT was believed to exist only in newborns and infants, in which the ratio between body surface and volume is greater than in adults, leading to increased heat loss, and the motor coordination is still not enough developed to meet thermogenesis demands with shivering [52]. Recently, however, the presence of BAT has been confirmed in adult humans through positron-emission tomography-computed tomography and analysis of biopsies showing uncoupling protein 1 (UCP1)⁺ multilocular adipocytes [53-55] [56]. The amount and activation levels of BAT seem to be inversely correlated to BMI, blood glucose levels and age [54]. In humans, BAT activity has been mainly detected in the neck, supraclavicular para-aortic, paravertebral and suprarenal depots [53, 54]. Cold exposure seems to rapidly activate BAT in humans [57, 58].

BAT is highly vascularized, being supplied by lobular arteries and a dense capillary plexus drained by lobular veins, with direct arteriovenous anastomoses present – an important feature to deliver the heat produced by the brown adipocytes. This tissue is also densely innervated by the sympathetic nervous system, displaying numerous noradrenergic vasomotor and parenchymal nerve terminals [59]. In response to beta 3-adrenergic stimulation by cold exposure or pharmacological antagonists, angiogenesis is further stimulated through increased vascular endothelial growth factor (VEGF) expression, increasing BAT vascularization [60].

Introduction

Brown adipocytes are generally smaller than white adipocytes (15 -50 μm of diameter) and display a polygonal shape and multilocular morphology, i.e., stored triglycerides are distributed into multiple small lipid droplets, facilitating lipid mobilization through a higher surface-to-volume ratio than the large lipid droplets of white adipocytes, which increases the accessibility of proteins involved in lipolysis to the stored lipids [38]. Lipid droplet-associated proteins in brown adipocytes include PLIN5 [61] and CIDEA [62, 63]. Brown adipocytes have a central nucleus and numerous large, highly developed mitochondria exhibiting a spherical shape and many laminar cristae [38]. These cells also differ from white adipocytes regarding their secretome. For example, brown adipocytes generally do not express Leptin, although it can be detected in brown adipocytes of db/db mice [31]. Recently, BAT has been shown to release factors that could also have an impact on other tissues, called “batokines”, including fibroblast growth factor (FGF)21, IL6 and neuregulin 4 (reviewed in [64]).

Cold exposure and high-fat-diet feeding trigger sympathetic stimulation of BAT through norepinephrine [65]. Activation of beta 3-adrenergic receptors (B3-adrenergic receptors) by this neurotransmitter activates adenylate cyclase, increasing the intracellular cyclic adenosine monophosphate (cAMP) levels [66, 67]. In consequence, PKA phosphorylates and activates proteins involved in lipolysis, including PLIN5 – which then increases ATGL activity [61] – and HSL, increasing intracellular free fatty acid (FFA) concentrations and stimulating thermogenesis [68-70]. In parallel, following activation by PKA, p38 mitogen-activated protein kinase (p38 MAPK) phosphorylates the transcriptional factors activating transcription factor 2 (ATF2) and peroxisome proliferator activated receptor gamma (PPARG) co-activator alpha (PGC1A), leading to increased transcription of the *Ucp1* gene [71]. The response of brown adipocytes to B3-adrenergic stimulus during cold exposure is recapitulated *in vitro* by the increase in lipolysis and *Ucp1* mRNA levels following treatment with agents known to increase intracellular cAMP levels, such as the adenylate cyclase activator forskolin [72-75]. Importantly, inhibition of PKA activity prevents forskolin-induced increases in *Ucp1* expression [75]. Functional *in vitro* experiments also show UCP1-dependent increases in oxygen consumption rates of brown adipocytes in response to the beta-adrenergic agonist isoproterenol [76]. Importantly, the increase in glucose uptake by BAT in response to stimulation of B3-adrenergic receptors is also observed in humans [77].

The BAT response to cold is also under important influence of thyroid hormones. Within the first hours of cold exposure, serum levels of the thyroid hormones triiodothyronine (T3) and thyroxine (T4) become rapidly elevated [78]. The intracellular levels of T3 in brown adipocytes are further increased by the activity of type 2 iodothyronine deiodinase (also called D2, product of the *Dio2* gene), an enzyme which converts T4 into T3 [79]. T3, in turn,

upregulates *Ucp1* transcription through thyroid responsive elements (TREs) present in an enhancer region of the *Ucp1* gene [80]. In accordance, the transcriptional upregulation of *Ucp1* in response to cold is drastically reduced in hypothyroid rats [81] and euthyroid *Dio2*-knockout mice [82].

In addition, cold exposure also enhances BAT thermogenesis through the stimulation of proliferation of interstitial adipocyte precursors and their differentiation into brown adipocytes in rodents [83, 84].

1.2.4. UCP1

Non-shivering thermogenesis in brown adipocytes is only possible due to the activity of UCP1 [85], also called thermogenin, a 32-kDa [86] transmembrane protein located in their inner mitochondrial membrane (extensively reviewed in [51]). During the transfer of electrons through the components of the mitochondrial respiratory chain, located in the inner mitochondrial membrane, protons are transported from the mitochondrial matrix across the inner mitochondrial membrane, resulting in a proton concentration gradient and an electrical potential across the membrane, the so-called proton motive force. The F_0F_1 complex, also called adenosine triphosphate (ATP) synthase, phosphorylates adenosine diphosphate (ADP) into ATP as the protons move back across the inner membrane into the mitochondrial matrix, driven by the proton motive force [87]. UCP1 allows the re-entry of protons in the mitochondrial matrix without ATP production, converting the energy produced by substrate oxidation into heat [88, 89]. This process is illustrated in Figure 1.1.

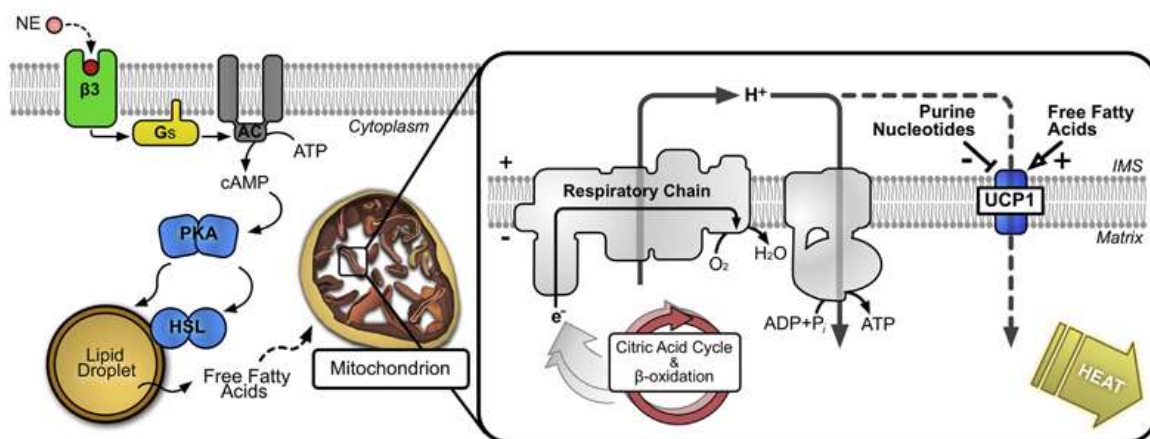


Figure 1.1: Mechanism of coupled and UCP1-dependent, uncoupled respiration in BAT mitochondria. In response to stimulation of B3-adrenergic receptors (indicated as β_3) by norepinephrine (indicated as NE), cAMP levels increase, stimulating lipolysis. The

Introduction

increase in intracellular FFA levels activates UCP1, located in the inner mitochondrial membrane, promoting the transfer of protons (indicated as H^+) from the intermembrane space (indicated as IMS) to the mitochondrial matrix without phosphorylation of ADP into ATP. G_s : $G_{\alpha s}$ protein, AC: adenylate cyclase. Adapted from [90].

In intact non-stimulated brown and brite adipocytes *in vitro*, UCP1 is not active, as demonstrated by experiments showing similar basal and oligomycin-resistant oxygen consumption between wild type and UCP1-knockout cells [76, 91]. Uncoupling and the resulting thermogenesis depend on activation of UCP1, which has been shown to occur via binding of long chain fatty acids (LCFAs), able to overcome the inhibition by purine nucleotides. According to this “shuttling model”, UCP1 is a LCFA/ H^+ symporter that simultaneously transports a LCFA anion and a proton; since the hydrophobic interactions between LCFA anions and UCP1 prevent their dissociation from each other, the net result is the transport of protons depending on binding by LCFAs [89]. Accordingly, oleate has been shown to increase UCP1 activity in mitochondria isolated from brown adipocytes [92]. UCP1 activity is inhibited by purine nucleotides such as guanosine diphosphate [89, 91, 92].

In response to B3-adrenergic stimulus (such as norepinephrine during cold exposure or CL316,243 – CL316 – treatment), intracellular cAMP levels increase in adipocytes, activating PKA and thereby a cascade that leads to lipolysis. The FFAs released from the adipocyte lipid droplets activate UCP1, promoting the dissipation of energy as heat (extensively reviewed in [51]).

Together with the already mentioned transcriptional regulation by norepinephrine (indirectly) and TREs, the *Ucp1* transcription has also been shown to be upregulated by increased cAMP levels via cAMP responsive element binding protein (CREB) [93]; by retinoic acid via retinoic receptor alpha and retinoid X receptor [94, 95]; by FFAs via PPARG [75] and peroxisome proliferator activated receptor alpha [96]; and by CCAAT/enhancer binding proteins (CEBPs) alpha (CEBPA) and beta (CEBPB) [97]. Transcriptional upregulation results from binding of these factors to their respective response elements in the *Ucp1* gene promoter and/or enhancer regions.

1.2.5. UCP1-expressing adipocytes in WAT

Together with the classical BAT depots, UCP1-positive, multilocular adipocytes can also be found in pockets within WAT following thermogenic stimulation [98]. These adipocytes have been described as inducible, beige or brite (from brown in white) [99]. The differences

in energy expenditure between C57Bl/6 (C57Bl/6) and 129S6/SvEvTac (Sv/129) mice provide a good example of the metabolic impact of these ectopic UCP1-positive adipocytes on energy expenditure: in comparison to obesity-prone C57Bl/6 mice, obesity-resistant Sv/129 display more UCP1-positive adipocytes within their perimuscular and intermuscular adipose tissue in the thigh, resulting in a higher energy expenditure and lower body mass gain under a high-fat diet [10].

Barbatelli et al. [15] observed that subcutaneous WAT of Sv/129 mice contains two types of UCP1-positive, brown-like adipocytes: (1) multilocular cells containing a central nucleus and large mitochondria, similar to the brown-adipocyte morphology, and (2) larger, paucilocular cells containing one central large lipid droplet and several smaller lipid droplets, with a peripheral nucleus and a mixture of elongated mitochondria, larger mitochondria similar to those from brown adipocytes, and mitochondria of an intermediary phenotype. In this study, cold exposure caused a 20-fold increase in the number of brown-like adipocytes in subcutaneous WAT, suggested to result from transdifferentiation of white into brown-like adipocytes. Indeed, lineage-tracing experiments confirmed that, in ingWAT of mice, transdifferentiation between white and brown adipocytes occurs in both directions. While white adipocytes acquire a brown-like phenotype in response to cold exposure, re-adaptation of animals to warmer temperatures reverses this process, and the transdifferentiated cells assume a white-adipocyte morphology [16]. Figure 1.2 illustrates the morphology of white and brite adipocytes in subcutaneous WAT, as well as the macroscopic changes in adipose tissue depots of Sv/129 mice in response to cold exposure.

Resembling B3-adrenergic stimulation during cold exposure, browning of ingWAT has also been reported following treatment with the B3-adrenergic agonist CL316 [10, 15, 17-19, 100]. Furthermore, UCP1 expression in ingWAT also increases following endurance-exercise training [11, 101, 102], although the mechanisms behind this response are still not fully understood, but could involve altered sympathetic tone, endothelial nitric oxide synthase activity and/or myokines secreted in response to exercise [103]. The increase in IL6 secretion by skeletal muscle has been suggested as a possible mechanism, since exercise-induced browning of ingWAT is completely blunted in IL6 knockout mice [102]. Furthermore, the myokines irisin [104] and meteorin-like [105] have been proposed to be secreted in response to exercise, thereby promoting browning of ingWAT.

The search for means of elevating energy expenditure through an increase in the amount and/or activation of UCP1-positive adipocytes in otherwise non-thermogenic WAT depots has prompted researchers to investigate the molecular mechanisms underlying the fate

Introduction

decision of adipocyte precursors into a white or brite phenotype, or the transdifferentiation of white into brite adipocytes. Examples of agents promoting the browning of WAT or white adipocytes *in vitro* include the PPAR γ agonist rosiglitazone [106]; FGF21, which upregulates PGC1A expression [107]; atrial natriuretic peptide (ANP), which signals through the natriuretic peptide receptor A to increase phosphorylation of p38 MAPK and its downstream targets mitogen-activated protein kinase-activated protein kinase 2 and ATF2 [108]; lactate (in the presence of PPAR γ stimulation by rosiglitazone) [109]; and bone morphogenic protein (BMP)7 [110], likely through phosphorylation of small mothers against decapentaplegic (SMAD) 1/5/8 and consequent phosphorylation of p38 MAPK and ATF2 [111]. BMP4, on the other hand, has been shown to play an opposite role, promoting a shift from a brown towards a white adipocyte phenotype in brown pre-adipocytes and adipocytes [112].

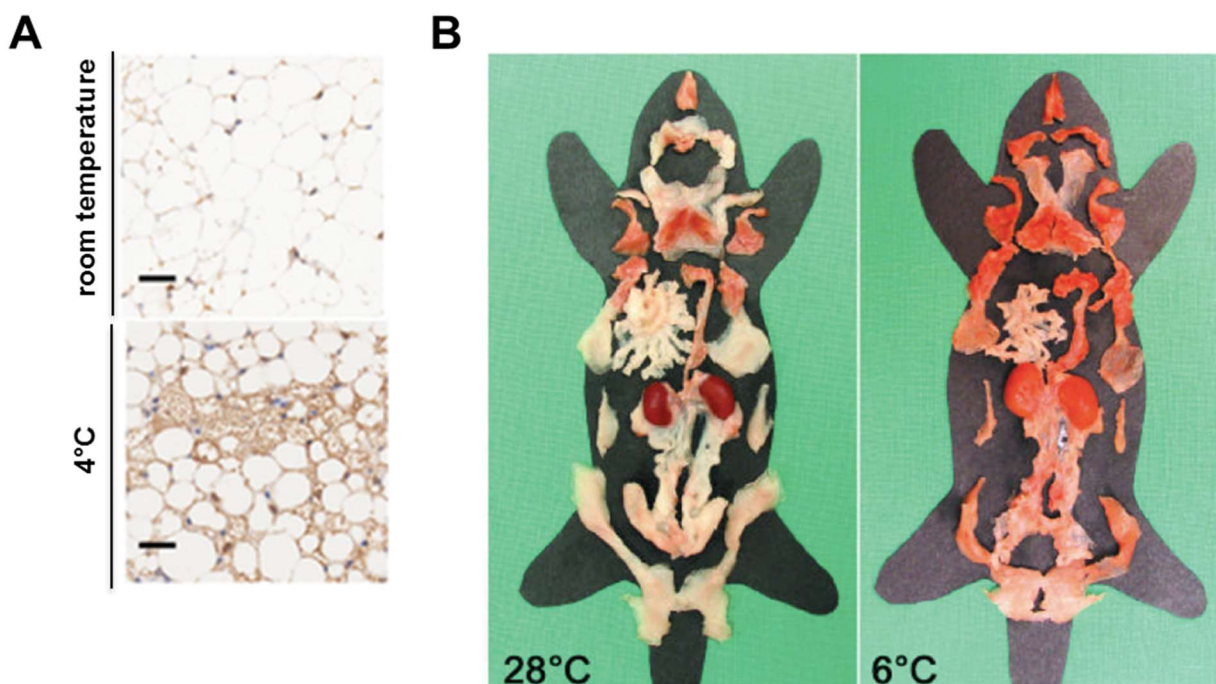


Figure 1.2: Browning of WAT. (A) UCP1 immunohistochemistry of WAT from mice kept at room temperature or exposed to cold. Adapted from [113]. (B) Adipose tissues from Sv/129 female mice kept at 28°C or following exposure to 6°C for ten days. Adapted from [44].

1.2.6. Adipocyte precursors in adult tissue

It is well known that the SVFs from BAT and WAT contain adipocyte precursors, since the SVF adherent cells can differentiate into adipocytes following *in vitro* expansion and treatment with adipogenic medium [114, 115]. The specific identity of brown, white and brite adipocyte precursors involved in *de novo* adipogenesis in adult tissue, however, is not yet fully clear.

Surprisingly, a previous study demonstrated that brown, but not white adipocytes, display a myogenic transcriptional signature [116], suggesting a different developmental origin for brown and white adipocytes. In line with these results, an additional study suggested that brown, but not white adipocytes, share a common myogenic factor 5 (*Myf5*)⁺ precursor with skeletal myoblasts. According to these findings, the expression of PR domain containing 16 (PRDM16) would direct these cells into a brown adipogenic fate, while its loss would promote the myogenic fate [100].

The distinction between brown and white adipocyte precursors based on *Myf5* expression, however, was subsequently challenged by lineage-tracing experiments showing that *Myf5*⁺ progenitors are also present in WAT depots, where they can give rise to white adipocytes; conversely, brown adipocytes were also shown to derive from *Myf5*⁻ cells in certain BAT depots [117]. Indeed, Schulz et al. [110] showed that mesenchymal cells derived from a *Myf5*-independent lineage and isolated from BAT and subcutaneous WAT based on expression of stem cell antigen-1 (SCA1) and negative staining for CD45 and macrophage-1 antigen could differentiate into UCP1⁺ cells following a brown adipogenic treatment *in vitro*. This SCA1⁺ precursor population highly overlaps with platelet-derived growth factor receptor alpha (PDGFRA)⁺ cells, which have been proposed as the precursor population generating all white adipocytes [118]. Furthermore, PDGFRA⁺SCA1⁺CD34⁺ progenitor cells from abdominal WAT are reportedly bipotent, being able to differentiate into brown or white adipocytes in response to B3-adrenergic stimulation or high-fat diet feeding, respectively [119].

It is likely that the progenitor populations analyzed in these studies are heterogeneous. Indeed, a CD24⁺ subpopulation of CD31⁻CD45⁻CD29⁺CD34⁺SCA1⁺ cells residing in WAT is able to reconstitute WAT following transplantation, while CD24⁻ cells contained in the same population are not [120]. Whether certain subpopulations of the PDGFRA⁺/SCA1⁺ adipocyte progenitor pool are more prone to differentiate into brown/brite adipocytes is also not clear. In this regard, WAT smooth muscle cells have been shown to differentiate into UCP1-positive adipocytes, and analysis of their transcriptome indicated that this population could be part of the previously identified pre-adipocyte populations expressing PDGFRA,

Introduction

SCA1 and zinc finger protein 423 (ZFP423), for example [121]. In addition, WAT perivascular, Nestin⁺ cells (adventitial cells and pericyte-like cells) from WAT were also reported to differentiate into adipocytes *ex vivo* [122].

Interestingly, obesity seems to affect the phenotype of WAT preadipocyte-derived adipocytes differentiated *in vitro*. For example, adipose stem cells isolated from obese women display lower lipid accumulation capacity, augmented IL6 secretion and decreased CCL2 and adiponectin secretion [123]. In addition, precursors isolated from subcutaneous abdominal WAT of obese humans express lower levels of UCP1 following *in vitro* differentiation compared to precursors isolated from lean counterparts [124].

1.2.7. Adipocyte differentiation

The differentiation of mesenchymal stem cells into adipocytes includes at least two phases: determination, in which the stem cells become pre-adipocytes committed to the adipogenic lineage, although morphologically not distinguishable from stem cells; and terminal differentiation, in which changes in cell morphology and the development of the machinery necessary to lipid synthesis and trafficking and other adipocyte functions occurs [125].

During the determination stage, BMP4 is one of the factors promoting commitment of mesenchymal cells to the adipogenic fate, increasing activation of the SMAD 1/5/8 signaling cascade [126]. BMP7, in turn, promotes the commitment of mesenchymal cells to the brown adipogenic lineage through activation of p38 MAPK [110, 111]. At the transcriptional level, *Zfp423* is expressed in both brown and white pre-adipocytes, enhancing BMP signaling and thereby *Pparg* expression [127].

Preadipocytes express the plasma membrane protein preadipocyte factor 1 (PREF1), which prevents adipogenesis; PREF1 expression is completely abolished as adipocyte differentiation proceeds [128]. *In vitro*, adipogenic differentiation is promoted by downregulation of PREF1 induced by the glucocorticoid dexamethasone, often added to adipogenic differentiation cocktails [129]. Furthermore, *Pref1* transcription is also inhibited by Krüppel-like factor (KLF)6, one of the KLFs promoting adipogenesis [130]. The differentiation of pre-adipocytes into adipocytes depends on the timely coordinated expression of different transcriptional factors. Important factors activated throughout the terminal differentiation include the CEBPs and PPARG [131].

Cocktails for *in vitro* differentiation of adipogenic precursors generally contain insulin, dexamethasone, indomethacin and isobutylmethylxanthine (IBMX) [132]. IBMX is a phosphodiesterase inhibitor and increases intracellular cAMP levels, leading to PKA activation, increased expression of PPARG [133] and CREB phosphorylation [134] early in

adipogenesis. CREB induces the expression of CEBPB [134], which then activates the transcription of *Cebpa* [135] and *Pparg* [135, 136]. CEBPA binds to the gene promoters of its own gene, *Pparg*, and the fatty acid binding protein 4 (*Fabp4*), upregulating transcription [135]. At early stages of adipocyte differentiation, PRDM16 seems to promote the brown adipogenic fate by simultaneously acting as a coregulator to activate PGC1A [137] and repressing the expression of white-adipocyte specific genes [138].

The transcriptional factor PPARG is the master regulator of adipogenesis, being simultaneously sufficient and strictly necessary for adipogenesis [139], and PPARG agonists such as rosiglitazone are often included in adipogenic media for *in vitro* differentiation [132]. PPARG regulates the transcription of several proteins involved in lipid metabolism and adipocyte function (reviewed in [139]). Not surprisingly, PPARG is also essential for the maintenance of white and brown adipocyte function, and inducing its knockout in adult tissue results in adipocyte death in both WAT and BAT [140].

1.3. Skeletal muscle

1.3.1. Skeletal muscle anatomy and function

Amounting to approximately 30% to 40% of total body mass in humans [141], skeletal muscle is part of the musculoskeletal system and is essential for movement and force production, maintenance of posture and vital functions such as respiration. Skeletal muscle is an extremely plastic tissue and its mass/volume, composition and internal organization can adapt to different stimuli. In response to resistance exercise training, for instance, increases in the rate of protein synthesis in myofibers lead to hypertrophy and increased muscle mass [142, 143]. On the other hand, a dramatic decrease in skeletal muscle mass and cross-sectional area, also termed muscle atrophy, is observed in situations of diminished activity and mechanical loading such as immobilization [144], spinal cord injury [145, 146], spaceflight [147], denervation [148], lower limb suspension [149-152] and bed rest [153-156]. In addition, loss of skeletal muscle mass and strength also occurs during aging, characterizing sarcopenia [157, 158].

The main cell type in skeletal muscle is the myofiber. Myofibers are elongated, cylindrical cells containing myofibrils – contractile structures composed by thick and thin myofilaments and other non-filamentous proteins –, highly developed mitochondria and sarcoplasmic reticulum, multiple peripheral nuclei of a flattened shape and other organelles. The main functional and contractile unit of a myofiber is the sarcomere, formed by thin actin filaments and thick myosin filaments. Single myofibers are ensheathed by a thin layer of connective tissue called endomysium; groups of myofibers form fascicles, which are surrounded by a

Introduction

middle layer of connective tissue denominated perimysium; finally, the entire muscle, composed by many fascicles, is enclosed in a thick layer of connective tissue, the epimysium. These connective tissue layers provide room for nerves and blood vessels, and merge into tendons and aponeuroses at the ends of the skeletal muscle [159]. These structures are illustrated in Figure 1.3. According to the expression of different myosin heavy chain (MYHC) isoforms, innervation, mitochondrial amount and metabolism, myofibers can be classified into slow oxidative type 1, or fast glycolytic type 2 fibers; type 2 fibers can be further classified into 2A or 2X in humans (with mice also displaying 2B fibers) (reviewed in [160]).

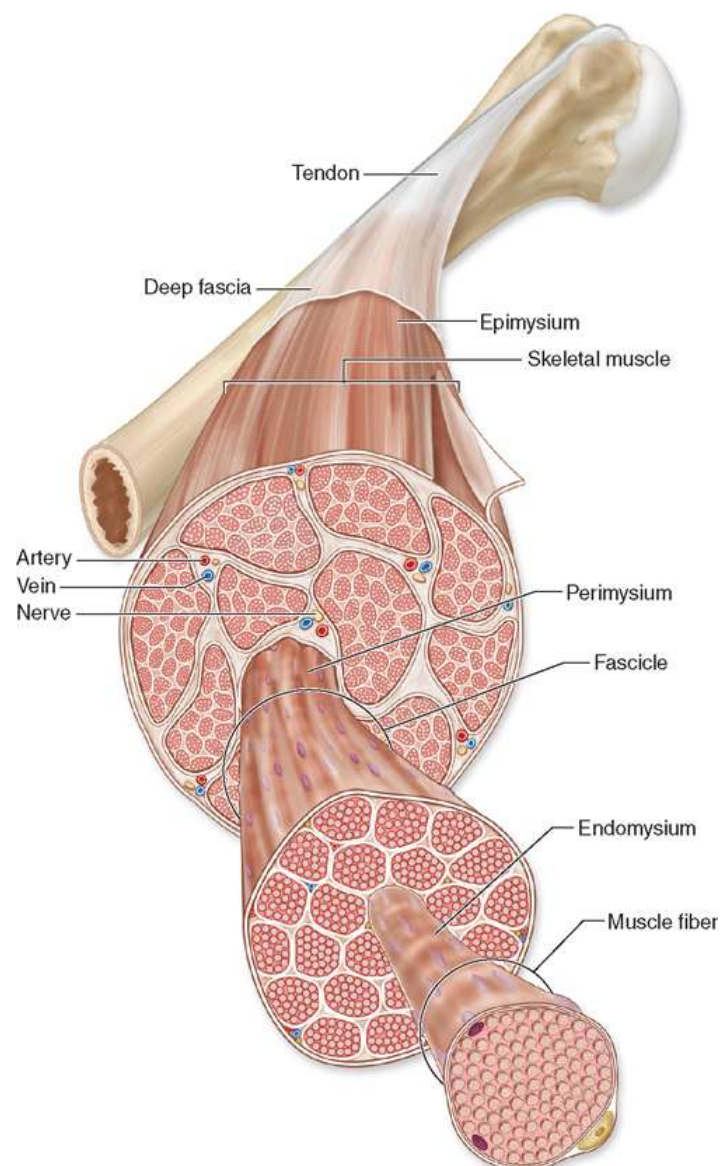


Figure 1.3: Structural organization of skeletal muscle. Skeletal muscle fibers, containing contractile myofibrils, are ensheathed by endomysium, and bundles of myofibers are grouped in fascicles surrounded by connective tissue constituting the

perimysium, where blood vessels and nerves are located. A further connective tissue layer, the epimysium, holds the fascicles together. These layers of connective tissue merge into tendons. Adapted from [3].

Healthy skeletal muscle is highly sensitive to insulin and responds for most of blood glucose clearance at the fed state [13, 14], playing an important role in metabolic health. Together with its role in movement production and glucose uptake, skeletal muscle has been also shown to function as a secretory organ, releasing cytokines and other peptides, named myokines, including IL6, IL15, IL8, brain-derived neurotrophic factor, FGF21 (extensively reviewed in [161]), irisin [104] and meteorin-like [105].

A remarkable trait of skeletal muscle is its high regeneration capacity. Minor disturbances in myofiber plasma membrane integrity seem to be rapidly repaired by the recruitment of intracellular vesicles to the damaged site [162]. In contrast, more severe damage caused by extensive eccentric exercise [163] or chemical injury [164-168] leads to a more complex regeneration response, characterized by sequential inflammatory response, recruitment of satellite cells (including their activation, proliferation and differentiation), and maturation of newly formed or repaired myofibers [169]. A widely used model to study skeletal muscle regeneration in rodents, and thereby the contribution of different cell populations to this process, is the intramuscular injection of myotoxins, such as cardiotoxin [170], notexin [164] and bupivacaine [168, 171]. Cardiotoxin causes an increase in the interstitial space between myofibers, myofibril disarrangements and subsarcolemmal accumulation of swollen mitochondria, followed by a rapid recruitment of immune cells [172]. Within few weeks, myogenic progenitors (MPs) are recruited to the injury site and repair the damaged myofibers or replace them with new myofibers [164] (described in more detail in section 1.3.2). Newly formed myofibers display central nuclei, which posteriorly migrate to the cell periphery [168].

In mice, bupivacaine-induced skeletal muscle regeneration seems to be impaired in diet-induced obese C57Bl/6 mice, possibly due to a diminished response of inflammatory (IL6 and TNFA levels) and anabolic (ribosomal protein S6 kinase – p70-S6K – levels) pathways [171].

1.3.2. Satellite cells

Satellite cells are mononuclear cells found juxtaposed between the plasma membrane of myofibers (the sarcolemma) and their basal lamina [173], which fuse to each other to form myofibers during embryogenesis or following myofiber damage, or contribute with new nuclei to damaged myofibers [174, 175]. Satellite cells derive from paired box (*Pax*)³⁺/

Introduction

Pax7⁺ embryonic progenitors [176] and PAX7 seems to be expressed exclusively by satellite cells in adult skeletal muscle [177]. To allow for the study of satellite cells *in vitro*, primary myoblasts can be isolated from skeletal muscle and fluorescence-activated cell sorting (FACS)-sorted based on expression of alpha-7 integrin (A-7 integrin) [178]. Skeletal muscle cells sorted based on exclusion of CD45⁺CD11b⁺TER119⁺CD31⁺SCA1⁺ cells and expression of beta-1 integrin/chemokine (CXC-motif) receptor 4, A-7 integrin/CD34, or vascular cell adhesion molecule 1 highly overlap and nearly 90% of these cells are *Pax7*⁺. Importantly, these three populations contain nearly 90% of the *Pax7*⁺ cells residing in skeletal muscle [179].

PAX7 expression is essential for satellite cell function [177, 180]. Deletion of this transcriptional factor in satellite cells from adult skeletal muscle causes drastic impairments in muscle regeneration following cardiotoxin injections, resulting in lower muscle mass and higher adipocyte deposition and fibrosis. This effects seem to be mediated by the induction of cell cycle arrest, decreased expression of MYF5 and myogenic differentiation 1 (MYOD), and precocious differentiation of the satellite cells [181]. Accordingly, ablation of PAX7⁺ cells in adult skeletal muscle prevents muscle hypertrophy induced by synergist ablation in mice [182] and impairs physical performance [183].

Two different subsets of satellite cells are found in skeletal muscle, resulting from asymmetric cell division: *Pax7*⁺*Myf5*⁻ stem cells (nearly 10% of the PAX7⁺ satellite cells) and *Pax7*⁺*Myf5*⁺ committed progenitors. The *Pax7*⁺*Myf5*⁻ cells divide asymmetrically into a basal *Pax7*⁺*Myf5*⁻ and an apical *Pax7*⁺*Myf5*⁺ cell, maintaining the homeostasis of satellite cells under normal physiological conditions. During skeletal muscle regeneration, on the other hand, symmetric division of *Pax7*⁺*Myf5*⁻ cells into two *Pax7*⁺*Myf5*⁻ sister cells seems to prevail [176]. Symmetric cell division is stimulated by wingless-type MMTV integration site family, member 7A (WNT7A) signaling via the Frizzled 7 receptor, and overexpression of WNT7A promotes the expansion of the satellite-cell pool and enhances skeletal muscle regeneration [184]. Notch signaling is critical for the maintenance of the undifferentiated state of *Pax7*⁺*Myf5*⁻ cells, and inhibition of Notch signaling promotes an increase in the PAX7⁺MYOD⁺ population at the expense of PAX7⁺MYOD⁻ cells [176]. A schematic view of satellite cell location and division is shown in Figure 1.4.

In response to skeletal muscle injury, satellite cells undergo massive proliferation [164]. MYOD expression indicates satellite cell activation [185] and primary myoblasts from MYOD-knockout mice differentiate poorly into myocytes *in vitro* and *in vivo* [186]. During terminal differentiation, the sequential and partially overlapping expression of the

transcriptional factors MYOD, myogenin and myocyte enhancer factor orchestrates the progression of satellite cells towards a myofiber phenotype (extensively reviewed in [169]).

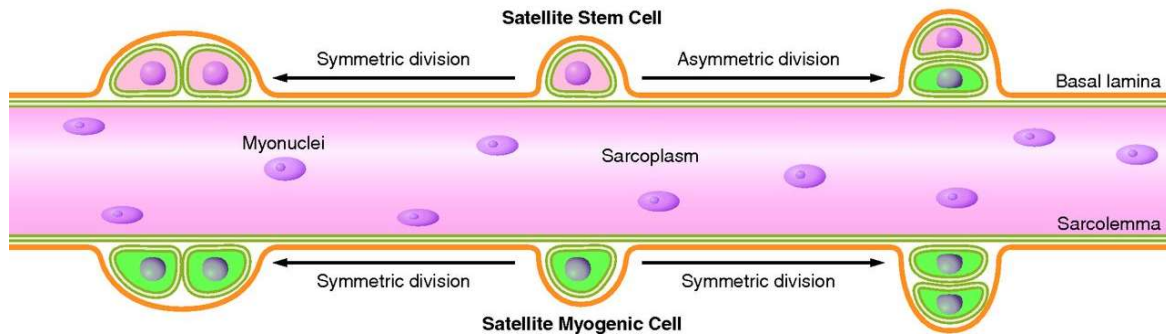


Figure 1.4: satellite cell location and division. Satellite cells are located juxtaposed between myofibers and their basal laminae. They can undergo both symmetric and asymmetric division. $Pax7^+Myf5^-$, represented as pink satellite cells, can give rise to both $Pax7^+Myf5^-$ and $Pax7^+Myf5^+$ (represented as green satellite cells) daughter cells; $Pax7^+Myf5^+$ are able to divide into two equal $Pax7^+Myf5^+$ daughter cells. Adapted from [169].

The amount and functionality of satellite cells seem to be affected by aging, diet and hormonal status. Aging seems to impair the generation of quiescent daughter cells by satellite cells due to higher levels of p38 MAPK activity, which prevent asymmetric p38 MAPK signaling during cell division [187]. Furthermore, 14-months old mice fed a high-fat diet feeding display a decreased number of satellite cells in the gastrocnemius muscle [188]. Accordingly, skeletal muscle regeneration following intramuscular injection of cardiotoxin is impaired in aged mice. Interestingly, exercise training was shown to restore these impairments in regeneration [189]. In addition, younger mice fed a high-fat diet also display impaired satellite cell functionality during cardiotoxin-induced muscle regeneration [190]. The effects of the hormonal microenvironment on satellite cell function are highlighted in ovariectomized mice, which display diminished satellite cell expansion, differentiation and self-renewal, suggesting a role for estrogens in the maintenance of skeletal muscle quality and regeneration capacity [191]. Together, these studies show the strong impact of the surrounding microenvironment on satellite cell function.

In addition to their potential to differentiate into myofibers, previous studies have proposed that satellite cells are also able to differentiate into adipocytes [100, 186, 192, 193] or osteocytes [186] following specific treatments. Such a potential for differentiation into

Introduction

multiple cell lineages, however, remains controversial, with other studies reporting on the strict commitment of satellite cells to the myogenic lineage [164, 194, 195].

1.3.3. Fibro/adipogenic progenitors (FAPs)

Recently, two research groups independently identified an additional mesenchymal stem cell population involved in skeletal muscle regeneration in mice: the FAPs. FAPs are mononuclear cells distinct from MPs, pericytes and smooth muscle cells, located in the interstitium between myofibers and circumferentially surrounding blood vessels, outside the capillary basement membrane [164, 165, 195]. These cells can be distinguished from other skeletal muscle side-population cells based on expression of SCA1, PDGFRA and transcription factor 4, and absence of CD31 and CD45 expression [148, 164, 165, 195]. Subsequently, a cell population equivalent to FAPs was also reported in the interstitium of human skeletal muscle, which can be isolated based on expression of PDGFRA, CD15 or the TE-7 antigen, and absence of CD56 [196-200].

In healthy conditions, skeletal muscle injury causes activation of FAPs, which proliferate and act as a “cellular filter” between alterations in their niche (caused by physical, metabolic and inflammatory signals) and satellite cells, supporting satellite cell activation and myogenesis [201]. Secreted by eosinophils during cardiotoxin-induced muscle regeneration, IL4 activates signal transducer and activator of transcription 6 signaling in FAPs, increasing their proliferation and inhibiting their adipogenic differentiation [202, 203]. Between two and four days following injury, FAP numbers reach a peak [164, 204]. Activated FAPs express collagen type 1, alpha 1 (COL1A1) and synthesize a transient extracellular matrix (ECM) [205]. They also promote a transient pro-differentiation niche for MPs during skeletal muscle regeneration, increasing the mRNA expression of *Il6* and *Il10* [164, 206]. Accordingly, FAPs enhance MP proliferation and myogenic differentiation in a dose-dependent manner *in vitro* [164, 205]. Furthermore, pharmacological inhibition of FAP expansion by the tyrosine-kinase inhibitor Nilotilib has been shown to impair myogenic regeneration, with reduced myofiber cross-sectional area at two and three weeks after injury [205]. In addition to the pro-myogenic role during muscle regeneration, FAPs seem to contribute to clearance of necrotic cellular debris from the damaged site through phagocytosis [202].

During the first days following skeletal muscle injury, inflammatory macrophages secrete TNF, which leads to FAP apoptosis through signaling via the receptors TNF receptor (TNFR)1 and TNFR2. As a result, FAP numbers reach pre-damage levels at day 5 post-injury. Following this initial stage of regeneration, macrophages switch to a pro-regenerative phenotype, decreasing TNF secretion and increasing transforming growth

factor beta (TGFB)1 synthesis, which promotes FAP survival through increased phosphorylation of p38 MAPK. Macrophages are also responsible for FAP clearance from the inflammation site. FAP death and clearance during regeneration are essential to prevent excessive deposition of extracellular matrix and fibrogenesis [204]. Besides the signals from immune cells involved in the regeneration process, myofibers also seem to influence FAP fate, inhibiting FAP adipogenic differentiation via direct interaction *in vitro* [195]. *In vitro* experiments have also shown that skeletal muscle CD31⁻CD45⁻SCA1⁺ mesenchymal stem cells, which very likely include FAPs (as discussed below), exhibit decreased expression of *Il6*, *Tgfb1*, *Tnfa* and *Vegfa* when grown on collagen compared to cells grown on laminin [207], pointing to a possible influence of the ECM on FAP gene expression.

In line with their role in skeletal muscle regeneration, FAPs seem to be involved in skeletal muscle adaptation to eccentric exercise. In fact, Valero et al.[208] observed a 2.2-fold increase in the number of CD31⁻CD45⁻SCA1⁺ mesenchymal stem cells in the gastrocnemius skeletal muscle following a bout of downhill-running exercise. These cells improved the expansion of PAX7⁺ cells and the synthesis of new myofibers in the exercised skeletal muscle. Although the authors identified more than 50% of these CD45⁻SCA1⁺ cells as pericytes, FAPs were also very likely included in this population based on the surface marker expression and location (interstitium and around blood vessels) described by the authors. A further study by the same research group showed that transplantation of these CD31⁻CD45⁻SCA1⁺ cells into the gastrocnemius skeletal muscle results in higher satellite cell number and myofiber nuclear content and hypertrophy after a two-week downhill-running training [209].

Despite their important contribution to regeneration in healthy skeletal muscle, FAPs are known to differentiate into adipocytes or fibroblasts under certain conditions. For example, in mice with murine X-linked muscular dystrophy, FAPs accumulate in fibrotic areas and express genes involved in fibrosis such as *Col1a1*, Collagen type 3 alpha 1 and connective tissue growth factor [165]. FAPs also differentiate into ECM-synthesizing fibroblasts in mice exposed to gamma radiation before intramuscular cardiotoxin injection [165], following skeletal muscle denervation and during BaCl₂-induced chronic muscle damage [148]. Fibrogenic differentiation of FAPs is stimulated by the TGFB isoforms 1, 2 and 3 [165, 197, 204, 210], as well as by platelet-derived growth factor AA [165], through independent signaling pathways.

Moreover, FAPs differentiate into unilocular white adipocytes during skeletal muscle fatty degeneration, as demonstrated in studies using intramuscular injection of glycerol to induce

Introduction

intramuscular fat deposition [164, 195]. FAP-derived adipocytes are also observed following intramuscular cardiotoxin-injection in IL4-knockout mice or in mice treated with the glucocorticoid dexamethasone [203]. In glycerol-injected muscle, FAP proliferation and adipocyte deposition decrease in response to hindlimb suspension-induced unloading [152]. *In vitro*, FAPs differentiate into white adipocytes spontaneously or following treatment with standard adipogenic medium, displaying lipid-filled vacuoles and expressing markers such as the *Pparg2*, Leptin, Adiponectin, Adipsin, *Cebpa*, *Cebpb*, early growth response 2 and *Fabp4* genes, and PLIN [164, 167, 195, 200, 203]. While human FAPs differentiated into adipocytes *in vitro* display similar levels of triglyceride synthesis and lipolysis compared to adipocytes derived from subcutaneous WAT, their insulin signaling is impaired, with a weak induction of AKT serine/threonine kinase 1 (AKT1) phosphorylation and unaltered phosphorylation of p44/42 mitogen-activated protein kinase in response to insulin treatment [200]. *In vitro*, adipogenic differentiation of FAPs is inhibited by IL4 [203], TNFA or cytokines from the TGFB family (TGFB1 and activin A) [200], besides the above-mentioned direct contact with differentiated myotubes [195]. The FGF receptor co-receptor beta-Klotho, in contrast, seems to enhance the FAP adipogenic differentiation [211].

1.3. Intramuscular fatty infiltration

1.3.1. Impact of intramuscular fatty infiltration on skeletal muscle function

In humans, the accumulation of adipose tissue between myofibers, called intramuscular fatty infiltration, is observed during aging [198, 212] and muscle disuse [213], as well as in patients with type-2 diabetes [20, 214], Duchenne muscular dystrophy [215], chronic obstructive pulmonary disease [216] and rotator cuff tears [217], among others. It is generally regarded as a negative process associated with insulin resistance [20, 214, 218], impaired muscle force production [219, 220] and, in the elderly, impaired mobility [21].

Despite the association between intramuscular adipocyte deposition and poor skeletal muscle health, the mechanisms underlying the possible effects of adipocytes on surrounding myofibers are not yet completely understood. *In vitro* studies with immortalized and primary cell lines have indicated that adipocytes can impair myotube function. Primary human myotubes treated with conditioned medium from subcutaneous [221] or mammary [222] WAT adipocytes display impaired phosphorylation of AKT1 in response to insulin treatment. The reduction in insulin-induced AKT1 phosphorylation seems to be even more pronounced when the myoblasts are treated with conditioned medium from omental WAT adipocytes [221]. This effect seems to be at least partially mediated by IL6 secreted by the adipocytes [221]. Similar results were observed in immortalized L6 myotubes co-cultured

with or exposed to conditioned medium from differentiated immortalized 3T3-L1 adipocytes [223]. Furthermore, in a three-dimensional co-culture system, Pellegrinelli et al. [224] observed that adipocytes isolated from visceral WAT of obese humans reduced titin expression levels, altered sarcomeric structure, and decreased basal phosphorylation levels of AKT1, p70-S6K and eukaryotic translation initiation factor 4E binding protein 1 compared to control cells and cells co-cultured with adipocytes isolated from subcutaneous WAT of lean humans. These studies not only suggest that adipocytes can negatively affect myotube metabolism, but also that adipocytes under different conditions, through an altered secretome, can differentially affect myotube function. We could not find studies investigating the effects of brown or brown-like adipocytes on myotube function.

Differentiated FAPs from human muscle have been characterized as white adipocytes [196, 200], and experiments have suggested these white adipocytes to be insulin-resistant [200]. On the other hand, Uezumi et al. [197] reported the detection of both Leptin and *UCP1* mRNA in human FAPs differentiated *in vitro*, indicating that these cells could have the ability to differentiate into both white and brown adipocytes.

In mice, intramuscular adipocyte deposition is a rare phenomenon even in aged mice [167]; to our knowledge, it has been only observed in type-2 diabetes model KKAy mice [225]. Thus, the study of intramuscular adipocyte accumulation in mouse models normally requires the stimulation of fatty degeneration, which can be achieved through intramuscular injections of glycerol [166, 167]. Transcriptome analysis of regenerating skeletal muscles suggests that, compared to intramuscular cardiotoxin injections used to stimulate skeletal muscle regeneration, intramuscular glycerol injections elicit a stronger inflammatory response and promotion of adipogenesis, resulting in a larger and more persistent accumulation of adipocytes between myofibers [166]. Glycerol injections seem to elicit the accumulation of unilocular, white adipocytes in skeletal muscle [167, 226, 227]

1.3.2. Origin of brown-like intramuscular adipocytes

While intramuscular adipocytes have been generally considered as harmful white adipocytes that impair skeletal muscle and systemic health, the formation of ectopic UCP1-expressing adipocytes or the transdifferentiation of white into brown-like adipocytes within skeletal muscle is still under debate. Browning of intramuscular adipocytes could not only contribute to an increment in whole-body energy expenditure – as proposed by Yin et al. [192] – but also to enhanced metabolism of fatty-infiltrated skeletal muscle. The development of therapies aiming at the browning of intramuscular adipocytes requires a better understanding of the potential of different cell populations residing in skeletal muscle to acquire a brown-like phenotype.

Introduction

Seale et al. [100] have shown that primary myoblasts isolated from new-born mice are able to differentiate into brown adipocytes when expression of the transcription factor PRDM16 is induced. Consistent with this, Yin et al. [192] reported the differentiation of 0.1% of PAX7⁺ cells isolated from skeletal muscle into PRDM16-positive adipocytes; in an additional experiment with monoclonal primary cultures, 8.1 % of PAX7⁺MYF5⁻ clones and 3.3% of PAX7⁺MYF5⁺ clones differentiated into adipocytes. *In vivo*, these authors showed that inhibition of miR-133 during cardiotoxin-induced skeletal muscle regeneration leads to the deposition of UCP1-positive adipocytes derived from PAX7⁺ cells. Importantly, the protocols used in these studies rely on the exclusive labeling of MPs by PAX7 and MYF5. Nevertheless, as previously mentioned, it has recently been shown that MYF5-positive progenitors are also present in WAT depots, where they can give rise to white adipocytes [117], indicating that the spectrum of cell lineages is broader than previously appreciated. Furthermore, a lineage tracing study reported that most adipocytes in skeletal muscle derive from a PAX3⁻ lineage and that adipocytes formed in aged mice during muscle regeneration derive from MYF5-independent cells [228].

On the other hand, there is also evidence that FAPs could constitute the brown adipocyte progenitor population residing in skeletal muscle. In this regards, it has been shown that FAPs, but not A-7 integrin⁺SCA1⁻ MPs, are able to differentiate into UCP1-positive adipocytes *in vitro* when pre-treated with BMP7. Interestingly, it was demonstrated that FAPs isolated from skeletal muscle of adult Sv/129 mice express higher levels of *Ucp1* and other BAT markers following *in vitro* differentiation compared with FAPs from C57Bl/6 mice [110], similarly to the differences observed in adipocyte precursors isolated from the subcutaneous WAT depots from these two mouse strains [110, 229].

In humans, CD34⁺CD56⁻CD146⁻ endothelial cells isolated from fetal skeletal muscle were shown to differentiate into UCP1⁺ adipocytes *in vitro*. In cells isolated from adult skeletal muscle, however, UCP1 protein could not be detected following brown adipogenic differentiation *in vitro* [230]. On the other hand, a study on PDGFRA⁺ progenitors isolated from human adult skeletal muscle showed that, following adipogenic differentiation *in vitro*, these cells expressed both leptin and *UCP1* at the mRNA level, suggesting that they could be able to differentiate into both white or brown adipocytes [197].

2. Research Aims

Intramuscular adipocytes are generally regarded as a metabolically and mechanically unfavorable feature of different diseases including obesity, diabetes, chronic obstructive pulmonary disease, muscle dystrophies, sarcopenia and muscle atrophy. Since brown adipocytes can act as a sink for excessive glucose in the circulation and their secretome differs from that of white adipocytes, it is tempting to speculate that the deposition of brown adipocytes instead of white adipocytes in skeletal muscle – or the transdifferentiation of intramuscular white adipocytes into brown adipocytes – could improve metabolism of fatty-infiltrated skeletal muscle. However, it remains unclear whether such a shift from the accumulation of white adipocytes to the accumulation of brown adipocytes is possible.

A first step towards the development of strategies to change the phenotype of intramuscular adipocytes is the identification of progenitor populations residing in skeletal muscle that could undergo brown adipogenic differentiation. Previous studies have suggested that skeletal muscle satellite cells/MPs or FAPs can differentiate into adipocytes under certain conditions. Therefore, the first aim of the present doctoral thesis was to assess the potential of MPs and FAPs to differentiate into brown-like, UCP1-expressing adipocytes. To this end, we analyzed intramuscular adipogenic differentiation *in vivo* and the response of MPs and FAPs to a brown adipogenic treatment *in vitro* in obesity-resistant and obesity-prone mice. Furthermore, we also tested the response of fatty-infiltrated skeletal muscle to beta 3-adrenergic stimulus, known to increase UCP1 expression in classical BAT and WAT depots. In Chapter 4, results from these experiments are described and discussed.

Modifiable lifestyle factors such as diet and physical activity are known to impact adipocyte metabolism and UCP1 expression in different adipose tissue depots. In addition, such factors can also affect the functionality of stem cells from different tissues. Following the identification of brown-like adipocyte precursors residing in skeletal muscle, the second aim of this thesis was to characterize the expression of *Ucp1* and other brown-adipocyte markers during intramuscular adipocyte deposition *in vivo*, as well as the brown adipogenic differentiation of primary FAPs *in vitro*, in mice fed a high-fat diet or in exercise-trained mice. Results from these experiments are shown and discussed in Chapter 5.

In addition to modifiable lifestyle factors, aging and estrogen-deficiency have also been reported to impact adipocyte differentiation and function in classical adipose tissue depots. Thus, the third aim of this doctoral thesis was to determine the effects of aging and ovariectomy on the expression of brown adipocyte markers in fatty-degenerated skeletal

Research Aims

muscle *in vivo* and on the *in vitro* differentiation of skeletal muscle FAPs into brown-like adipocytes in mice. The results of experiments related to this aim are presented and discussed in Chapter 6.

3. Material and Methods

3.1. Chemicals

Unless specified in sections 3.3 to 3.9 or purchased from Sigma-Aldrich, chemicals used in the experiments are described in the list provided in Table 3.1.

Chemical	Manufacturer	Catalog number	Stock solution
T3	Sigma-Aldrich	T6397	4.98 ug/ml (diluted to 1mg/ml in 1 N NaOH, further diluted 1:200 in low-glucose DMEM)
7-Aminoactinomycin D (7AAD)	Sigma	SML1633	1 mg/ml
ANP (1-28) (rat)	Tocris Bioscience	1912	0.03 ug/ul in double-distilled H ₂ O (ddH ₂ O)
BMP7	R&D Systems	354BP-010	6 ng/ul in 4 mM HCl with 0.1% bovine serum albumin (BSA)
BSA	Sigma-Aldrich	05479-50G	-
Cardiotoxin	Sigma-Aldrich	C9759	140 uM in phosphate-buffered saline (PBS)
CL316	Sigma-Aldrich	C5976	0.06 mg/ml in mouse saline
Collagen 1, from rat tail	Gibco	A10483-01	-
Collagenase, type 2	Gibco	17101015	-
cOmplete, ethylene diamine tetra acetic acid (EDTA)-free protease inhibitor cocktail	Roche	5056489001	0.5 tablet/ml in radio immunoprecipitation assay (RIPA) buffer

Material and Methods

4',6-diamino phenylindole (DAPI)	-2- Roth	6335.1	1 mg/ml in ddH ₂ O
Dexamethasone	Sigma-Aldrich	D4902	64 mM in dimethyl sulfoxide (DMSO)
Ham's F-10 Nutrient Mix (F10)	Gibco	31550-023	-
Fetal bovine serum (FBS)	Gibco	10270	-
FGF-Basic Recombinant Human Protein (FGFB)	Gibco	PHG0266	2.5 ug/ml in low-glucose DMEM with 10% FBS
Forskolin	Sigma-Aldrich	F6886	10 mM in DMSO
Gelatin	Fluka	48722	-
Glycerol	Sigma-Aldrich	G2025	-
Goat serum	Gibco	16210064	-
Hank's Balanced Salt Solution (HBSS)	Gibco	14175-053	10 x
High-glucose Dulbecco's modified Eagle's medium (DMEM)	Gibco	41966029	-
Horse serum	Gibco	10270-106	-
Indomethacin	Sigma-Aldrich	I7378	100 mM in DMSO
Insulin	Sigma-Aldrich	I9278	10 mg/ml
IBMX	Sigma-Aldrich	I5879	100 mM in DMSO
Isoflurane (Forane)	Abbot	-	-
Isoproterenol	Sigma-Aldrich	I5627	Freshly prepared, 100 nM in ddH ₂ O
Low-glucose DMEM	Gibco	31885023	-

Penicillin/Streptomycin (P/S)	Gibco	15140122	100 x
PhosSTOP phosphatase inhibitor	Roche	4906837001	1 tablet/ml in RIPA buffer
Recombinant Mouse Activin Receptor type 2B (ACTR2B) Fc Chimera	R&D Systems	3725-RB-050	1 ug/ml in PBS
Rosiglitazone	Sigma-Aldrich	R2408	14 mM in DMSO
Rotiphorese Gel 30 (37.5:1)	Carl Roth	3029.1	-
TEMED	Carl Roth	2367.1	-
Trizol	Thermo Fisher Scientific	15596018	-

Table 3.1.: Chemicals.

3.2. Antibodies

A list of the antibodies used in the experiments is provided in Table 3.2.

Antigen	Conjugate	Manufacturer	Catalog number	Reactivity	Application	Used dilution
A-7 integrin	PE	R&D Systems	FAB3518P	Mouse	FACS	1:100
Actin beta (ACTB)	-	ProteinTech	20536-1-AP	Mouse, human, rat, zebrafish, monkey, hamster	Western blot	1:2000
CD31	Alexa Fluor® 488	BioLegend	102414	Mouse	FACS	1:1000
CD45	Alexa Fluor® 488	BioLegend	103121	Mouse	FACS	1:1000
FABP4	-	Cell Signaling	3544	Mouse, (human)	Western blot	1:1000

Material and Methods

Glyceraldehyde 3-phosphate dehydrogenase (GAPDH)	-	ProteinTech	10494-1-AP	Mouse, human, rat, pig, bombyx, monkey, mussel, oriental river prawns, sea cucumbers, tree shrews, zebrafish	Western blot	1:2000
Sca1	APC	BioLegend	108111	Mouse	FACS	1:1000
Mouse IgG, heavy and light chains	Peroxidase	Merck Millipore	401253	Mouse	Western blot	1:8000
MyHC	-	Developmental Studies Hybridoma Bank	MF 20	Mammalian, avian and amphibian	Western blot	1:100
Rabbit IgG, heavy and light chains	Peroxidase	Merck Millipore	401393	Rabbit	Western blot	1:800
UCP1	-	Abcam	ab10983	Mouse, human, rat	Immunofluorescence	1:1000
UCP1	-	Merck Millipore	662045	Mouse, human, rat	Western blot (unless otherwise stated)	1:1000
UCP1		Thermo Fisher Scientific	PA1-24894	Rabbit	Immunohistochemistry	1.250

Table 3.2: Antibodies. Species enclosed between parentheses are predicted to react based on 100% homology. APC: allophycocyanin; PE: phycoerythrin.

3.3. Animal Procedures

3.3.1. Animal Husbandry

All mice used in the experiments were maintained in a 12-h light/dark cycle at room temperature in a specific pathogen-free animal facility. Mice were provided with *ad libitum* access to standard laboratory animal chow (Kliba Nafag, code 3336) and water. C57Bl/6J and Sv/129 mice were purchased from Harlan Laboratories and Taconic, respectively. For experiments using ovariectomized mice, ovariectomized Sv/129 mice were purchased from Taconic. The ethics committee of the Cantonal Veterinary Office Zurich approved all animal studies and the principles of laboratory animal care were followed.

3.3.2. Glycerol and cardiotoxin intramuscular injections

To induce skeletal muscle injury, and consequently the proliferation and differentiation of FAPs and MPs *in vivo*, mice were anesthetized with isoflurane and one of the tibialis anterior (TA) muscles was injected with cardiotoxin (50 μ l, 10 μ M in PBS) or glycerol (50 μ l, 50% v/v in HBSS); the contralateral muscle was used as a control.

3.3.3. CL316 treatment

To stimulate B3-adrenergic receptors, thereby promoting *Ucp1* expression in otherwise white adipocytes, mice were treated for five consecutive days with daily intraperitoneal injections of CL316 (0.5 mg/kg body mass).

3.3.4. High-fat diet-feeding

For high-fat diet feeding, mice were fed for 12 or 16 weeks *ad libitum* with chow containing 58%, 25.5% and 16.4% of kcal provided by lipids, carbohydrates and proteins, respectively (Research Diets, code D12331, 5.56 kcal/g). Control mice were fed with standard laboratory animal chow as described above.

3.3.5. Exercise training protocol

The exercise training protocol consisted of 20 treadmill-running sessions split into four weeks (five training sessions per week). A five-lane mouse treadmill was used (Panlab LE8710M, Harvard Apparatus). Each session had a total duration of 45 min, comprising a 5-min warm-up phase at 6 m/min followed by a slow increment in speed (0.6 m/min-increment every 30 s) until reaching the target speed maintained until the end of the session. The target speed of the training sessions started at 10.2 m/min and was gradually increased up to 15.6 m/min throughout the training period, as shown in Figure 3.1. To stimulate the running behavior, the electrical shock grid behind the treadmill belt was set

Material and Methods

to two pulses per second at 0.2-0.3 mA. Before each training session, mice were placed and left undisturbed on the treadmill for 15 min, with the belt unmoving and the electrical grid switched off, but the treadmill motor switched on for noise adaptation. Control mice underwent only the 15-min noise adaptation five times per week during four weeks.

Ten to 15 days before the start of the training period, mice were acclimated to the treadmill by being placed and left undisturbed on the stopped treadmill for 15 min; the treadmill speed was then gradually increased to 6 m/min and kept at this level for 5 min (warm-up). Finally, the treadmill speed was slowly increased (0.6 m/min-increase per min) to 10.2 m/min. After 1 min at 10.2 m/min, the treadmill speed was slowly decreased until the belt stopped. During acclimation, mice touching the electrical shock grid behind the belt received a 0.2-mA electrical stimulus. Both experimental and control groups were acclimated to the treadmill.

Since laboratory mice prefer darkened areas, during all familiarization and exercise training sessions a dark area was created at the front-end of the treadmill by covering it with cardboard to promote a consistent running behavior.

Exercise was immediately stopped and the mice were placed back in their cages when any of the following situations occurred:

1. Mouse spent more than 3 s in contact with the electrical shock grid without attempting to reengage on the treadmill.
2. Mouse jumped or was not able to reengage into running behavior after return from the electrical shock grid.
3. Mouse was willing to remain on the electrical shock grid for 2 s or more without returning to the moving belt for three times.

3.4. Physiological Analysis

3.4.1. Blood Parameters

For the measurement of blood glucose levels, blood was collected from the tail vein and analyzed with an Accu-Check Aviva blood glucose meter (Roche) using Accu-Check Aviva Plus test strips (Roche).

For plasma insulin measurements, blood was collected from the tail vein into ice-cold Microvette® 100 K3E EDTA-coated tubes (Sarstedt, catalog number 20.1278) and centrifuged at 2000 g for 5 min. The supernatant was collected into a new tube and immediately stored at -80°C until further analysis. Determination of plasma insulin levels

was conducted using the Ultra Sensitive Mouse Insulin ELISA kit (Crystal Chem, catalog number 90080) according to the manufacturer's instructions.

The homeostasis model of insulin resistance index (HOMA-IR) was calculated using the equation [fasting serum glucose (in mM)* fasting serum insulin / 22.5], as previously described. Lower HOMA-IR values indicate higher insulin sensitivity [231].

3.4.2. Body mass and TA mass

Body and TA mass were measured using a digital scale balance (PJ360 Delta Range, Mettler Toledo). To measure TA mass, excessive blood eventually surrounding the tissue was carefully removed following dissection.

3.5. Tissue sections

For histological analysis of control and glycerol-injected TAs, TA skeletal muscles were excised from mice and immediately flash frozen in isopentane cooled in liquid nitrogen. Samples were stored in liquid nitrogen and, posteriorly, 30-um sections were prepared from different TA areas using a cryostat (CM1850, Leica Biosystems) and placed on glass slides (Superfrost™ Plus Gold Adhesion Slides, catalog number 10143351, Thermo Fisher Scientific). Sections were stained with hematoxylin and eosin (H&E), dehydrated and cover slipped with Entellan (Merck Millipore, catalog number 1079600500).

For UCP1 immunostaining on paraffin sections, TA skeletal muscles and ingWAT were excised from mice, washed in PBS and fixed for 16-18 h in 10% formalin at 4°C. Tissue samples were then maintained in ddH₂O until sequential immersion in ethanol, xylene and paraffin using a benchtop tissue processor (TP1020, Leica Biosystems), followed by embedding in paraffin. Sections of 4-um thickness were prepared using a microtome (RM2255, Leica Biosystems) and deparaffinized. Sections were immunostained as described in section 3.9.3. Following immunostaining, sections were counterstained with hematoxylin, dehydrated and cover slipped with Pertex (Histolab, catalog number 00811).

Images of cryosections and paraffin sections were obtained using a digital camera (Zeiss AxioCam HRc) connected with a microscope (Zeiss Axioplan2).

3.6. Isolation of primary cells

3.6.1. Isolation of skeletal muscle FAPs and MPs

For isolation of FAPs and MPs, skeletal muscle tissue was excised from the hindlimbs (when indicated, paraspinal muscle was also included), minced with scissors and digested with 2 mg/ml type-2 collagenase in collagenase buffer (2% BSA in HBSS) for 1 h in a

Material and Methods

shaking water bath at 37°C. Following erythrocyte lysis (erythrocyte lysis buffer: 154 mM NH₄Cl, 10 mM KHCO₃, 0.1 mM EDTA) and filtration through 40-um cell strainers, cells were incubated for 45 min at 4°C with APC-conjugated anti-mouse SCA1, Alexa Fluor® 488-conjugated anti-mouse CD31, Alexa Fluor® 488-conjugated anti-mouse CD45 and PE-conjugated anti-mouse A-7 integrin antibodies diluted in PBS containing 0.5% BSA.

Using FACS (BD FACSAria III, BD Biosciences), FAPs were sorted based on positive staining for SCA1 and absence of staining for A-7 integrin, CD31 and CD45 [164], while MPs were sorted based on positive staining for A-7 integrin and absence of SCA1, CD31 and CD45 [232]. To exclude dead cells, 7AAD was added to the samples shortly before the sort. Sorts were performed using an 85-um nozzle, with sheath pressure set at 45 psi. An example of the gating strategy used is displayed in Figure 3.2. For analysis of monoclonal cell colonies, single FAPs and MPs were sorted directly into 96-well cell culture plates containing growth medium using the FACS-sorter coupled to an Automated Cell Deposition Unit (Becton Dickinson).

3.6.2. Isolation of cells from WAT SVF

For isolation of primary cells from WAT SVF, ingWAT was excised and digested with 2 mg/ml type-2 collagenase in collagenase buffer (25 mM NaHCO₃, 12 mM KH₂PO₄, 1.2 mM MgSO₄*7H₂O, 4.8 mM KCl, 120 mM NaCl, 1.4 mM CaCl₂*2H₂O, 5 mM glucose, 2.5% BSA, 1% P/S) for 1 h shaking at 37°C. After centrifugation, the resulting pellet containing the SVF was washed, erythrocytes were lysed, and cells were filtered through a 40-um strainer and plated for cell culture.

3.7. Tissue Culture

3.7.1. Immortalized Cell Lines

3T3-L1 immortalized preadipocytes were cultured in high-glucose DMEM supplemented with 10% FBS and 1% P/S. All cells were cultured in a 5% CO₂ atmosphere at 37°C.

3.7.2. Primary Cell Lines

MPs were cultured on collagen-coated plates in culture medium containing 40% F10, 40% low-glucose DMEM, 20% FBS, 1% P/S and 5 ng/ml FGFB. FAPs were grown in low-glucose DMEM containing 20% FBS, 1% P/S and 5 ng/ml FGFB. WAT SVF cells were grown on collagen-coated plates in high-glucose DMEM with 10% FBS and 1% P/S. All cells were cultured in a 5% CO₂ atmosphere at 37°C.

3.7.3. Differentiation and Stimulation

Myogenic differentiation medium contained 2% horse serum and 1% P/S in low glucose DMEM. To stimulate adipogenic differentiation, cells were treated for two days with high-glucose DMEM supplemented with 10% FBS, 1% P/S, 5 ug/ml insulin, 125 uM indomethacin, 5 uM dexamethasone, 0.5 mM IBMX, 1 nM T3 and 1 uM rosiglitazone (brown adipogenic induction medium); subsequently, cells were kept in high-glucose DMEM containing 10% FBS, 1% P/S, 5 ug/ml insulin, 1 nM T3 and 1 uM rosiglitazone (brown adipogenic differentiation medium) for up to eight days. Where indicated, T3 was not added to the brown adipogenic induction and differentiation media.

Where indicated, UCP1 expression in differentiated adipocytes was stimulated by the addition of 10 uM forskolin to the culture medium for 4 h before cell lysis.

3.7.4. Staining of Cultured Cells

To quantify differentiated adipocytes following FAP differentiation, cells were expanded and differentiated in 96-well plates (Greiner Bio-One, catalog number 655090). At day 10 of differentiation, cells were fixed in 10% formalin for 20 min at room temperature, washed in PBS and maintained in PBS at 4°C until further analysis. For lipid droplet staining, cells were incubated for 30 min with LD540 (100 ng/ul) and DAPI diluted in PBS at room temperature in the dark. After washing, 17 pictures were taken per well using an automated microscope imaging system (PerkinElmer Operetta High Content Imaging System). For UCP1 immunofluorescence, cells were further processed as described in section 3.9.4.

3.8. Gene Expression Analysis

3.8.1. RNA Extraction and Purification

Total RNA was isolated using the Trizol reagent according to the manufacturer's instructions, followed by DNase digestion of total RNA (DNA-free DNA Removal kit, Invitrogen, catalog number AM1906) according to the manufacturer's instructions.

The concentration and ratio of UV absorbance at 260 nm and 280 nm (A_{260}/A_{280}) of the RNA samples were measured with a spectrophotometer (NanoDrop Lite, Thermo Scientific Inc.); only samples with ratios equal to or higher than 1.8 were used for further analysis. To evaluate RNA integrity, approximately 300-500 ng RNA (1-2 ul RNA sample dissolved in 3.5-4.5 ul ddH₂O, 3.5 ul formaldehyde, 2 ul 10x 3-(N-morpholino)propanesulfonic acid – MOPS, 10 ul formamid and 1 ul EtBr₂) were run on a 1%-agarose gel (in MOPS, 1.1% formaldehyde, pre-ran for 5 min at 80 V before loading samples) to visualize 28S and 18S rRNA bands. Samples were stored at -80°C for further analysis.

Material and Methods

3.8.2. Reverse transcription and quantitative polymerase chain reaction (qPCR)

Complementary DNA was synthesized from 0.5 to 1.0 ug RNA with random hexamer primers using Super Script III Reverse Transcriptase (SuperScript® III First-Strand Synthesis System, Invitrogen, catalog number 18080051). All procedures were conducted according to the manufacturer's instructions.

mRNA levels were posteriorly analyzed by qPCR with a 7500 Fast Start Real-Time PCR system (Applied Biosystems) using the FastStart Universal SYBR Green Master Mix (Roche). Transcript levels were normalized to 18S rRNA levels. Primer sequences are show in Table 3.3. Primers were stored as stock solutions at -20°C and diluted to for qPCR.

Target	Forward	Reverse
18S	5'- GACACGGACAGGATTGACAGATTG	5'- AAATCGCTCCACCAACTAAGAACG
Cebpa	5'-TGGACAAGAACAGCAACGAG	5'-GTCACTGGTCAACTCCAGCA
Cidea	5'-ATCACAACCTGGCCTGGTTACG	5'-TACTACCCGGTGTCCATTTCT
Cox7a1	5'-AGAAAACCGTGTGGCAGAGA	5'-CAGCGTCATGGTCAGTCTGT
Elovl3	5'-GATGGTTCTGGGCACCATCTT	5'-CGTTGTTGTGTGGCATCCTT
Eva1	5'-CCACTTCTCCTGAGTTTACAGC	5'-GCATTTTAACCGAACATCTGTCC
Fabp4	5'-GATGAAATCACCGCAGACGACA	5'-ATTGTGGTCGACTTTCCATCCC
Leptin	5'-TCAAGACCATTGTCACCAGG	5'-TGAAGCCCAGGAATGAAGTC
Pgc1a	5'-GCGAACCTTAAGTGTGGAAC	5'-CACCACGGTCTTGCAAGAGG
Pparg2	5'-TGCTGTTATGGGTGAACTCTG	5'-CTGTGTCAACCATGGTAATTTCT
Prdm16	5'-CAGAGGTGTCATCCCAGGAG	5'-ACGGATGTACTTGAGCCAGC
Ucp1	5'-GGACGACCCCTAATCTAATGAG	5'-GCAAAACCCGGCAACAAG

Table 3.3: primers used for qPCR. All primers were purchased from Sigma-Aldrich. Cox7a1: Cytochrome c oxidase subunit 7a 1; Elovl3: Elongation of very long chain fatty acids (FEN1/Elo2,SUR4/Elo3, yeast)-like 3; Eva1: Myelin protein zero-like 2.

3.9. Protein Expression Analysis

3.9.1. Protein Extraction

To prepare samples for protein extraction, frozen tissues were pulverized with a mortar and pestle in liquid nitrogen and cell cultures were briefly washed with PBS and scraped on ice.

Cells homogenates and ground tissues were then lysed on ice for 30 min in RIPA buffer (25 mM Tris HCl, pH 7.6; 150 mM NaCl; 1% NP-40; 1% sodium deoxycholate; 0.1% sodium dodecyl sulfate – SDS) freshly supplemented with protease and phosphatase inhibitors. Lysates were subsequently sonicated for approximately 20 s and centrifuged at 14000 g for 15 min at ~4°C. The supernatant was taken into a new tube. The protein concentration of the samples was measured using a bicinchoninic acid protein assay kit (Pierce, catalog number 23225) according to the manufacturer's instructions and a microplate spectrophotometer (PowerWave 340, BioTek).

3.9.2. SDS polyacrylamide gel electrophoresis (SDS-PAGE) and Western Blotting

For Western blotting, equal amounts of protein (4 ug to 30 ug) were denatured and reduced at 95°C for 5 min using Laemmli buffer [233], and loaded into the wells of SDS-PAGE gels, along with a molecular weight size marker (indicated as M in the figures, PageRuler Prestained Protein Ladder, Thermo Scientific, catalog number 26616). Handcast (12% or 14%) or precast (4-15% Mini-PROTEAN TGX Stain-Free, BioRad, catalog number 4568086 or 4568083) mini gels were used. Electrophoresis and wet transfer of proteins to polyvinylidene difluoride membranes (Roche, catalog number 0301004001) were conducted using a Mini-PROTEAN Tetra Cell and a Mini Trans-Blot Cell (BioRad, catalog numbers 1658000 and 1703930).

Following protein transfer, membranes were blocked in Tris-buffered saline containing 0.1% Tween 20 and 4% skim milk for one hour and incubated with primary antibodies diluted in NET-G buffer (150 mM NaCl, 5 mM EDTA, 50 mM Tris, 0.05% Triton X-100, 0.25% gelatin, pH 7.4) for approximately 18 h at 4°C on a roller.

3.9.3. Immunohistochemistry on Tissue Sections

For UCP1 immunostaining on paraffin sections of ingWAT and glycerol-injected skeletal muscle, endogenous peroxidase activity was blocked by incubation in 3% H₂O₂ for 15 min at room temperature in the dark, followed by heat-induced epitope retrieval in sub-boiling 0.01M Sodium Citrate (pH = 6) for 8 min and gradual cooling for 1 h at room temperature. Tissue sections were encircled using a hydrophobic pen (Super PAP PEN Mini, Daido Sangyo) and blocked in 10% goat serum in PBS for 1 h at 37°C. Tissue sections were then incubated with anti-UCP1 diluted in blocking buffer for 18 h at 4°C. After washing, sections were incubated for 30 min with SignalStain® Boost IHC Detection Reagent (HRP, rabbit, Cell Signaling, catalog number 8114) according to the manufacturer's instructions. For detection, sections were incubated with SignalStain® Diaminobenzidine (DAB) Chromogen Concentrate freshly diluted 1:100 in SignalStain® DAB Diluent (SignalStain® DAB

Material and Methods

Substrate kit, Cell Signaling, catalog number 8059) until positive signal was observed, followed by washing in ddH₂O. Incubation time was controlled for the first tissue section and the remaining sections were incubated with DAB for the same time.

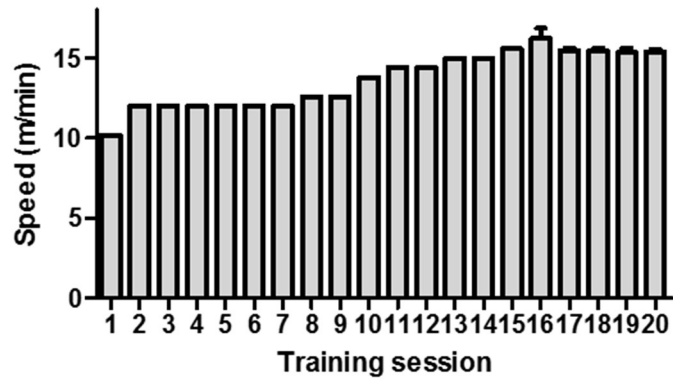
3.9.4. Immunofluorescence of Cell Cultures

For immunofluorescence of differentiated FAPs, cells fixed and stained with LD540 and DAPI as described in section 3.7.4 were incubated with 5% acetic acid in ethanol for 10 min at -20°C to destroy lipid droplets and, after washing, blocked with 1% BSA in PBS-0.05% Triton for 1 h at room temperature. Cells were then incubated for 18 h with anti-UCP1 diluted in blocking buffer, washed, and incubated with secondary antibody diluted in blocking buffer for 45 min at room temperature.

3.10. Statistical Analysis

Student's t-tests were used for pairwise comparisons and one-way or two-way Analyses of Variance (ANOVAs) with Bonferroni post-hoc tests were used for comparisons between more than two groups. A significance level of 0.05 was considered for all tests. Results are shown as mean and standard error of the mean (S.E.M.). All statistical analyses were conducted using GraphPad Prism 5. When gene or protein expression values did not show a normal distribution of residuals, data were log transformed before statistical analysis. In these cases, for experiments in which at least one sample had an undetermined cycle threshold (C_t) value for a given gene, half of the lowest detectable value of the experiment was added to all samples, allowing for logarithmic transformation.

Maximal running speed per training session



Running distance per training session

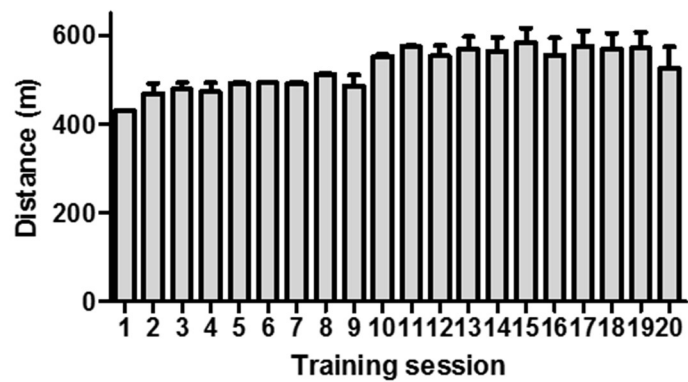


Figure 3.1: Maximal running speed and running distance attained in each training session throughout the treadmill-running exercise training protocol. Data are shown as mean and S.E.M. of speed (m/min) and distance (m) per training session.

Material and Methods

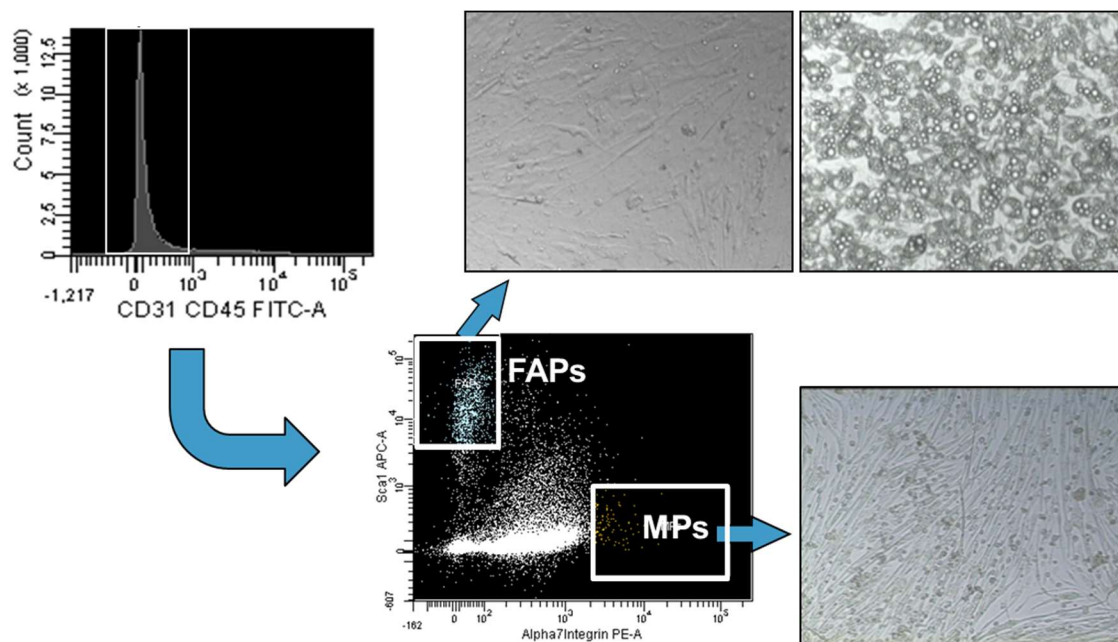


Figure 3.2: Gating strategy for FACS-sort of MPs and FAPs. CD31⁻CD45⁻ cells (negatively stained for Alexa-488, detected in the fluorescein channel – indicated as FITC) were sorted as FAPs based on positive staining for SCA1-APC and negative staining for A-7 integrin-PE, or as MPs based on positive staining for A-7 integrin-PE and negative staining for SCA1-APC. Following *ex vivo* expansion, FAPs were able to differentiate into either fibroblasts or adipocytes (100 x magnification) and MPs differentiated into myotubes (50 x magnification).

4. FAPs differentiate into brown-like adipocytes¹

4.1. Expression of UCP1 and other brown-adipocyte markers in skeletal muscle is nearly negligible and does not respond to cold exposure

Although UCP1 expression has been reported in intermuscular and perimuscular adipose tissue near the quadriceps skeletal muscle [10] – and, controversially, even in myofibers of certain mouse strains [234, 235]–, it is not clear whether intramuscular adipocytes eventually interspersed within skeletal muscle (i.e., between myofibers) also express *Ucp1* and other genes highly expressed in brown adipocytes. Thus, the expression of these genes was first measured in non-stimulated skeletal muscle, carefully dissected to avoid contamination by surrounding adipose tissue. Since different skeletal muscle groups vary in fiber-type content, capillarization, innervation and energy metabolism, which could affect intramuscular adipocyte deposition and *Ucp1* expression, a wide range of skeletal muscle groups – quadriceps, TA, gastrocnemius, soleus and paraspinal – was analyzed; ingWAT was used as a positive control. Based on the differences in ectopic *Ucp1* expression reported between mouse strains [10], male and female C57Bl/6 and Sv/129 mice were included in this panel, as shown in Figure 4.1.

In contrast to ingWAT, most skeletal muscle groups analyzed displayed barely detectable mRNA levels of brown and general adipocyte markers; in many skeletal muscle samples, mRNA expression of *Ucp1* was under the qPCR detection limit. The quadriceps of Sv/129 female mice was the only skeletal muscle group in which mRNA expression of *Ucp1* could be consistently detected at levels closer to those of ingWAT. A possible explanation for this is the expression of *Ucp1* in the intermuscular and perimuscular adipose tissue near this muscle in Sv/129 mice, previously reported in the literature [10]. Since the quadriceps muscle group includes four muscles, careful dissection preventing contamination by

¹ Parts of this chapter were included in an oral presentation at the 2015 Annual Meeting of the Swiss Society of Endocrinology and Diabetology (Gorski T, Modica S, Wolfrum C and Krützfeldt J. Fibro/adipogenic progenitors from skeletal muscle differentiate into brown-like adipocytes); in a poster presentation at the ENDO2016: 98th Annual Meeting and Expo of the Endocrine Society (Gorski T, Modica S, Wolfrum C and Krützfeldt J. Fibro/Adipogenic Progenitors from Skeletal Muscle Differentiate into Thyroid-Hormone Responsive Brown-like Adipocytes); and in a manuscript submitted for publication in a peer-reviewed journal (Gorski T and Krützfeldt J. UCP1 expression in adipocytes derived from skeletal muscle fibro/adipogenic progenitors is under genetic and hormonal control).

FAPs differentiate into brown-like adipocytes

surrounding adipose tissue may not be sufficient to avoid inclusion of adipose tissue interspersed between the four muscles in the samples. The low expression levels of the adipocyte markers *Fabp4* and *Pparg2* in all skeletal muscle groups reflect the absence of significant amounts of intramuscular adipose tissue in healthy adult mice. The low and highly variable expression of *Ucp1* in skeletal muscle, not detectable by qPCR in many samples, seems to be of no physiological relevance.

It is well known that UCP1 expression increases in response to cold exposure in BAT [15, 16, 236, 237] and in certain WAT depots [15, 16, 237]. Furthermore, a previous study reported upregulation of *Ucp1* mRNA levels in trunk muscles (supraspinatus, intercostal and paraspinal), but not in the TA, of C57Bl/6 mice exposed to cold for one week [192]. We confirmed that the low *Ucp1* mRNA expression in the TA muscles of not only C57Bl/6, but also Sv/129 male mice was not upregulated in response to cold exposure for one week (Figure 4.2). Moreover, UCP1 protein was not detectable by immunoblotting in any of the analyzed muscle groups of male mice kept at room temperature or exposed to cold (~4°C) for one week, including the paraspinal muscle (Figure 4.3). In these experiments, we noticed that the anti-UCP1 antibody from Abcam detected a protein band of slightly lower molecular weight than UCP1. To ensure that this protein band was not specific, soleus samples from UCP1-knockout mice (kindly provided by M. Klingenspor, Technische Universität München) were tested using the same antibody. The protein band could still be detected in skeletal muscle of UCP1-knockout mice, confirming that UCP1 is not detectable by immunoblotting in skeletal muscle of male Sv/129 and C57Bl/6 mice (Figure 4.4). Together, these data show that non-stimulated skeletal muscle contains only negligible amounts of *Ucp1* mRNA and protein levels are not detectable by immunoblotting even following cold exposure.

4.2. Intramuscular adipocytes express UCP1 and respond to beta 3-adrenergic stimulus

The irrelevant mRNA levels of *Ucp1* and other adipocyte markers in skeletal muscle could simply reflect the absence of adipocytes in this tissue. Intramuscular adipocyte deposition in mice is rare compared to humans, but can be induced by intramuscular injection of glycerol [167] or cardiotoxin [166], for example. To induce intramuscular adipocyte deposition in mice, allowing for the characterization of brown-adipocyte markers in intramuscular adipocytes, the TA muscles of male and female Sv/129 mice, as well as male C57Bl/6 mice, were injected with glycerol and analysed after four weeks. Since cardiotoxin and glycerol-induced intramuscular adipogenesis are characterized by different gene expression patterns [166], which could affect *Ucp1* expression in skeletal muscle, a group

FAPs differentiate into brown-like adipocytes

of Sv/129 female mice was treated with cardiotoxin injections into the TA. The contralateral, non-injected TA muscles were used as a control. In line with previous reports [166], adipocyte formation was observed in the TA muscles of mice injected with both glycerol and cardiotoxin, but was more pronounced following glycerol injection (Figure 4.5A). Accordingly, the mRNA levels of the general adipocyte markers *Pparg2* and *Fabp4* were significantly increased in both models, but significantly higher in glycerol-injected muscles than in cardiotoxin-injected muscles (Figure 4.5C). In line with the microscopy results, FABP4 protein levels were increased in response to both models of intramuscular adipogenesis (Figure 4.5B). The brown adipocyte markers *Ucp1* and *Cidea*, however, were significantly increased only in response to the glycerol injections in Sv/129 mice (Figure 4.5C). These results suggest that intramuscular *Ucp1* expression depends on adipocyte formation and on genetic background.

The increase in *Ucp1* expression in response to cold exposure via the stimulation of beta-adrenergic receptors is a remarkable feature of brown [235, 238] and beige [15, 235] adipocytes. Ectopic *Ucp1* expression in ingWAT, for example, increases by up to nearly five-fold following treatment with the B3-adrenergic agonist CL316 [10, 234]. To test the response of intramuscular *Ucp1* levels to beta 3-adrenergic stimulation *in vivo*, Sv/129 female mice were treated with CL316 for five consecutive days four weeks after injection of glycerol into the TA muscles. Notably, intramuscular mRNA levels of *Ucp1* and *Cidea* were markedly higher in CL316-treated compared to control mice, similarly to ingWAT, and independent from adipocyte differentiation as measured by intramuscular *Pparg2* expression (Figure 4.6A). This gene expression response was observed specifically in the glycerol-injected, but not in the control skeletal muscles, reinforcing the skeletal muscle adipocytes as the source of general and brown adipocyte markers expression (Figure 4.6B). Importantly, we could confirm the expression and CL316-induced upregulation of UCP1 at the protein level, together with the multilocular morphology of several intramuscular adipocytes, by immunohistochemistry (Figure 4.6C). Thus, similarly to previous results on brown and beige adipocytes, intramuscular UCP1 expression can be regulated through a classical brown-adipocyte pathway.

4.3. FAPs, but not MPs, differentiate into UCP1-expressing adipocytes

At least two stem cell populations have been proposed as the precursors for intramuscular UCP1-expressing adipocytes: satellite cells/MPs [192] and FAPs [110]. To define the potential of MPs and FAPs to differentiate into UCP1⁺ adipocytes, these two populations were isolated from skeletal muscle and FACS-sorted based on expression of A-7 integrin or SCA1, respectively.

FAPs differentiate into brown-like adipocytes

First, we addressed the potential of MPs to form adipocytes, expanding them as myoblasts under cell culture conditions. Confluent myoblasts were treated with myogenic or brown adipogenic medium for eight days. As expected, myoblasts treated with myogenic medium differentiated into MYHC-expressing myotubes (Figure 4.7A). Remarkably, myoblasts were still able to form MYHC⁺ myotubes and did not differentiate into adipocytes even when treated with brown adipogenic medium (Figure 4.7A). In contrast, SVF cells isolated from ingWAT, used as a control, readily differentiated into FABP4⁺ adipocytes upon treatment with the same medium (Figure 4.7A). Adipocyte formation was also not observed when myoblasts from Sv/129 and C57Bl/6 mice were treated with brown adipogenic medium further supplemented with different compounds reported to promote brown adipogenic differentiation – namely BMP7, FGF21, ANP, isoproterenol and ACTR2B inhibitor (Figure 4.7B).

Since polyclonal cell culture conditions could be disadvantageous for adipogenic subclones, we next sorted single MPs directly into 96-well plates and, after expansion, treated the monoclonal colonies for 10 days with brown adipogenic medium. Similarly to the initial results, adipogenesis was again not observed and myotube formation occurred to different extents, confirming the commitment of MPs to the myogenic fate (Figure 4.8). Importantly, more than 30% of monoclonal colonies derived from single-sorted FAPs contained adipocytes following the same treatment (Figure 4.8). These results demonstrate that the lack of adipocyte formation in monoclonal colonies of MPs cannot simply be explained by the cell culture conditions. Together, these data suggest that MPs are strictly committed to the myogenic lineage and do not have the potential to differentiate into adipocytes even under adipogenic conditions.

In contrast to MPs, FAPs readily differentiated into adipocytes in response to the brown adipogenic treatment, as assessed by light microscopy (Figure 4.9A) and FABP4 immunoblotting (Figure 4.9B). Importantly, FAPs also showed a marked upregulation of UCP1 expression during differentiation, which could be already detected at day 6 and increased until the 10th day of differentiation (Figure 4.9B). To stimulate further increases in UCP1 expression in differentiated FAPs, cell cultures were also treated with the adenylate cyclase activator forskolin (10 μ M) for 4 h before collection for protein analysis (Figure 4.9B, indicated as “+F”). As previously reported in 3T3-L1 adipocytes [239], in which forskolin induces secretion of FABP4, treatment with forskolin decreased FABP4 protein levels in differentiated FAPs. However, we did not observe consistent increases in UCP1 protein levels following treatment with forskolin in different cell cultures.

FAPs differentiate into brown-like adipocytes

When treated with the same brown adipogenic medium as FAPs for up to 13 days, differentiated 3T3-L1 cells did not express detectable levels of UCP1 (Figure 10). This indicates that FAPs possess the necessary machinery to differentiate into brown-like adipocytes, which might not be common to all adipocyte lineages.

Besides *Ucp1*, other genes highly expressed in brown adipocytes were also significantly upregulated in FAPs in response to the brown adipogenic treatment, including *Pgc1a*, *Cidea*, *Prdm16*, *Elovl3* and *Eva1* (Figure 4.11B). Therefore, the experiments show that FAPs, but not MPs, are a likely source for UCP1-expressing intramuscular adipocytes.

4.4. UCP1 levels in FAP-derived adipocytes depend on mouse strain

Previous studies have shown that adipocyte precursors residing in WAT and skeletal muscle from C57Bl/6 and Sv/129 mice differ in their potential to express UCP1 after brown adipogenic differentiation [110, 229]. In line with these findings, we observed higher levels of UCP1 in skeletal muscle FAPs isolated from Sv/129 mice than in those isolated from C57Bl/6 mice after brown adipogenic differentiation (Figures 4.9B and 4.11A). This suggests that, similar to the intrinsic differences reported for WAT SVF cells from C57Bl/6 and Sv/129 mice [229], FAPs isolated from skeletal muscle of different mouse strains retain intrinsic differences that affect UCP1 expression under culture conditions.

4.5. UCP1 expression in FAP-derived adipocytes responds to the thyroid hormone T3

The thyroid hormone T3 plays an important role in the activation of brown adipocytes and thyroidectomized rats exhibit impaired BAT activation and thermoregulation in response to cold [240, 241]. *In vitro*, it has been shown that T3 upregulates UCP1 levels in fetal rat brown adipocytes [242] and human multipotent adipose-derived stem cells (hMADS) under adipogenic conditions [243]. Similarly, we observed higher UCP1 expression levels in FAPs differentiated with medium supplemented with T3 (+T3) compared to cells differentiated with brown adipogenic medium lacking addition of T3 (-T3), despite no increases in the expression of the adipocyte marker FABP4 in response to addition of T3 to the medium (Figure 4.11A). Thus, the increased UCP1 expression was not a by-product of enhanced differentiation. *Ucp1* was also upregulated in response to T3 at the mRNA level together with the inducer of mitochondrial biogenesis *Pgc1a* (Figure 4.11B). Upregulation of the transcriptional coregulator of *Pgc1a*, *Prdm16*, during differentiation also depended on addition of T3 to the medium, while other brown adipocyte markers remained unchanged (*Eva1*, *Cidea*) or showed a slightly lower expression (*Elovl3*) in response to T3 supplementation in the differentiation medium (Figure 4.11B). mRNA levels of the general

FAPs differentiate into brown-like adipocytes

adipocyte markers *Pparg2* and *Fabp4* did not differ between cells differentiated with medium +T3 and medium -T3, indicating no effect of T3 supplementation on adipocyte differentiation (Figure 4.11B). To further define the mechanisms for higher UCP1 expression in cells differentiated with medium +T3, differentiated FAPs were stained for lipid droplets (LD540 dye) and for nuclei (DAPI), and posteriorly immunostained for UCP1; UCP1⁺ cells and differentiated adipocytes were then quantified using an automated microscope imaging system. We observed a slightly higher percentage of UCP1⁺ adipocytes in cultures differentiated in medium +T3 compared to cells differentiated with medium -T3 (Figure 4.12B); while the percentage of differentiated cells was similar in both conditions. This supports the notion that the increased UCP1 expression in response to T3 is independent of effects on cell differentiation, with the underlying mechanisms including both a slightly higher percentage of cells expressing UCP1 and higher UCP1 expression levels per cell.

4.6. UCP1 expression in FAP-derived adipocytes is sex-dependent

UCP1 protein and mRNA expression in adipocytes can be sex-dependent as previously shown for rat BAT [244] and in differentiated stem cells from human perirenal adipose tissue [56], respectively. We also observed a tendency for higher *Ucp1* expression levels in glycerol-injected TA muscles from female compared to male Sv/129 mice *in vivo* (Figure 4.5C). Therefore, we compared the potential of skeletal muscle FAPs from male and female mice to express UCP1 following brown adipogenic differentiation *in vitro*. Interestingly, FAPs isolated from Sv/129 female mice reached higher UCP1 levels after differentiation compared to FAPs isolated from Sv/129 male mice (Figure 4.13A and B). The expression levels of the adipocyte marker FABP4 were not different between groups, indicating that the differences in UCP1 levels were not dependent on differentiation (Figure 4.13B). The difference in UCP1 expression after differentiation between FAPs isolated from male and female mice was also observed in C57Bl/6 mice (data not shown).

Together, these results demonstrate that FAPs isolated from skeletal muscle of not only different mouse strains, but also different sexes retain intrinsic differences which influence UCP1 expression following differentiation.

4.7. Discussion

This chapter provides a comprehensive analysis of UCP1 expression in skeletal muscle based on two *in vivo* models of intramuscular adipogenesis and the prospective isolation of two different progenitor cell populations residing in skeletal muscle. It shows that *Ucp1* expression increases in skeletal muscle following glycerol-induced intramuscular

FAPs differentiate into brown-like adipocytes

adipogenesis in an obesity-resistant mouse strain and that intramuscular UCP1 expression is responsive to beta 3-adrenergic stimulation. Furthermore, it was observed that skeletal muscle FAPs, but not MPs, are able to differentiate into UCP1⁺ adipocytes *ex vivo*, with UCP1 levels being affected by both intrinsic factors (genetic background and sex) and hormonal signaling (T3 treatment).

The low and highly variable mRNA levels and the undetectable protein expression of UCP1 observed in our skeletal muscle samples – carefully dissected to prevent contamination by adipose tissue (with exception of the quadriceps muscle, in which adipose tissue can be interspersed between the four adjacent muscles that are excised together) – suggest that, if at all expressed, intramuscular UCP1 has a negligible impact on skeletal muscle and whole-body metabolism of C57Bl/6 and Sv/129 mice. This is in line with previous studies reporting UCP1 to be expressed exclusively in BAT and in pockets of cells within WAT [245, 246]. Indeed, Almind et al. [10] observed that UCP1 was only detected by immunoblotting in skeletal muscle when the adipose tissue surrounding the samples was not removed before analysis; furthermore, immunohistochemistry for UCP1 showed that the protein was expressed exclusively in adipocytes surrounding skeletal muscle, but not within myofibers of Sv/129 and C57Bl/6 mice. Only few studies have suggested that UCP1 can be also detected in skeletal muscle mitochondria (from the diaphragm and triceps surae muscles) from rats [247] and obese KKAY [235] and ICR mice [234], as well as in uterine longitudinal smooth muscle from mice [248]. The study by Nibbelink et al. [248] reporting UCP1 expression in uterine smooth muscle cells was later challenged by Rousset et al. [246], who showed that the antibody against UCP1 used in the former study cross-reacted with a mitochondrial protein of slightly lower molecular weight than UCP1, equivocally regarded as a specific protein band. The UCP1 antibody used in the present study (Abcam, code ab10983) also detected a protein band very close to the specific UCP1 signal (Figure 4.3), but immunoblotting of skeletal muscle samples from UCP1-knockout mice proved it to be non-specific (Figure 4.4). Since Garcia-Cazarin et al. [247] did not include BAT as a positive control in the immunoblotting figures showing UCP1 expression in rat skeletal muscle mitochondria, the hypothesis that UCP1 signal reported by these authors is a mere product of cross-reaction with a protein of similar molecular weight cannot be rejected. Using immune-electron microscopy and immunohistochemistry, one research group showed that mitochondria surrounding the myofibrils become positive for UCP1 following a two-weeks treatment with daily CL316 injections in obese ICR [234] and KKAY mice, but not in C57Bl/6 mice [235]. However, we could not find confirmation of these data by other research groups in the literature.

FAPs differentiate into brown-like adipocytes

The intramuscular injections of either cardiotoxin or glycerol are widely established protocols to induce muscle regeneration and the formation of intramuscular adipocytes [164, 166, 167, 228]. Both models involve the proliferation of satellite cells and FAPs followed by satellite cell fusion to damaged myofibers and intramuscular adipogenesis. Similarly to the present results, intramuscular adipogenesis was previously reported to be stronger and more persistent following intramuscular glycerol injections [166]. Additionally, the present results show that these two skeletal muscle injury models also differ regarding the induction of brown-adipocyte markers: significant increases in the mRNA levels of *Ucp1* and *Cidea* were only observed in response to glycerol injections. Thus, intramuscular glycerol injection provides a suitable model to study intramuscular formation of adipocytes expressing *Ucp1* in obesity-resistant mice.

The difference in *Ucp1* mRNA levels following intramuscular adipogenesis between C57Bl/6 and Sv/129 mice recapitulates the differences in ectopic UCP1 expression reported in subcutaneous and intermuscular/perimuscular WAT between these mouse strains [10], pointing out to the possibility that factors influencing UCP1 regulation in these WAT depots could also regulate UCP1 expression in intramuscular adipocytes. This speculation is supported by the increased mRNA levels of *Ucp1* observed in glycerol-injected muscles following treatment with CL316. In addition to *Ucp1* expression during intramuscular adipogenesis, genetic background also seems to affect intramuscular adipogenesis per se, since the mRNA levels of general adipocyte markers were lower in glycerol-injected muscles of C57Bl/6 compared to Sv/129 mice. This is in line with a recent report on the differences in fatty infiltration in response to intramuscular glycerol injection between these two mouse strains in which the authors described 129S1/SvImJ mice as more susceptible to fatty infiltration than C57Bl/6 mice [226]. The similar *in vitro* differentiation levels of FAPs isolated from these two strains in the present study indicates that extrinsic factors, including the ECM composition and other skeletal muscle cells, could depend on genetic background and influence FAP adipogenic differentiation *in vivo*.

In humans, intramuscular adipose tissue is generally associated with impaired myofiber function, both from a mechanical [220] and a metabolic point of view [214, 249]. Although this adipose tissue depot is not yet fully characterized, studies analysing cardiotoxin- and glycerol-induced adipogenesis in murine skeletal muscle describe the intramuscular adipocytes as white rather than brown [166, 167, 228]. In contrast, the increase in *Ucp1* expression in skeletal muscle observed during glycerol-induced adipogenesis in Sv/129 mice suggests that intramuscular adipocyte precursors can also adopt a brown-like phenotype in an obesity-resistant mouse strain. The further increase in intramuscular *Ucp1* and *Cidea* expression in response to beta 3-adrenergic stimulation resembles the browning

FAPs differentiate into brown-like adipocytes

process of WAT depots and points to intramuscular adipocytes as a possible and accessible target for therapies promoting the brown adipocyte-like phenotype. It remains to be shown whether brown-like intramuscular adipocytes could improve skeletal muscle metabolism and insulin sensitivity in humans affected by skeletal muscle fatty infiltration.

The identity of the skeletal muscle progenitor population able to differentiate into brown-like adipocytes is currently under debate. Previous studies claimed that MPs are able to differentiate into white [186, 193, 250] or brown-like adipocytes [100, 192] under certain conditions. However, most of these studies relied on single muscle fiber isolations [186, 193, 250] or on preplating of collagenase-digested tissue [186] to obtain the progenitor populations, which could potentially result in the isolation of non-myogenic, interstitial cells surrounding myofibers. Indeed, Starkey et al. [194] reported that most adipogenic clones that derived from single myofibers could be removed by adding two myofiber-washes to the isolation protocol before plating the cells. Moreover, studies that observed adipogenic differentiation of MPs identified the MPs by labeling for *Pax7* or the myogenic regulatory factor *Myf5*. However, it has recently been shown that *Myf5* expression can be more widely distributed than previously appreciated and also labels white adipocyte precursors [117]. Likewise, a subpopulation of cells from extraocular muscle which descending from *Myf5*⁺ precursors expresses SCA1 and is adipogenic [251]. In this study, we relied on a prospective isolation strategy to obtain MPs from skeletal muscle by FACS based on the absence of CD31, CD45 and SCA1, and the presence of A-7 integrin which results in highly pure myogenic cultures [232]. Analyzing both polyclonal and monoclonal cell cultures, we could not identify any MP subpopulation with adipogenic potential. These results further support previous work showing that MPs are committed to the myogenic fate [164, 194, 195, 200, 211] and that FAPs constitute the adipocyte precursor population residing in murine [110, 164, 165, 195, 203] and human [197, 198, 200, 252] adult skeletal muscle. Although one cannot reject the hypothesis that a small subpopulation of satellite cells could form brown adipocytes – as shown by Yin et al. [192] relying on the expression of *Pax7* exclusively in muscle satellite cells – the present results suggest that FAPs are a more likely source for intramuscular adipocytes and bear the necessary machinery to express UCP1.

Notably, the present experiments show that FAPs differentiate into brown-like adipocytes more readily than previously appreciated, i.e. without any pre-differentiation exposure to adipocyte browning agents such as BMP7 [253]. The differences in UCP1 expression following FAP differentiation between this study and previous studies could be explained at least partially by differences in cell culture conditions. Firstly, *Ucp1* expression in response to BMP7 in FAPs differentiated in the absence of a PPARG agonist has been

FAPs differentiate into brown-like adipocytes

reported to be highly dependent on the serum batch used [253]. This could explain the low *Ucp1* expression in protocols that do not include the PPARG agonist rosiglitazone in the differentiation medium [110, 195, 228]. Moreover, we show that the thyroid hormone T3 is critical for UCP1 expression in differentiated FAPs and this hormone was not always included in the differentiation medium [164, 195]. Lastly, studies using cells that have been passaged or frozen-thawed prior to differentiation report low *Ucp1* levels in FAP-derived adipocytes [252]. Similarly, a decrease in differentiation and UCP1 expression following cell passaging has been previously reported for CD34⁺ cells isolated from human fetal skeletal muscle [230]. We have also noticed a decrease in the proliferation and differentiation capacity of FAPs after trypsinization and re-seeding, and therefore used only freshly isolated cells expanded for a maximum of 10 days for the experiments.

The upregulation of UCP1 mRNA and protein levels in response to T3 treatment in differentiated FAPs underscores the importance of T3 for UCP1 expression in adipocytes, already observed in studies with rat BAT cells [242] and hMADS [243]. Importantly, in the present study, this effect was dependent on a direct effect of T3 on UCP1 levels rather than on FAP differentiation, as indicated by similar mRNA and protein levels of adipocyte markers and automated microscopy analysis of differentiation. We speculate that the increase in UCP1 gene and protein expression in FAPs differentiated in medium supplemented with T3 could result at least partially from the stimulation of TREs in the *Ucp1* gene promoter [80], increased stability of *Ucp1* mRNA [242] and/or enhanced mitochondriogenesis (extensively reviewed in [254]). In addition to intramuscular adipocytes being a target for T3-induced thermogenesis, our results also point to FAPs as a possible tool to further dissect the effects of T3 on thermogenesis and UCP1 expression.

Two intrinsic factors affecting UCP1 levels in differentiated FAPs could be identified in the present study: genetic background and sex. The differences in UCP1 expression after differentiation between FAPs isolated from C57Bl/6 and Sv/129 mice are in line with previous results obtained in adipogenic progenitors isolated from skeletal muscle [110], subcutaneous WAT and epididymal WAT [110, 229] of these strains and highlight the importance of genetic background on the ectopic expression of UCP1 [10, 19, 255]. Regarding differences in brown and brown-like adipocytes between sexes, evidence is scarcer and mostly derives from human studies. For example, previous studies have reported that functionally active BAT [54] and UCP1⁺ adipocytes in perirenal adipose tissue [56] are more frequently found in women than in men. Additionally, perirenal mesenchymal stem cells isolated from women express higher mRNA (but not protein) levels of *UCP1* after differentiation than those isolated from men [56]. Further analysis of the differences between FAPs isolated from male and female mice or from mice of different genetic

FAPs differentiate into brown-like adipocytes

backgrounds could identify factors leading to enhanced UCP1 expression in intramuscular adipose tissue and potentially also in WAT depots. Finally, the observation that intrinsic differences affect the potential of skeletal muscle FAPs to express UCP1 following differentiation could have implications for the development of interventions to promote a brown phenotype in intramuscular adipocytes in specific populations.

In summary, the present results show that intramuscular *Ucp1* expression can be triggered during skeletal muscle fatty infiltration in an obesity-resistant mouse strain and that FAPs, the adipocyte precursors residing in skeletal muscle, are able to differentiate into brown-like adipocytes. Therefore, FAPs could be a target for therapies promoting a brown phenotype in intramuscular adipocytes, with potential to improve the microenvironment of skeletal muscle affected by fatty infiltration.

FAPs differentiate into brown-like adipocytes

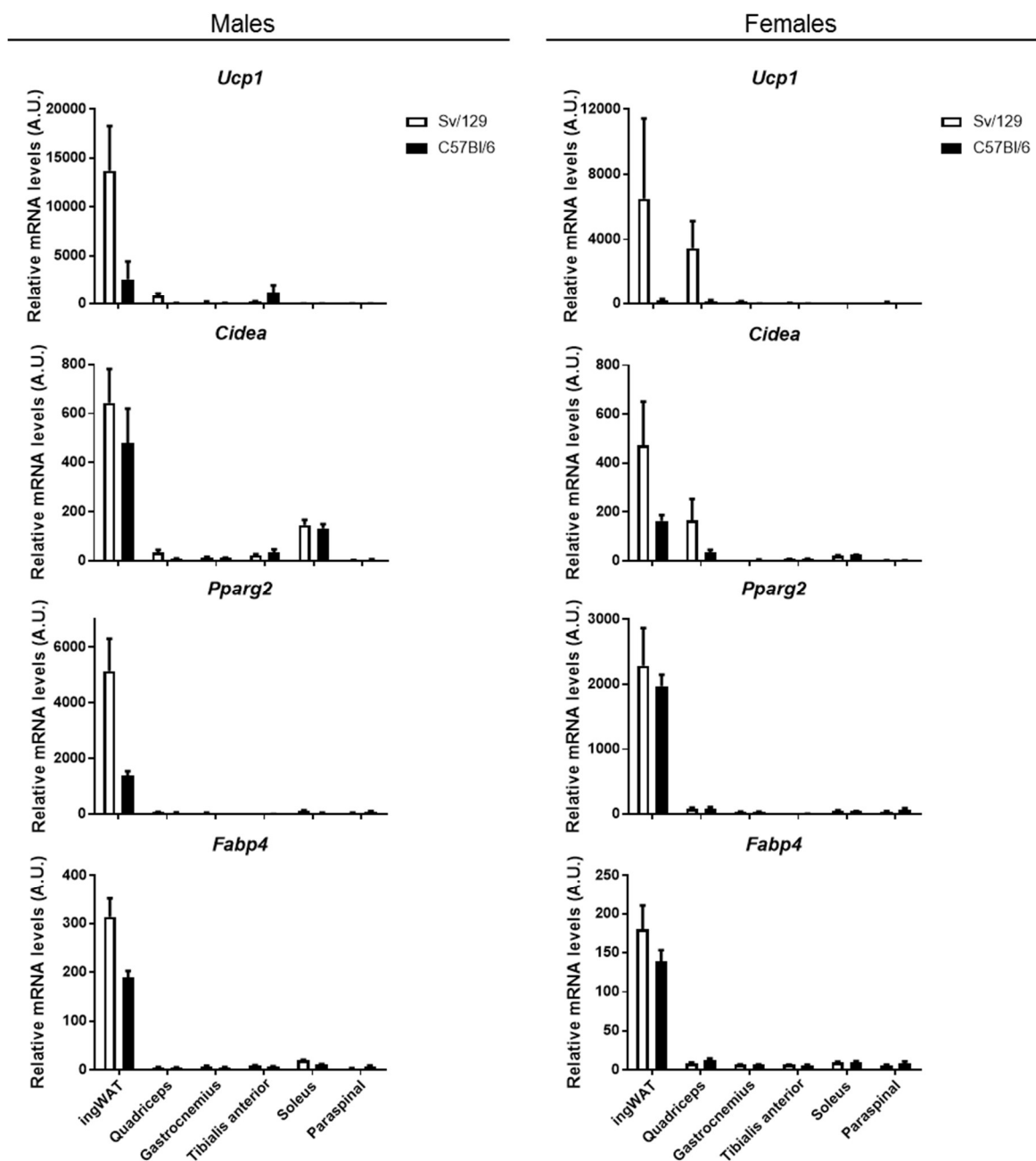


Figure 4.1: mRNA levels of *Ucp1* and other genes highly expressed in brown adipocytes are nearly negligible in different skeletal muscle groups of Sv/129 and C57Bl/6 male and female mice maintained at room temperature. Results are shown as mean and S.E.M. of gene expression levels normalized to 18S rRNA expression levels in arbitrary units (A.U.), n = 5 mice per group.

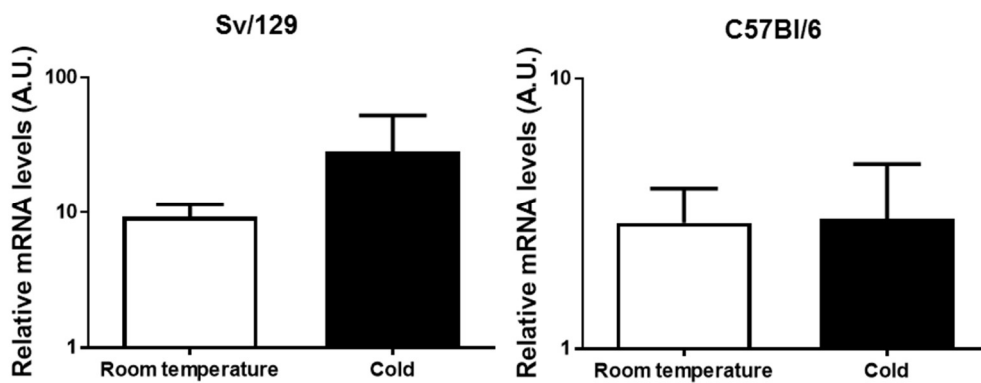


Figure 4.2.: mRNA levels of *Ucp1* in the TA of C57Bl/6 and Sv/129 mice kept at room temperature or exposed to cold (~4°C) for one week are similar. Results are shown as mean and S.E.M. of *Ucp1* expression levels normalized to 18S rRNA expression levels in A.U., n = 5 Sv/129 and 7 C57Bl/6 male mice kept at room temperature, 5 Sv/129 and 6 C57Bl/6 male mice exposed to cold for one week. Log-transformed data were compared using unpaired Student's t tests. For *Ucp1* expression in C57Bl/6 mice, half of the lowest detectable value (1.879) was added to all measurements to allow for logarithmic transformation despite null values (undetermined C_t values).

FAPs differentiate into brown-like adipocytes

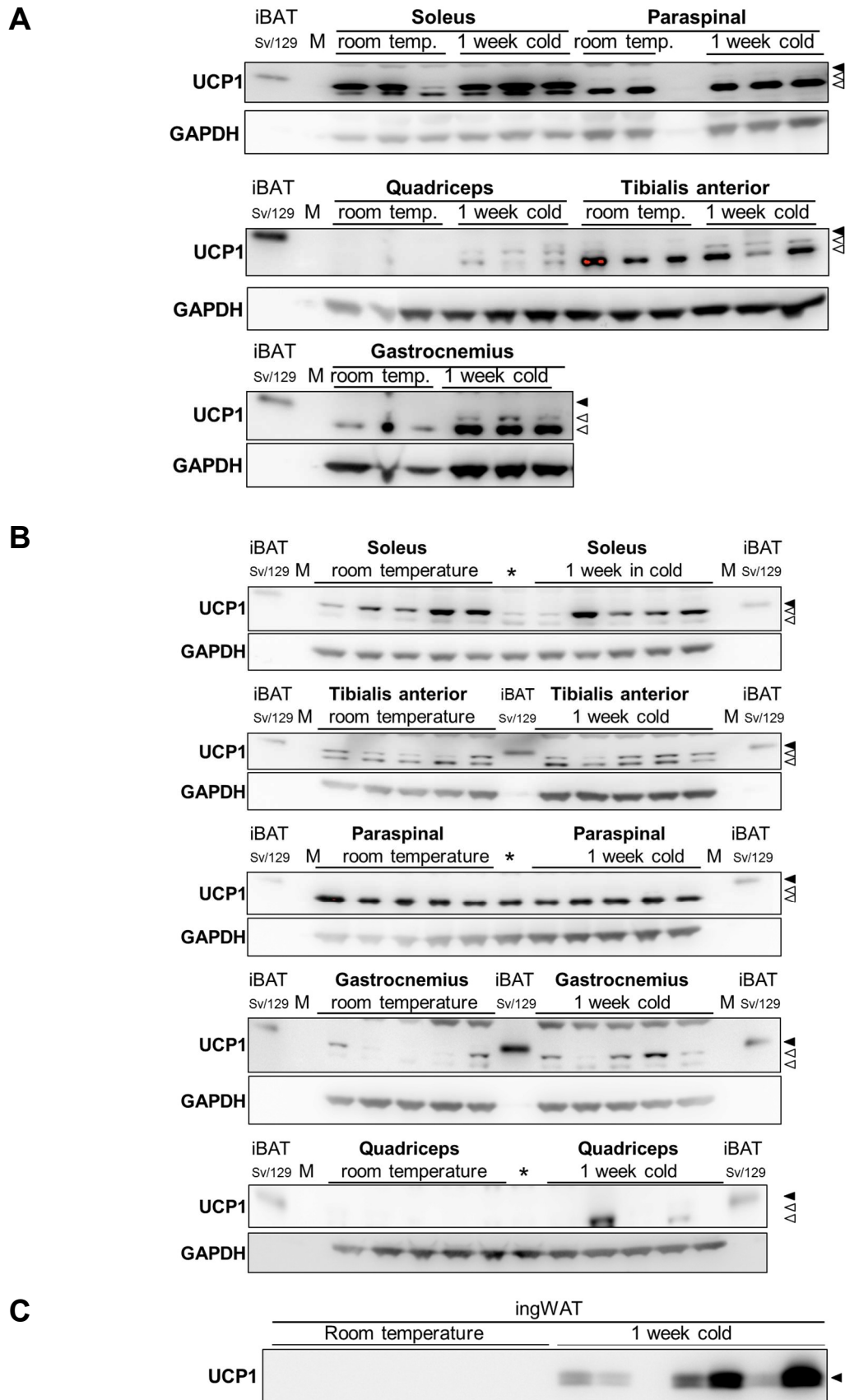


Figure 4.3: UCP1 is not detectable in different skeletal muscle groups of mice kept at room temperature or exposed to cold (~4°C) for one week. UCP1 immunoblotting

FAPs differentiate into brown-like adipocytes

for the soleus, paraspinal, gastrocnemius, quadriceps and TA of male C57Bl/6 (A, n = 3 mice at per group) and Sv/129 (B, n = 5 mice per group) mice kept at room temperature or exposed to cold (~4°C) for one week. iBAT from a male Sv/129 mouse (iBAT Sv/129) was used as a positive control and GAPDH was used as a loading control. In iBAT Sv/129 lanes, only 1/50 of the protein amount loaded in other lanes was loaded, to avoid overloading. (C) Immunoblotting for UCP1 in ingWAT samples from C57Bl/6 mice kept at room temperature or exposed to cold (~4°C) for one week, showing upregulation of UCP1 protein expression in most mice in response to cold exposure. In A, B and C, black arrowheads indicate the specific UCP1 protein band, while white arrowheads indicate the two non-specific bands slightly below the specific band. In immunoblots of skeletal muscle from Sv/129 mice (B), iBAT Sv/129 or a repeated skeletal muscle protein sample (indicated as *) was loaded in the central lane of the gel to discard the shift in position of the specific band between central and lateral lanes as a cause for the difference in height seen between the specific band in iBAT and the highest non-specific band in skeletal muscle samples.

FAPs differentiate into brown-like adipocytes

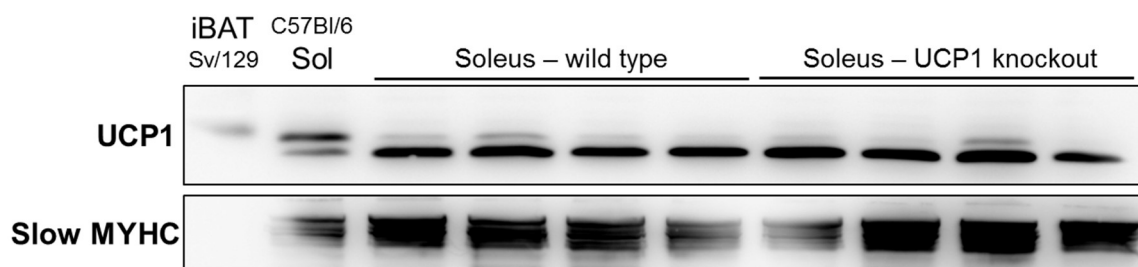


Figure 4.4: The protein band detected by the UCP1 antibody (Abcam) close to UCP1 is not specific. Immunoblotting for UCP1 in soleus skeletal muscle samples from UCP1 knockout and wild type male mice (n = 4 mice per group). Brown adipose tissue from a male Sv/129 mouse (iBAT Sv/129) was used as a positive control for UCP1 expression and a soleus sample from a C57Bl/6 mouse (indicated as C57Bl/6 Sol) was used as a positive control for the non-specific band close to UCP1. In the iBAT Sv/129 lane, only 1/50 of the protein amount loaded in the other lanes was loaded, to prevent overloading. The black arrowhead indicates the specific UCP1 protein band and the white arrowheads indicate the two non-specific bands slightly below the specific band.

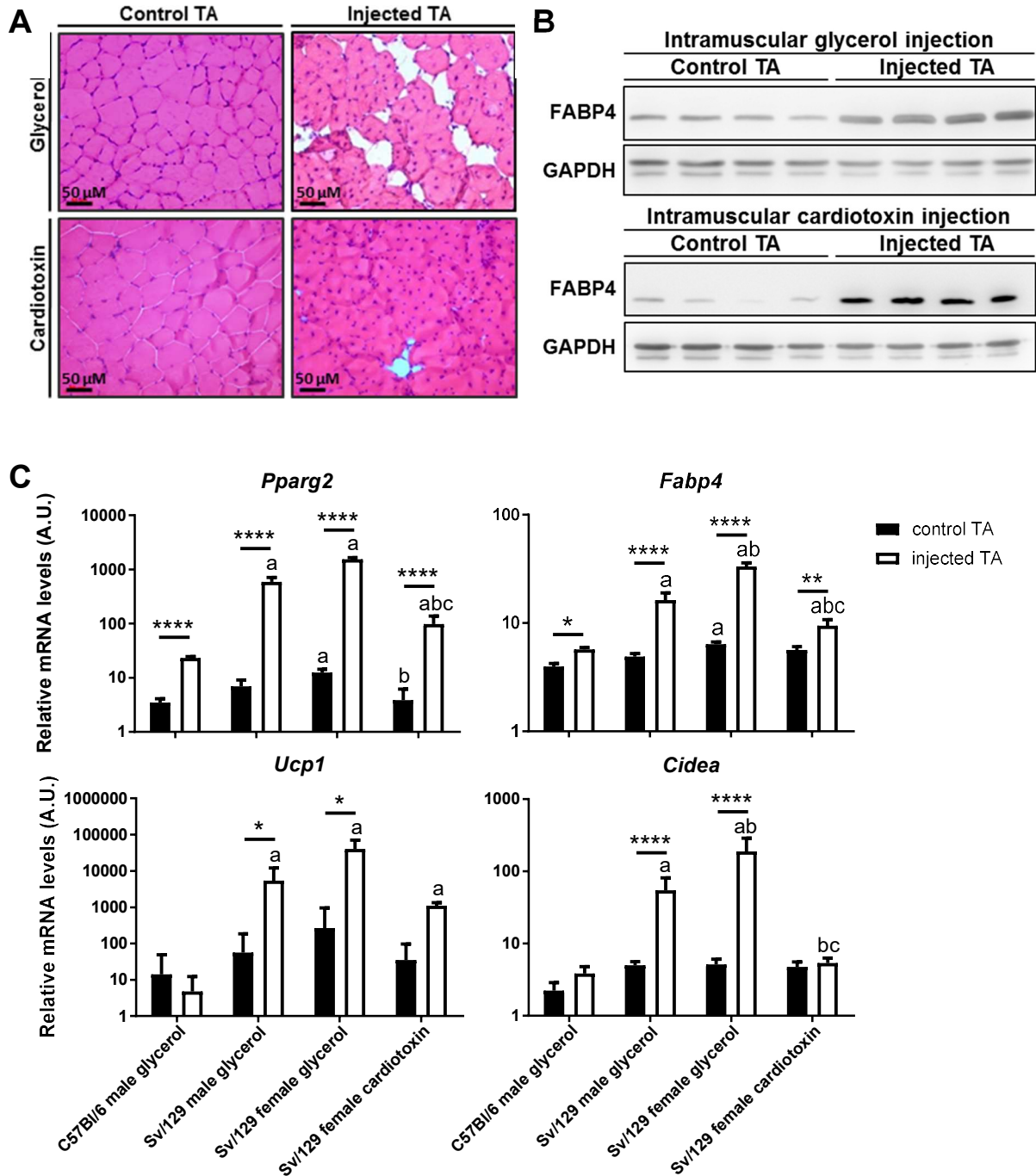


Figure 4.5: Glycerol, but not cardiotoxin, induces intramuscular adipogenesis and *Ucp1* expression in skeletal muscle. (A) Representative images of H&E staining of TA cross sections four weeks after intramuscular injection of cardiotoxin or glycerol. (B) Immunoblotting for FABP4 in control and glycerol- or cardiotoxin-injected TAs four weeks after intramuscular injection of glycerol or cardiotoxin; GAPDH was used as a loading control, n = 4 female Sv/129 mice per experiment. (C) mRNA levels of general (*Pparg2* and *Fabp4*) and brown (*Ucp1* and *Cidea*) adipocyte markers in TA muscles four weeks after intramuscular glycerol injection in male C57Bl/6 mice and male and female Sv/129 mice,

FAPs differentiate into brown-like adipocytes

as well as four weeks after intramuscular cardiotoxin injection in Sv/129 female mice, n = 5 mice at 15 weeks of age per group. * $P < 0.05$, ** $P < 0.01$, **** $P < 0.0001$, a: significantly different than C57Bl/6 male glycerol, b: significantly different from Sv/129 male glycerol, c: significantly different than Sv/129 female glycerol, repeated measures two-way ANOVA. Results are shown as mean and S.E.M. of mRNA levels normalized to 18S rRNA levels, in A.U..

FAPs differentiate into brown-like adipocytes

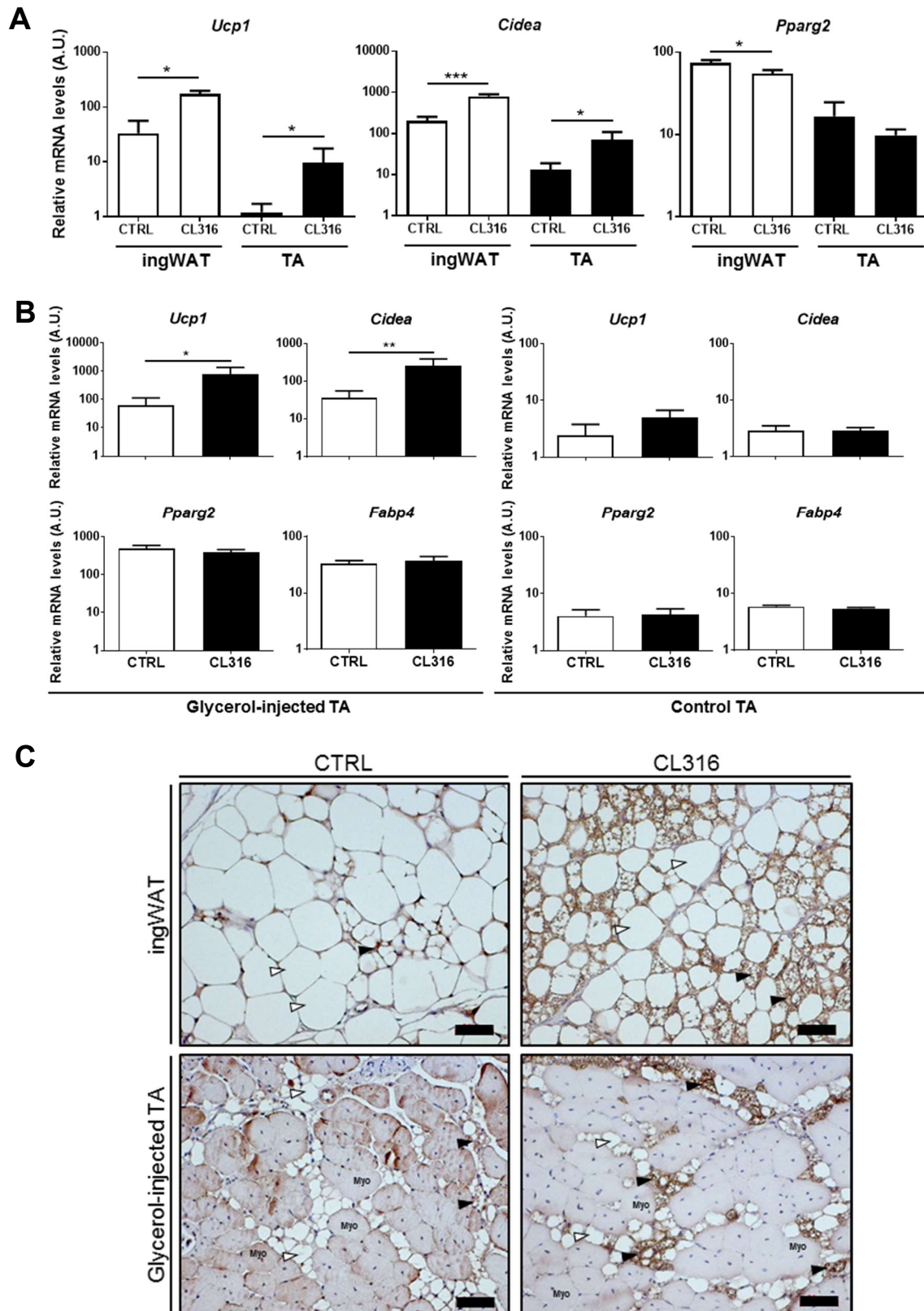


Figure 4.6: Intramuscular Ucp1 expression responds to a beta 3-adrenergic stimulus. Four weeks after intramuscular glycerol injection in the TA muscles, mice were treated with

FAPs differentiate into brown-like adipocytes

daily intraperitoneal injections of CL316 for five days and TA muscles were excised for quantification of mRNA levels of brown and general adipocyte marker. (A) Expression of *Ucp1*, *Cidea* and *Pparg2* in ingWAT, used as a control, and glycerol-injected TAs of control (CTRL) and CL316-treated (CL316) animals, n = 5 Sv/129 female mice at 17-weeks of age per group. (B) Expression levels of *Ucp1*, *Cidea*, *Pparg2* and *Fabp4* in the glycerol-injected and in the control TA muscles from CTRL and CL316-treated mice, n = 5 Sv/129 female mice at 16-weeks of age per group. In A and B, results are shown as mean and S.E.M. of mRNA levels normalized to 18S rRNA levels, in A.U.; * p < 0.05, ** p < 0.01 *** p < 0.001, unpaired Student's t test. (C) Representative images of UCP1 immunostaining on paraffin sections of ingWAT and glycerol-injected TA from CTRL and CL316-treated Sv/129 females at 17-weeks of age. White arrowheads indicate white, UCP1-negative adipocytes; black arrowheads indicate brown-like, UCP1-positive adipocytes; Myo indicates myofibers. Scale bar, 50 um.

FAPs differentiate into brown-like adipocytes

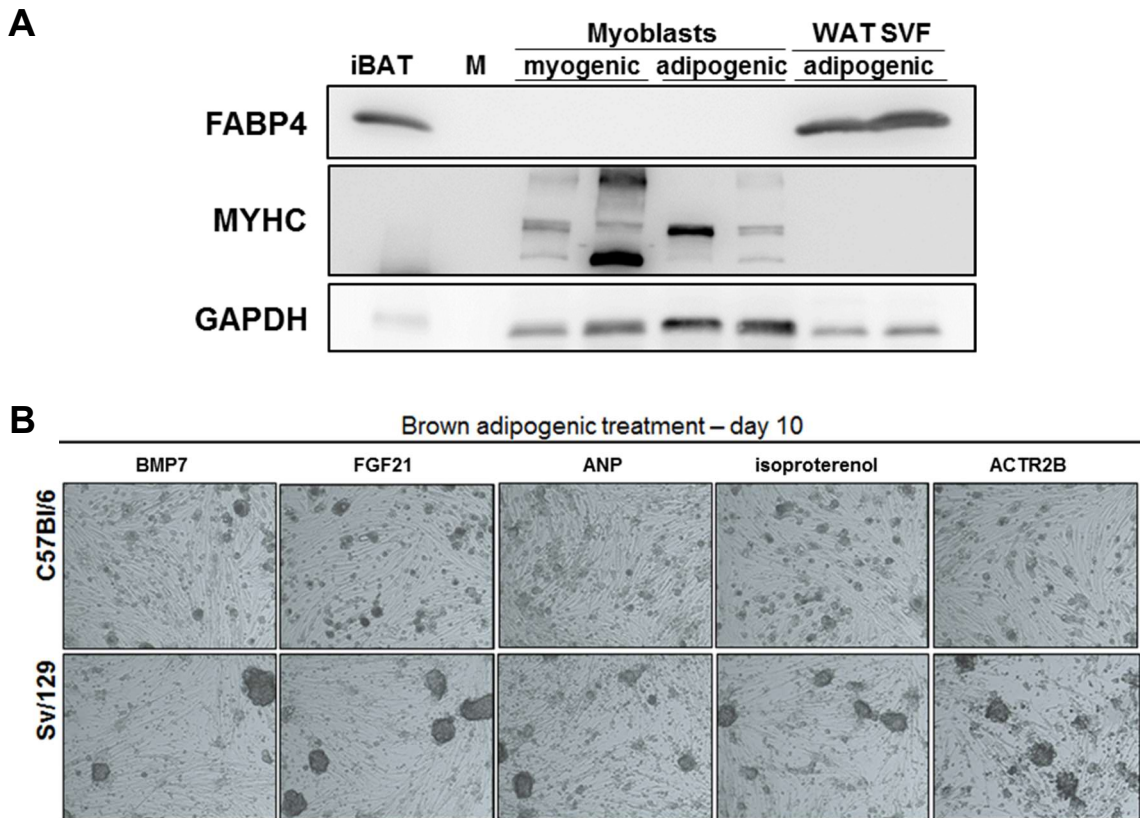


Figure 4.7: Myoblasts are committed to the myogenic fate under treatment with brown adipogenic medium. (A) Expression of the adipocyte marker FABP4, different isoforms of the myotube marker MYHC and GAPDH (loading control) in primary mouse myoblasts following eight days of differentiation in myogenic or brown adipogenic medium. Cells from the ingWAT SVF differentiated for eight days with adipogenic medium were used as a control, n = 2 cultures from individual mice per condition. iBAT was used as a positive control. (B) Representative light microscopy images of myoblasts isolated from C57Bl/6 and Sv/129 mice following 10 days of differentiation in brown adipogenic medium supplemented with the indicated compounds, 50x magnification.

FAPs differentiate into brown-like adipocytes

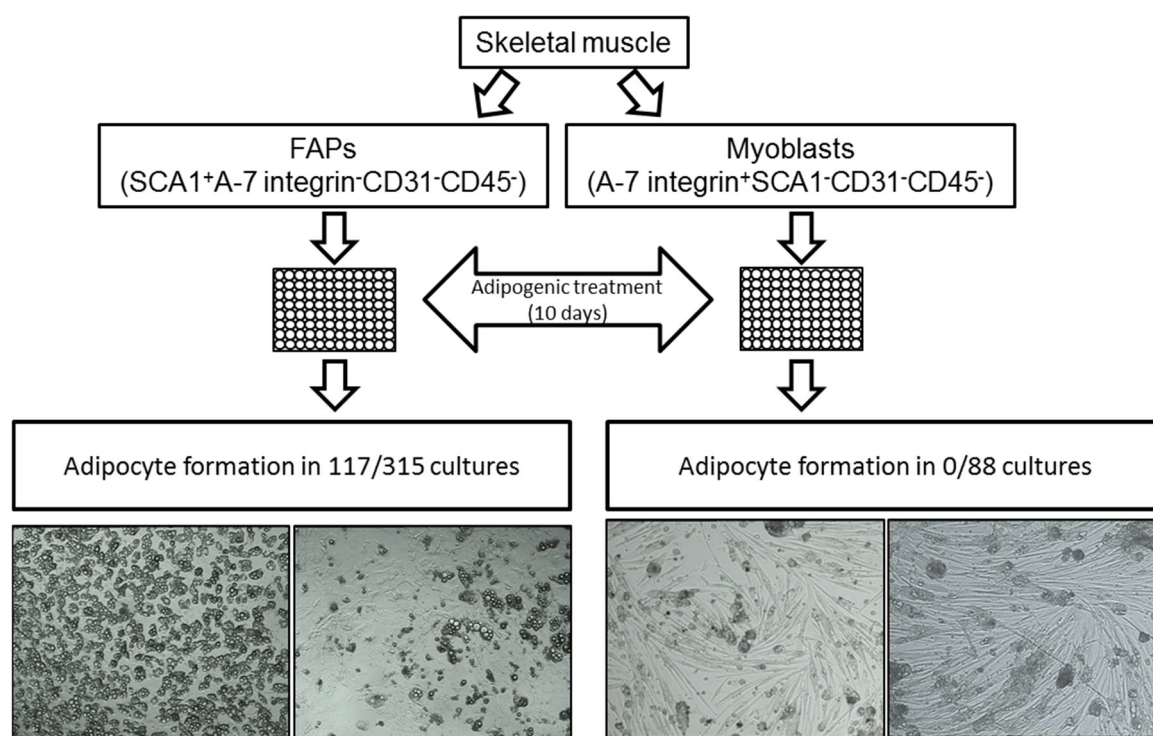


Figure 4.8: Monoclonal cultures of FAPs, but not myoblasts, have the potential to differentiate into adipocytes. FAPs and myoblasts were isolated from skeletal muscle (hindlimbs and paraspinal) and single cells were FACS-sorted directly into 96-well plates. Nearly confluent cells were treated for 10 days with brown adipogenic medium. Adipocyte formation was assessed through microscopy in 315 FAP and 88 myoblast monoclonal cultures. Shown are representative light microscopy images of monoclonal colonies of FAPs (x100 magnification) and myoblasts (x50 magnification).

FAPs differentiate into brown-like adipocytes

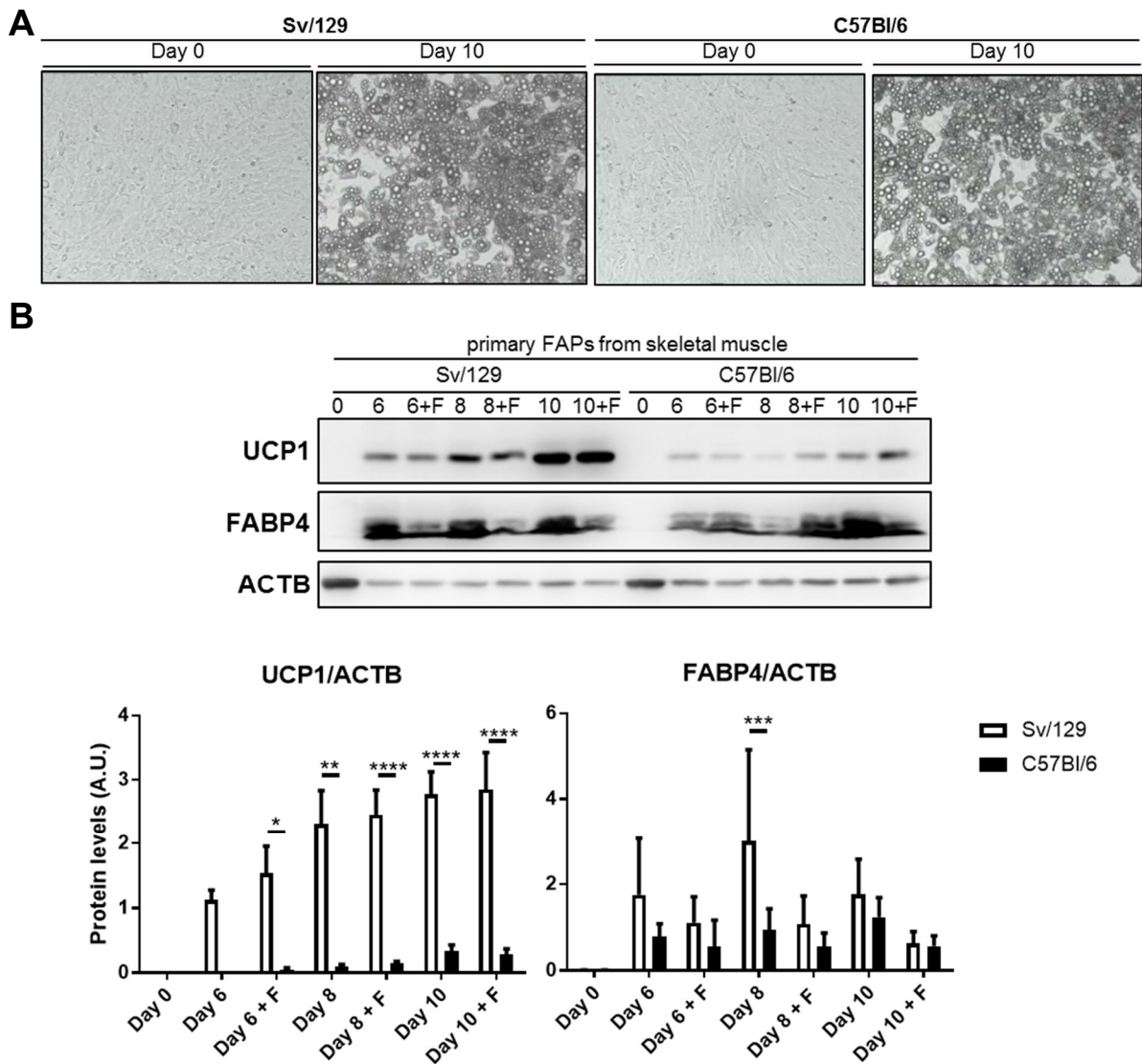


Figure 4.9: FAPs readily differentiate into UCP1-expressing adipocytes. (A) Representative images of FAPs isolated from Sv/129 and C57Bl/6 mice at day 0 and at day 10 of brown adipogenic differentiation (x100 magnification). (B) Immunoblotting for UCP1 and FABP4 in FAPs at days 0, 6, 8 and 10 of brown adipogenic differentiation. +F indicates stimulation with 10 μ M forskolin for 4 h before cell lysis. ACTB was used as a loading control. The graphs show mean and S.E.M. of UCP1 and FABP4 protein levels normalized to ACTB levels in FAPs through the brown adipogenic differentiation protocol quantified by densitometry, $n = 6$ Sv/129 and 6 C57Bl/6 female mice. * $P < 0.05$, ** $P < 0.01$, *** $P < 0.001$, **** $P < 0.0001$, repeated-measures two-way ANOVA.

FAPs differentiate into brown-like adipocytes

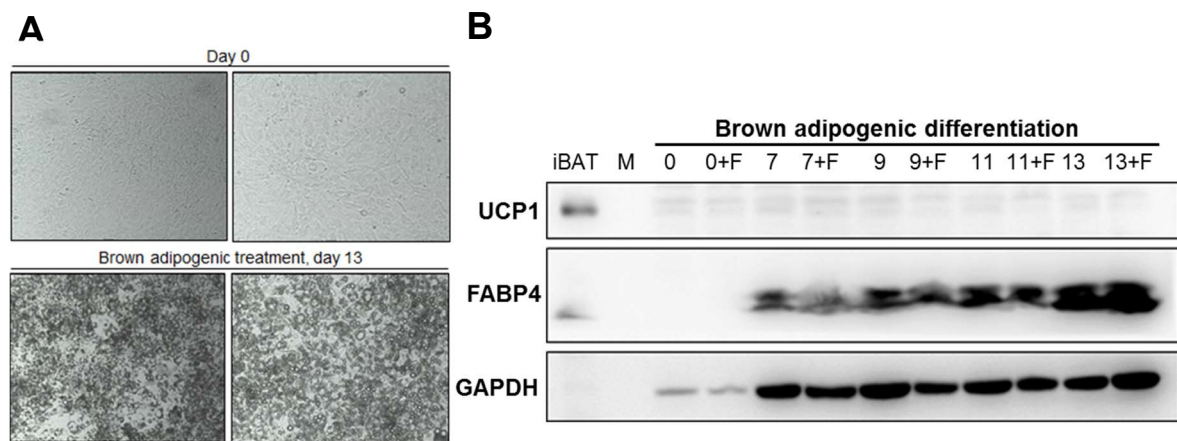


Figure 4.10: 3T3-L1 cells do not differentiate into UCP1-expressing adipocytes in response to treatment with brown adipogenic medium. (A) Representative images of 3T3-L1 cultures at day 0 and at day 13 of adipogenic differentiation. (B) Immunoblotting for UCP1 and FABP4 in 3T3-L1 cells at days 0, 7, 9, 11 and 13 of treatment with brown adipogenic medium. +F indicates stimulation with 10 μ M forskolin for 4 h before cell lysis. GAPDH was used as a loading control and iBAT from an Sv/129 male mouse was used as a positive control for UCP1 expression (2.5-fold less protein was loaded in the iBAT lane).

FAPs differentiate into brown-like adipocytes

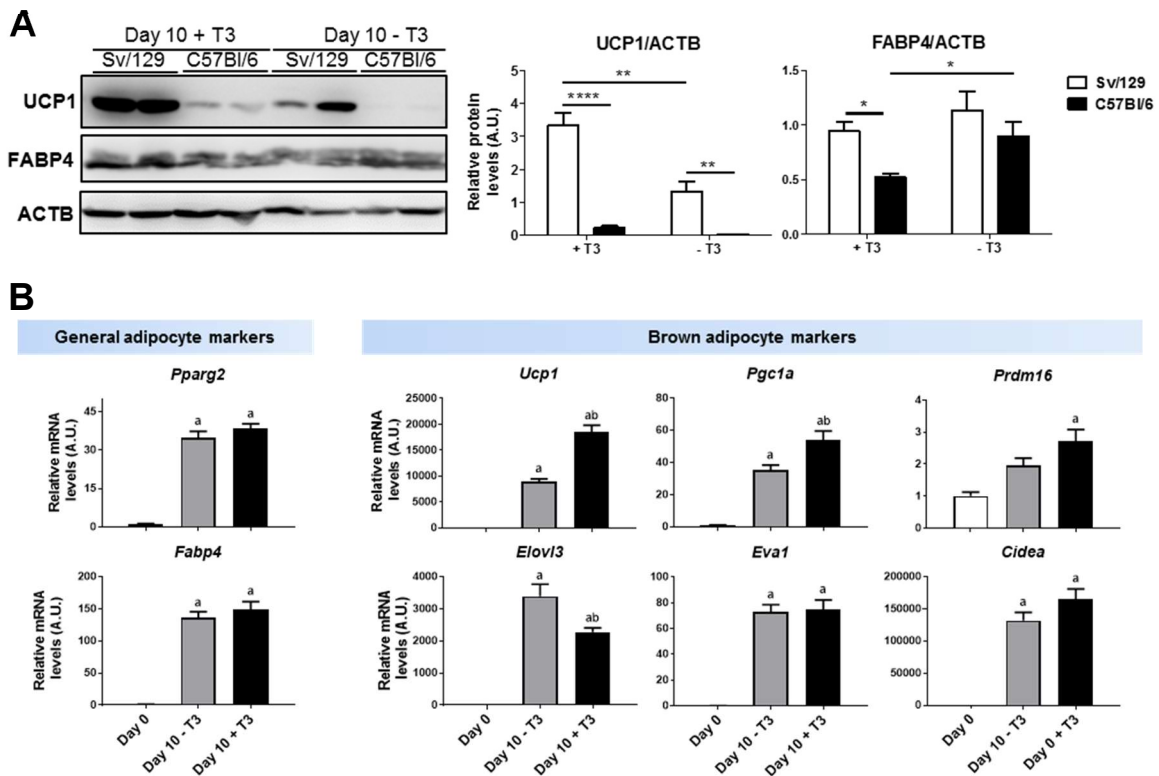


Figure 4.11: FAPs differentiate into brown-like adipocytes in a strain- and T3-dependent manner. FAPs were isolated from skeletal muscle (hindlimbs) of Sv/129 and C57Bl/6 mice and, upon confluence, differentiated for 10 days with brown adipogenic medium supplemented (+T3) or not (-T3) with T3. (A) UCP1, FABP4 and ACTB (loading control) protein expression in differentiated FAPs. Results are shown as mean and S.E.M. of relative protein expression levels normalized to ACTB relative levels in A.U., $n = 6$ mice; * $P < 0.05$, ** $P < 0.01$, **** $P < 0.0001$, repeated measures two-way ANOVA. (B) mRNA levels of general and brown adipocyte markers in FAPs at day 0 and at day 10 of differentiation in medium +T3 or medium -T3. Results are shown as mean and S.E.M. of gene expression levels normalized to 18S rRNA levels, in A.U., $n = 6$ Sv/129 female mice; a: significantly different from undifferentiated cells, b: significantly different from cells differentiated with medium -T3, repeated measures one-way ANOVA.

FAPs differentiate into brown-like adipocytes

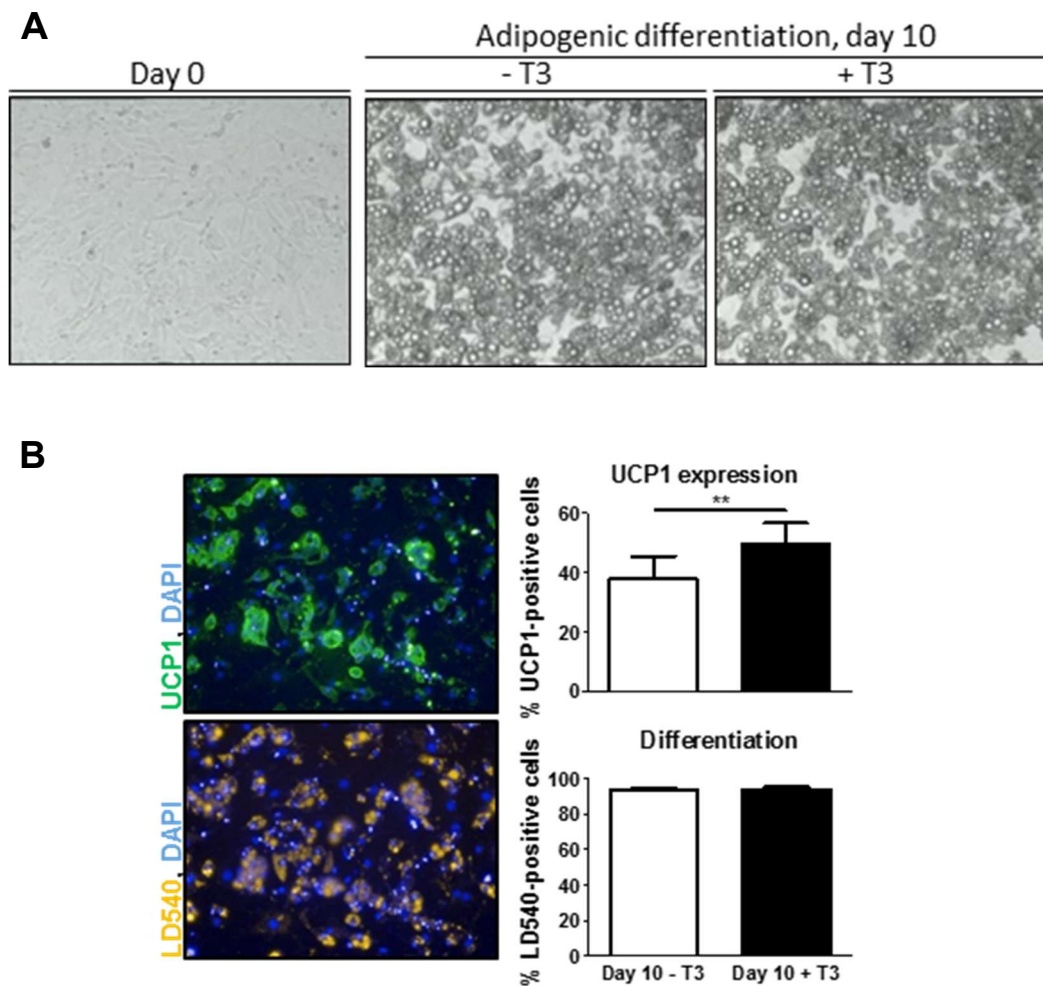


Figure 4.12.: T3 affects UCP1 expression in differentiated FAPs independent of differentiation. (A) Representative light microscopy images (100x magnification) of FAPs at day 0 and at day 10 of differentiation with medium +T3 or -T3. (B) FAPs at day 10 of differentiation (+T3 or -T3) were stained for nuclei (DAPI) and lipid droplets (LD540) and immunostained for UCP1. Automated image acquisition was followed by automated quantification of cells positive for UCP1 and of differentiated cells (i.e., cells containing lipid droplets). Results are shown as mean and S.E.M. of percentage of cells positive for UCP1 or percentage of differentiated cells; n = 10 Sv129 female mice, ** P < 0.01, paired Student's t test.

FAPs differentiate into brown-like adipocytes

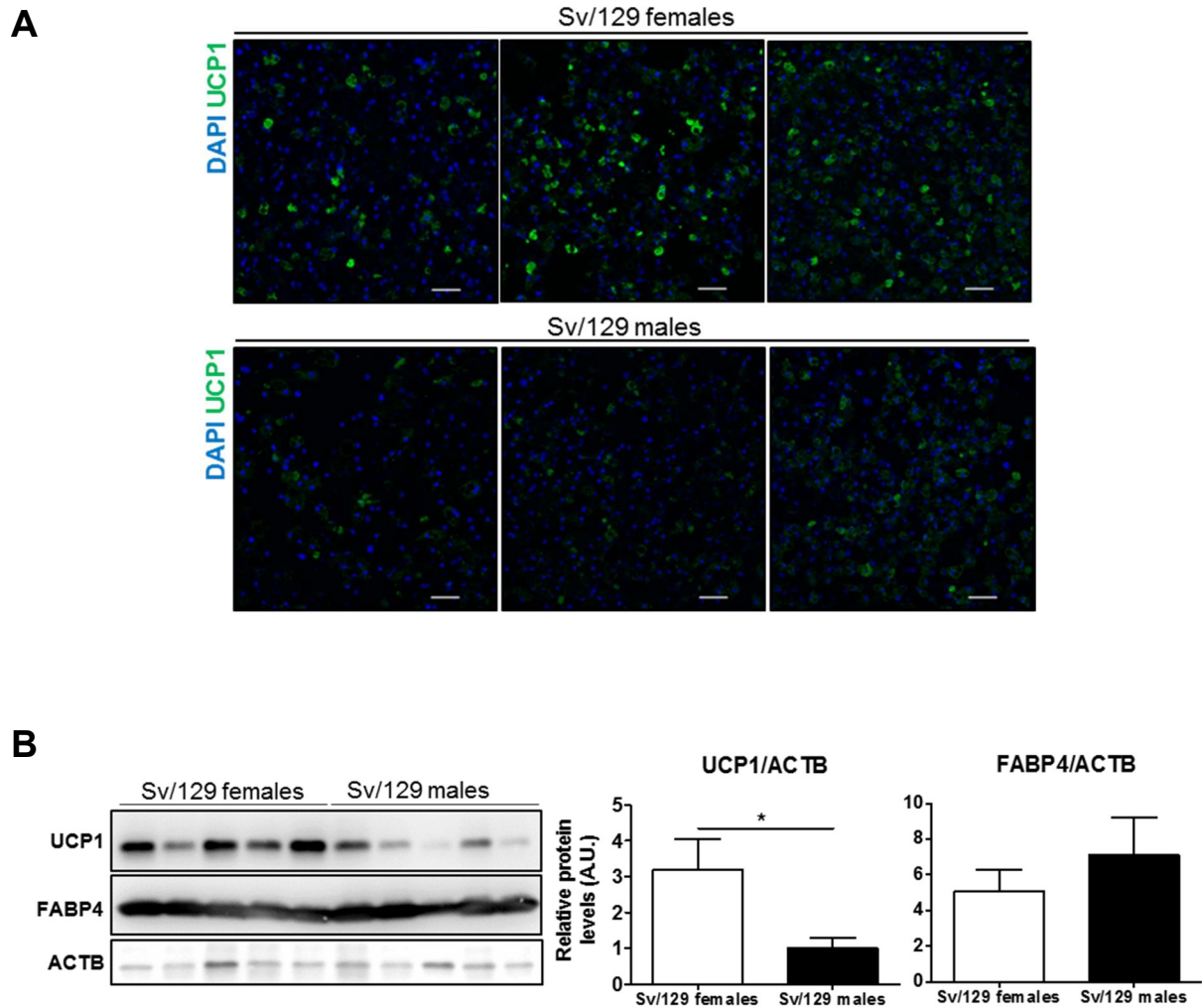


Figure 4.13: UCP1 expression in differentiated FAPs is sex-dependent. (A) FAPs isolated from skeletal muscle (hindlimbs) of male and female Sv129 mice were differentiated for 10 days, stained for nuclei (DAPI) and immunostained for UCP1, $n = 3$ cell cultures from individual Sv/129 mice per group. Scale bar = 50 μM . (B) UCP1, FABP4 and ACTB (loading control) protein expression in FAPs isolated from Sv/129 male and female mice at day 10 of differentiation. Results are shown as mean and S.E.M. of relative protein expression levels normalized to ACTB relative levels in A.U., $n = 5$ cell cultures from individual mice per group. $*P < 0.05$, unpaired Student's t test.

FAPs differentiate into brown-like adipocytes

5. Intramuscular Ucp1 expression is not influenced by high-fat diet feeding or exercise-training status in an obesity-resistant mouse strain

5.1. High-fat diet feeding mildly increases body mass and blood glucose levels of Sv/129 female mice

In rodents, high-fat diet feeding has been reported to differentially regulate UCP1 expression. BAT displays upregulation of UCP1 expression [101, 256], while in subcutaneous WAT UCP1 levels are reportedly decreased or unaffected (reviewed in [257]). Research on the effects of a high-fat diet on intramuscular adipose tissue is limited, but the pool of CD34⁺ brown-adipocyte progenitors in the skeletal muscle of obese humans seems to be diminished compared to their normal-weight counterparts [258] and skeletal muscle FAPs isolated from obese subjects acquire a rather white-adipocyte phenotype upon differentiation [252]. To investigate the effects of high-fat diet feeding and its metabolic consequences on intramuscular adipocytes, Sv/129 female mice were fed a high-fat diet for 12-weeks.

As shown in Figure 5.1, there were no differences in body mass between the high-fat diet-fed (HFD) and the control-diet-fed (CTRL) group at the beginning of the experiment (week zero), while at week 12 HFD mice had a slightly, but significantly higher body mass compared to the CTRL group. Blood glucose levels measured at random-fed state and after a 6-h fast were higher in HFD than in CTRL mice, although insulin levels in both states did not differ between groups. Consequently, HOMA-IR was slightly higher in HFD than in CTRL mice. These differences suggest that at experimental week 12, mice were at an early stage of metabolic disturbance, but not obese or diabetic.

5.2. FAPs isolated from Sv/129 female mice fed a high-fat diet maintain their potential to differentiate into brown-like adipocytes *in vitro*

To determine the effects of a high-fat diet on the potential of FAPs to differentiate into brown-like adipocytes, we isolated cells from skeletal muscle of the HFD and CTRL groups at week 12 and, after cell expansion and the brown adipogenic treatment, compared their UCP1 expression. As shown by FABP4 immunoblotting, adipogenic differentiation was not impaired in the FAPs from HFD mice compared to those from CTRL mice (Figure 5.2). Moreover, UCP1 expression following differentiation was also similar between skeletal

Effects of exercise and high-fat diet on FAPs

muscle FAPs isolated from both groups, suggesting that the intrinsic factors determining UCP1 expression in these cells remain unaltered following a high-fat diet period, at least while the metabolic disturbance caused by the diet is still mild.

5.3. High-fat diet feeding does not influence intramuscular *Ucp1* expression following glycerol injection in Sv/129 female mice

High-fat diet can impair skeletal muscle satellite cell function during muscle regeneration [190], but it remains unclear whether it also affects skeletal muscle FAPs function during regeneration or FAPs potential to differentiate into *Ucp1*-expressing adipocytes. To investigate the effects of high-fat diet feeding on the *in vivo* adipogenic differentiation of FAPs, HFD and CTRL mice received an intramuscular injection of glycerol into the TA to induce intramuscular fatty infiltration at experimental week 12. Four weeks later, no significant differences in body mass and random-fed blood glucose levels were observed between groups (Figure 5.3A), with blood glucose levels after a 6-h fast slightly higher in the HFD group (Figure 5.3B). The ratio between the mass of the injected and the non-injected TA muscles was similar in both groups, indicating that high-fat diet feeding did not impair skeletal muscle regeneration following glycerol injection (Figure 5.3B).

In ingWAT, used as an experimental control, HFD and CTRL mice displayed similar mRNA levels of the brown-adipocyte markers (*Ucp1* and *Cidea*) and the general adipocyte markers *Cebpa* and *Fabp4*. Leptin and *Pparg2* mRNA levels, on the other hand, were higher in HFD compared to CTRL mice. Regarding mitochondria-related genes, there were no differences between groups in *Pgc1a* expression, and *Cox7a1* mRNA expression was higher in the HFD than in the CTRL group (Figure 5.4).

In both HFD and CTRL mice, the glycerol-injected TA displayed higher mRNA levels of the general adipocyte markers *Pparg2*, *Cebpa*, *Fabp4* and leptin, as well as of the brown adipocyte markers *Ucp1* and *Cidea*, compared to the contralateral, non-injected TA, as expected (Figure 5.5). The mRNA expression of the brown adipocyte markers *Ucp1* and *Cidea* did not differ between the injected TA of HFD and CTRL mice. The general adipocyte markers *Pparg2*, *Cebpa* and *Fabp4* were expressed at similar levels in CTRL and HFD mice, suggesting that the amount of intramuscular adipocyte deposition was similar in the two groups. Expression of leptin, however, was higher in the injected TA of HFD compared to CTRL mice. Regarding the mitochondria-related genes, *Pgc1a* mRNA levels in the injected TA did not differ between HFD and CTRL mice, while the expression of *Cox7a1* was higher in both injected and control TAs of HFD compared to CTRL mice, indicating a response of the entire muscle rather than a specific response of intramuscular adipose

tissue to a high-fat diet. Thus, the effect of high-fat diet feeding on the expression of the analysed genes in the injected, adipocyte-infiltrated TAs mostly resembled the effects observed in the ingWAT of the same animals, with leptin expression consistently increased in both tissues.

5.4. A four-week exercise training intervention causes only minor changes in gene expression of ingWAT in Sv/129 male mice

Besides high-fat diet, aerobic/endurance exercise training is also reported to differentially regulate UCP1 expression in BAT and WAT. In BAT, conflicting studies report either a downregulation [101] or no differences [259, 260] in UCP1 expression in response to different exercise training protocols. In subcutaneous WAT, on the other hand, UCP1 expression is consistently reported to increase in response to exercise training [101-104, 261]. It remains unclear whether exercise training could also have an impact on UCP1 expression in intramuscular adipocytes. To investigate this hypothesis, male Sv129 mice underwent a four-week treadmill-running training period, composed by five weekly sessions of 45 min. As shown in Figure 5.6, body mass of the exercise-trained (EXE) and the non-trained control (CTRL) group were similar at baseline (week zero). Following the four-week training period, body mass remained similar between groups, as did blood glucose levels at random-fed state and after a 6-h fast. In ingWAT, used as a control, *Pparg2* and *Fabp4* mRNA levels were slightly increased in EXE compared to CTRL mice, but the expression of *Ucp1*, other general and brown adipocyte markers, and mitochondria-related genes remained similar between groups (Figure 5.7A). Protein levels of UCP1 in ingWAT were highly variable within each experimental group and upregulation was not observed in response to exercise training (Figure 5.7B). In the TA, mRNA levels of all analysed genes were similar in the EXE and CTRL groups (Figure 5.8).

5.5. FAPs from exercise-trained and from untrained Sv/129 male mice express similar levels of UCP1 following *in vitro* differentiation

Exercise training has been reported to impair the *ex vivo* adipogenic differentiation of WAT SVF cells [262], but also to improve *ex vivo* differentiation of BAT preadipocytes from mice fed a high-fat diet [263]. To assess the effect of endurance exercise training on the potential of FAPs to differentiate into brown-like adipocytes *in vitro*, FAPs were isolated from skeletal muscle of EXE and CTRL mice between one and three days after the last treadmill-running session. Following *ex vivo* expansion and treatment with brown adipogenic medium for 10 days, there were no differences in UCP1 and FABP4 expression between cells isolated from EXE and CTRL mice (Figure 5.9). These data suggest that, at least in male Sv/129

Effects of exercise and high-fat diet on FAPs

mice, the intrinsic capacity of FAPs to differentiate into brown-like adipocytes is not altered by exercise training, or that any eventual *in vivo* changes are not retained following *ex vivo* expansion.

5.6. Intramuscular expression of *Ucp1* after glycerol-induced adipogenesis is similar in exercise-trained and untrained Sv/129 male mice

To investigate the effects of exercise-training state on FAP differentiation *in vivo*, CTRL and EXE mice received intramuscular injections of glycerol one day after the last exercise training session. Skeletal muscles and adipose tissue were excised four weeks later (week eight). At week eight, body mass and blood glucose levels at random-fed state did not differ between the two groups. Blood glucose levels following a 6-h fast, in contrast, were slightly lower in EXE mice than in their CTRL counterparts. As observed in response to high-fat diet feeding, no differences in the ratio between the mass of the glycerol-injected TA and of the contralateral, non-injected TA were observed between EXE and CTRL mice, indicating that skeletal muscle regeneration was not affected by exercise-training status (Figure 5.10).

Intriguingly, exercise-training effects on the expression of brown adipocyte markers and mitochondria-related genes in ingWAT were more pronounced following the four-week detraining period, with EXE mice displaying higher mRNA levels of *Ucp1*, *Cidea* and *Cox7a1* than their CTRL counterparts. *Pparg2* mRNA expression remained higher in EXE mice compared to CTRL mice (Figure 5.11).

As shown in Figure 5.12, the intramuscular expression of general and brown adipocyte markers, as well as *Pgc1a*, reached similar levels in EXE and CTRL mice four weeks following intramuscular glycerol injection. *Cox7a1* expression levels were slightly higher not only in the glycerol-injected TA of the EXE group compared to the CTRL group, but also in the non-injected TA, likely reflecting an effect of exercise training on the entire muscle, and not specifically on the intramuscular adipocytes. Leptin levels were significantly lower in the control TAs of EXE compared to CTRL mice, although very low in both groups. We speculate that this could reflect changes in a small number of intramuscular adipocytes that could eventually be interspersed between muscle fibers of the non-injected TAs.

5.7. Discussion

Lifestyle factors such as high-fat diet feeding and physical-exercise training are known to differentially affect the expression of UCP1 in BAT and subcutaneous WAT depots [101, 257], but the regulation of UCP1 in intramuscular adipose tissue is much less understood.

Effects of exercise and high-fat diet on FAPs

Here, we show that, in an obesity-resistant mouse strain, intramuscular adipocytes respond to high-fat diet feeding with increased leptin mRNA expression and unchanged *Ucp1* mRNA expression, similarly to ingWAT. Moreover, while exercise-trained mice displayed an increased expression of brown-adipocyte genes in ingWAT following a four-week detraining period, training status did not influence *Ucp1* expression in intramuscular adipocytes differentiated during detraining.

Previous studies have shown that high-fat diet feeding differentially regulates UCP1 expression in BAT and in subcutaneous WAT [101, 257]. The similar expression of *Ucp1* and other brown adipocyte markers in fatty-infiltrated skeletal muscle of mice fed a high-fat or a control diet indicates that intramuscular adipocytes respond to high-fat diet feeding similarly to white adipocytes rather than brown adipocytes. This is further supported by the increased mRNA expression of leptin in fatty-infiltrated skeletal muscle of HFD animals, which resembles the upregulation of this gene in ingWAT, also observed in previous studies with other mouse strains and rats [264-266]. We speculate that the increased *Cox7a1* mRNA expression in ingWAT and skeletal muscle (glycerol-injected and non-injected) reflects an adaptation of the oxidative machinery to the increased circulating levels of FFAs resulting from high-fat diet feeding, rather than the browning of adipocytes in these tissues. In fact, high-fat diet feeding has been shown to increase mitochondrial content in the skeletal muscle [267-269] and *Cox7a1* expression in epididymal WAT [270] of rodents.

In line with the *in vivo* *Ucp1* mRNA levels in the TA following intramuscular glycerol injection, UCP1 protein levels did not differ between *in vitro*-differentiated FAPs isolated from the HFD and the CTRL groups. This result suggests that, at least at an early stage of metabolic disturbance, the potential of FAPs to differentiate into UCP1-expressing adipocytes is still preserved. Additionally, the similar FABP4 protein expression in differentiated FAPs from the two groups suggests that the differentiation capacity of FAPs was also not affected by diet and the consequent metabolic adaptations. SVF cells isolated from abdominal subcutaneous WAT of obese humans display lower levels of UCP1 following *in vitro* differentiation compared to those isolated from lean subjects [124] and FAPs isolated from skeletal muscle of obese humans exhibit a white- rather than a brown-adipocyte phenotype following differentiation [252]. Whether FAPs from skeletal muscle of lean humans acquire a different phenotype after differentiation was not investigated. Furthermore, an increased BMI seems to correlate with impaired *in vitro* differentiation of SVF cells from abdominal subcutaneous WAT [271] and mammary adipose tissue [272]. Due to the use of female mice of an obesity-resistant genetic background in the high-fat diet-study, we did not observe an overt weight gain in the HFD group and were consequently not able to assess the effects of obesity on FAP differentiation into UCP1-

Effects of exercise and high-fat diet on FAPs

positive adipocytes. Thus, it remains to be elucidated whether FAPs isolated from mice at more advanced stages of metabolic dysfunction – i.e., obese and/or glucose-intolerant – have a decreased capacity of differentiation into brown-like adipocytes.

In opposition to high-fat diet feeding, exercise training has been suggested to promote upregulation of UCP1 expression in ingWAT and decreased expression in BAT [101-103]. Nevertheless, we did not observe increases in UCP1 expression in ingWAT of male Sv129 mice immediately after a four-week endurance training protocol, indicating that exercise-induced regulation of UCP1 might be strain-dependent. Indeed, among the analysed genes, only *Pparg2* and *Fabp4* displayed a slight upregulation in ingWAT at the mRNA level, the latter not mirrored at the protein level. Previous studies have also reported increased mRNA levels of *Pparg2* [273] in different WAT depots in response to exercise training. A possible cause for the *Pparg2* response is the release of FFAs into the circulation during the exercise bouts: FFAs are known ligands for PPARG [274], which in turn upregulates its own transcriptional levels directly [275] or via upregulation of other factors that bind to its promoter, such as CEBPs [276]. Binding of PPARG to a peroxisome-proliferator-responsive element in the *Fabp4* promoter [277] could be a possible explanation for the increased *Fabp4* mRNA levels. It is intriguing that the differences observed between exercise-trained and untrained mice in gene expression in skeletal muscle and ingWAT, as well as in blood glucose levels at fasted state, became more pronounced following the four-week detraining period. We speculate about at least two possible causes for this: 1) an indirect effect of other training adaptations on the browning of ingWAT or 2) a different systemic response to intramuscular injections of glycerol between groups. Regarding the first hypothesis, alterations in basal lipid metabolism (increased lipolysis) and/or prolonged PPARG2 signalling sustained after the training period could have led to an increase in *Ucp1* transcriptional levels at week eight in the EXE group. Exercise training-induced alterations in the preadipocyte niche could also have directed the differentiation of preadipocytes towards a brown-like phenotype during the detraining period. In addition, a possible loss of adipose tissue mass during the exercise-training period could diminish body insulation, increasing the demand for non-shivering thermogenesis, and consequently sympathetic tone, at a given environmental temperature in EXE compared to CTRL mice. The effects of adrenergic stimuli in the ingWAT of the trained mice could also have been intensified by an enhanced sensitivity of the adipocytes to adrenergic stimulus, previously reported in parametrial adipocytes from rats in response to exercise training [278]. Concerning the second hypothesis, muscles from trained and untrained mice could respond to the intramuscular injection of glycerol in a different manner, affecting inflammatory signalling from skeletal muscle, skeletal muscle secretome

Effects of exercise and high-fat diet on FAPs

and, therefore, the crosstalk between skeletal muscle and other tissues, including ingWAT. Since we did not assess the mentioned factors (PPARG2 signalling, FFAs and WAT mass following the training period, and myokines and inflammation parameters following glycerol injection) in this study, further experiments are needed to depict the mechanisms underpinning the appearance of training status-dependent differences in gene expression and blood glucose levels only after four weeks of detraining.

In contrast to the high-fat diet experiment, in which the response of leptin and *Ucp1* mRNA expression displayed a similar pattern in ingWAT and injected TA, the differences in *Pparg2*, *Ucp1* and *Cidea* expression between EXE and CTRL mice observed at week eight in ingWAT were not observed in fatty-infiltrated skeletal muscle. Thus, microenvironment or cell autonomous factors affecting the capacity of FAPs to differentiate into UCP1-positive adipocytes during fatty degeneration are unlikely to be modified by exercise training, at least on the short term. This is further supported by the *in vitro* results showing unaltered UCP1 expression in FAPs isolated from EXE mice following differentiation. A limitation of this experiment is the exposure of quiescent FAPs only, and not activated and differentiated cells, to the exercise stimulus. It remains to be elucidated whether exercise training during or following muscle degeneration could affect FAP differentiation and UCP1 expression or the transdifferentiation of white intramuscular adipocytes into brown-like adipocytes. To answer this question, exercise training could be included in the experimental protocol four weeks following the intramuscular injections of glycerol, analogous to the injections of CL316 in the experiment described in Chapter 4.2. Such an experiment would also contribute to a better understanding of intramuscular adipose tissue response to exercise in general. While it is known that skeletal muscle hypoactivity induced by hindlimb unloading greatly decreases intramuscular adipocyte deposition resulting from glycerol injections [152], the effects of systematic exercise training on intramuscular adipocyte accumulation and phenotype are still unclear. Notably, the establishment of a protocol to verify the impact of exercise training on FAP fate decisions during glycerol-induced muscle degeneration would be potentially more challenging, if not practically or ethically impossible, given the discomfort and movement limitations possibly experienced by the mice during the first days following intramuscular injections of glycerol.

In conclusion, we show that neither high-fat diet-feeding nor exercise-training have short-term effects on the potential of skeletal muscle FAPs to express UCP1 after differentiation, at least in an obesity-resistant mouse strain known to express elevated levels of UCP1 in WAT compared to other strains. Intramuscular adipocytes seem to resemble subcutaneous adipocytes in their response to high-fat diet feeding, with increased leptin and unaffected

Effects of exercise and high-fat diet on FAPs

Ucp1 mRNA expression levels, while their response to exercise training remains to be investigated.

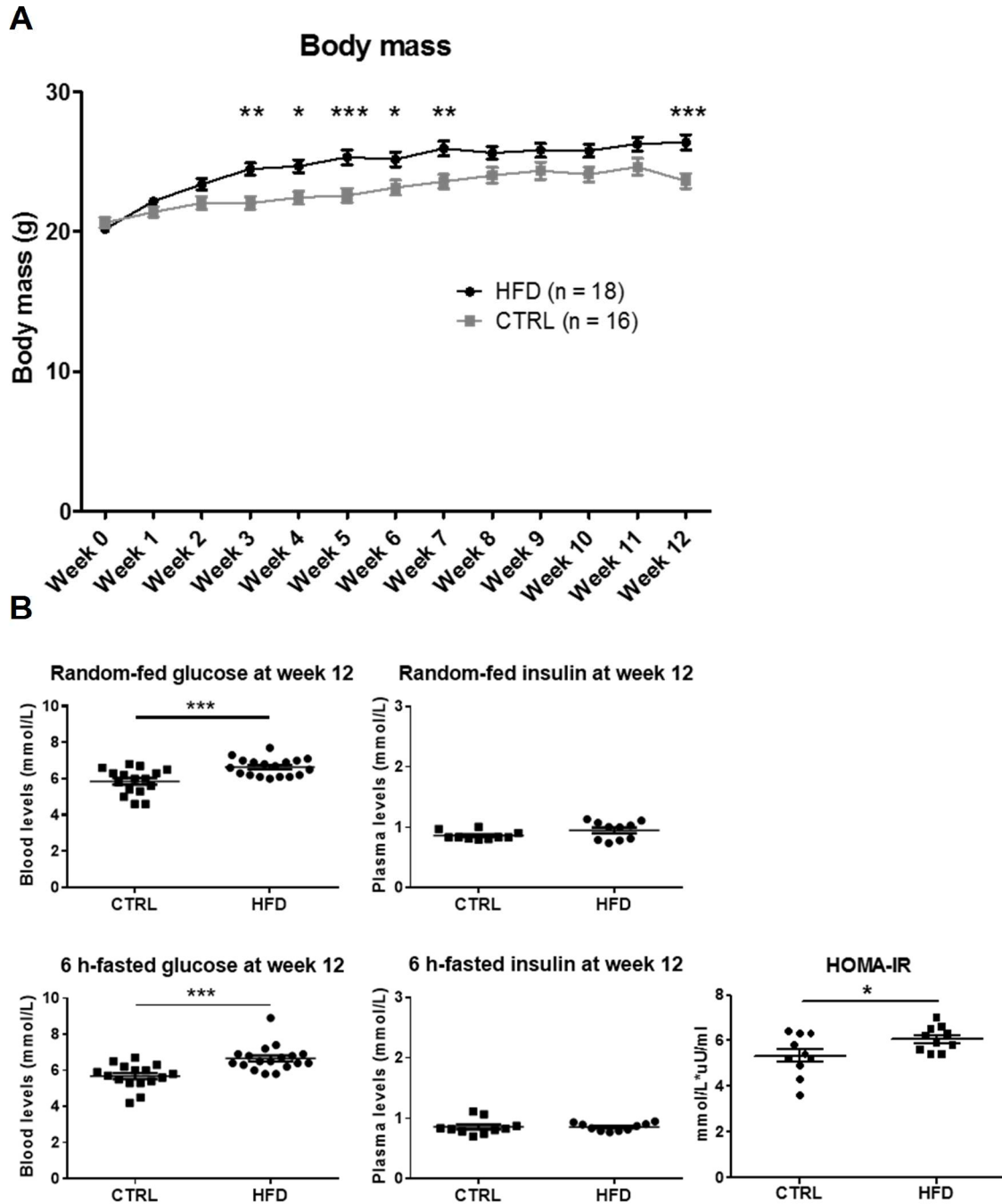


Figure 5.1: HFD mice display mildly increased body mass and blood glucose levels following 12 weeks of high-fat diet feeding. (A) Mean and S.E.M. of body mass of HFD (n = 18) and CTRL (n = 16) mice throughout the high-fat diet-feeding period. * p < 0.05, ** p < 0.01, *** p < 0.001, repeated-measures two-way ANOVA. (B) Mean and S.E.M. of blood glucose and plasma insulin levels at random-fed state and following a 6-h fast, and of HOMA-IR values in CTRL (n = 10 – 16) and HFD (n = 10 – 18) mice at experimental week 12. * p < 0.05, *** p < 0.001, unpaired Student’s t-test.

Effects of exercise and high-fat diet on FAPs

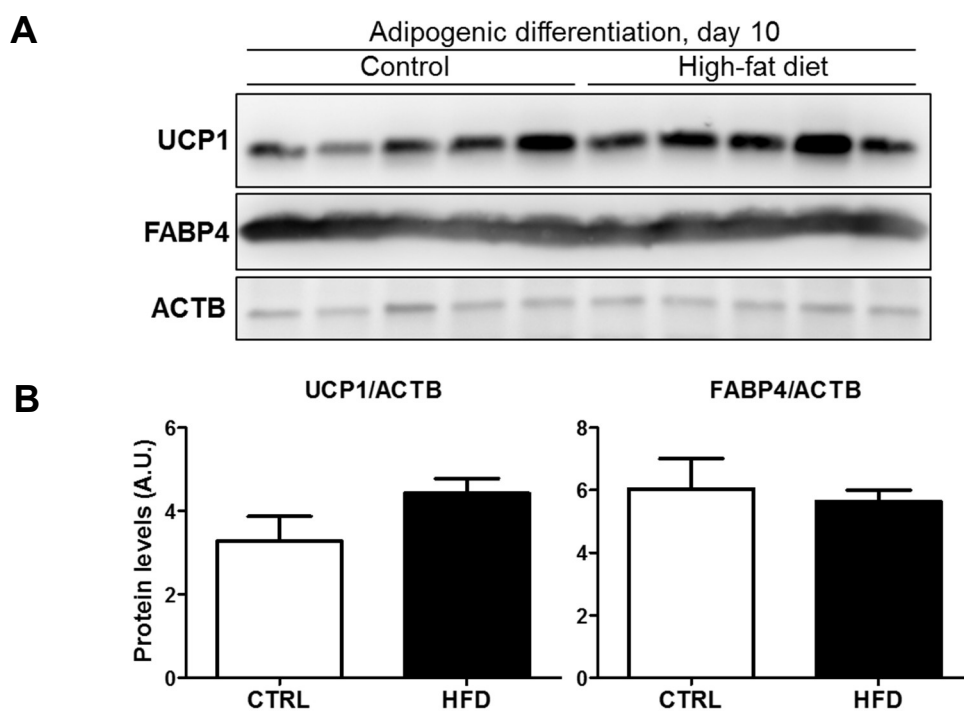


Figure 5.2: UCP1 expression in FAPs isolated from HFD and CTRL mice is similar following brown adipogenic differentiation. FAPs were isolated from CTRL and HFD mice at experimental week 12, followed by *in vitro* expansion and differentiation. (A) Immunoblotting for UCP1 and FABP4 in FAPs isolated from CTRL and HFD mice following 10 days of brown adipogenic treatment *in vitro*. ACTB was used as a loading control. (B) Mean and S.E.M. of relative UCP1 and FABP4 protein levels normalized to ACTB levels measured by densitometry (n = 5 CTRL and 5 HFD mice), in A.U.; unpaired Student's t-test.

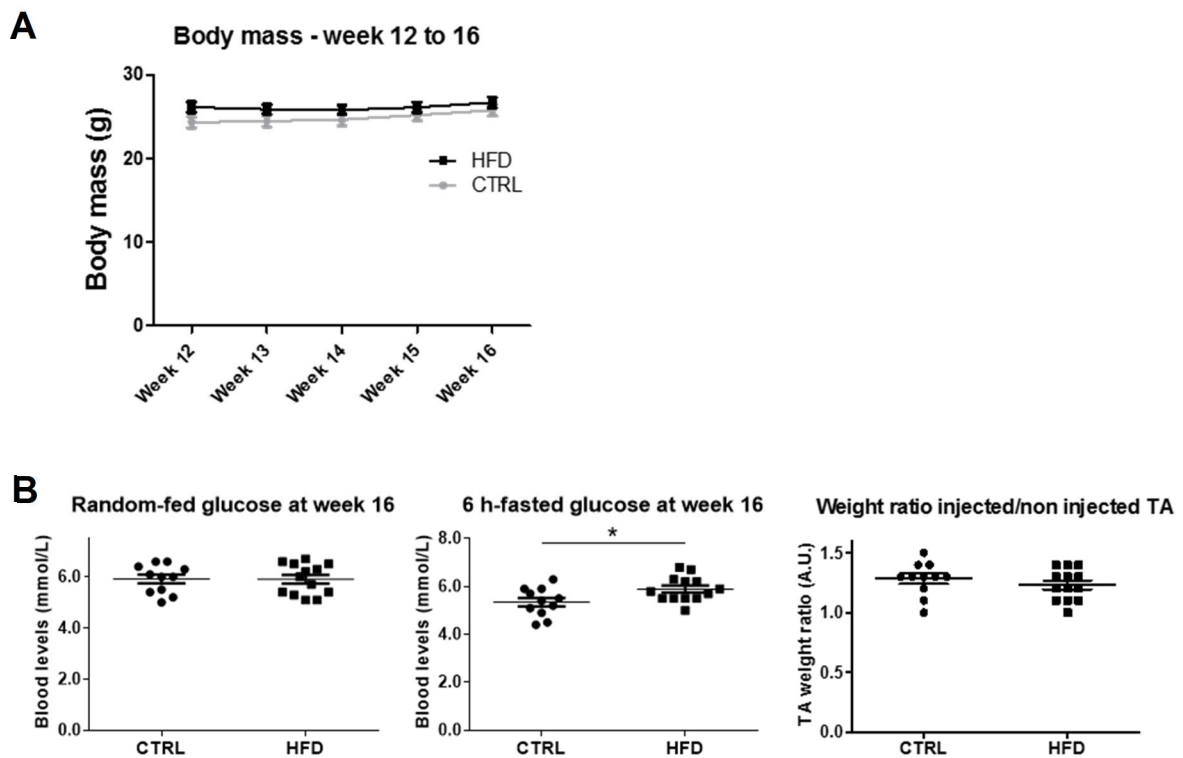


Figure 5.3: High-fat diet feeding mildly increases fasted-state blood glucose levels, but does not impair skeletal muscle regeneration four weeks after glycerol-injection. (A) Mean and S.E.M. of body mass of HFD (n = 13) and CTRL (n = 11) mice from week 12 to week 16 of the high-fat diet experiment. Repeated-measures two-way ANOVA. (B) Mean and S.E.M of blood glucose levels at random-fed state and after a 6-h fast, and ratio between mass of injected and non-injected TA in HFD (n = 13) and CTRL (n = 11) mice. * p<0.05, unpaired Student's t-test.

Effects of exercise and high-fat diet on FAPs

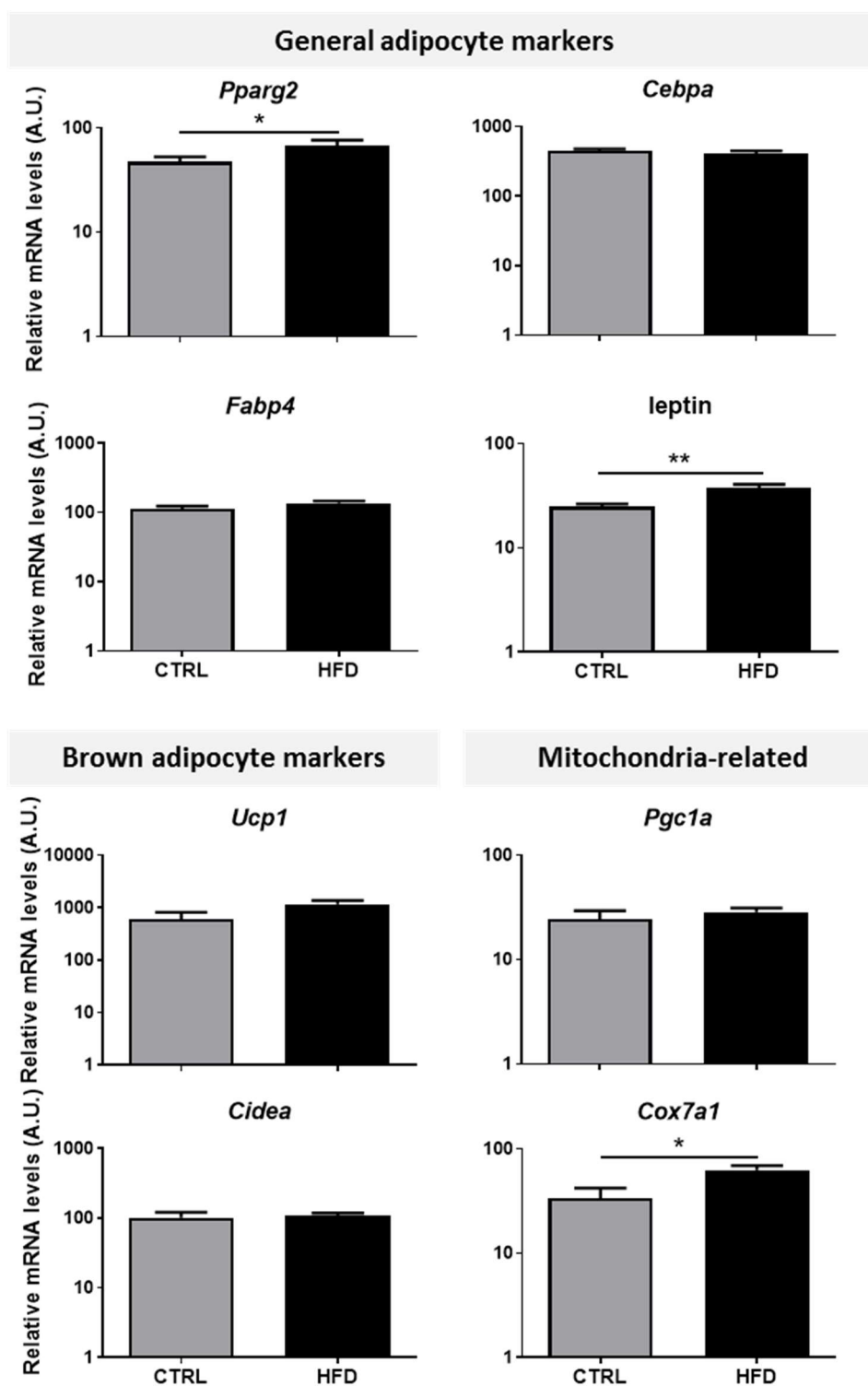


Figure 5.4: High-fat diet feeding does not affect *Ucp1* mRNA levels in ingWAT. IngWAT was excised from HFD and CTRL mice following a 16-week high-fat diet period. Data are shown as mean and S.E.M. of relative mRNA levels (in A.U.) of general adipocyte markers, brown adipocyte markers and mitochondria-related genes normalized to 18S rRNA levels in HFD (n = 10) and CTRL (n = 8) mice. * p < 0.05, ** p < 0.01, unpaired Student's t-test.

Effects of exercise and high-fat diet on FAPs

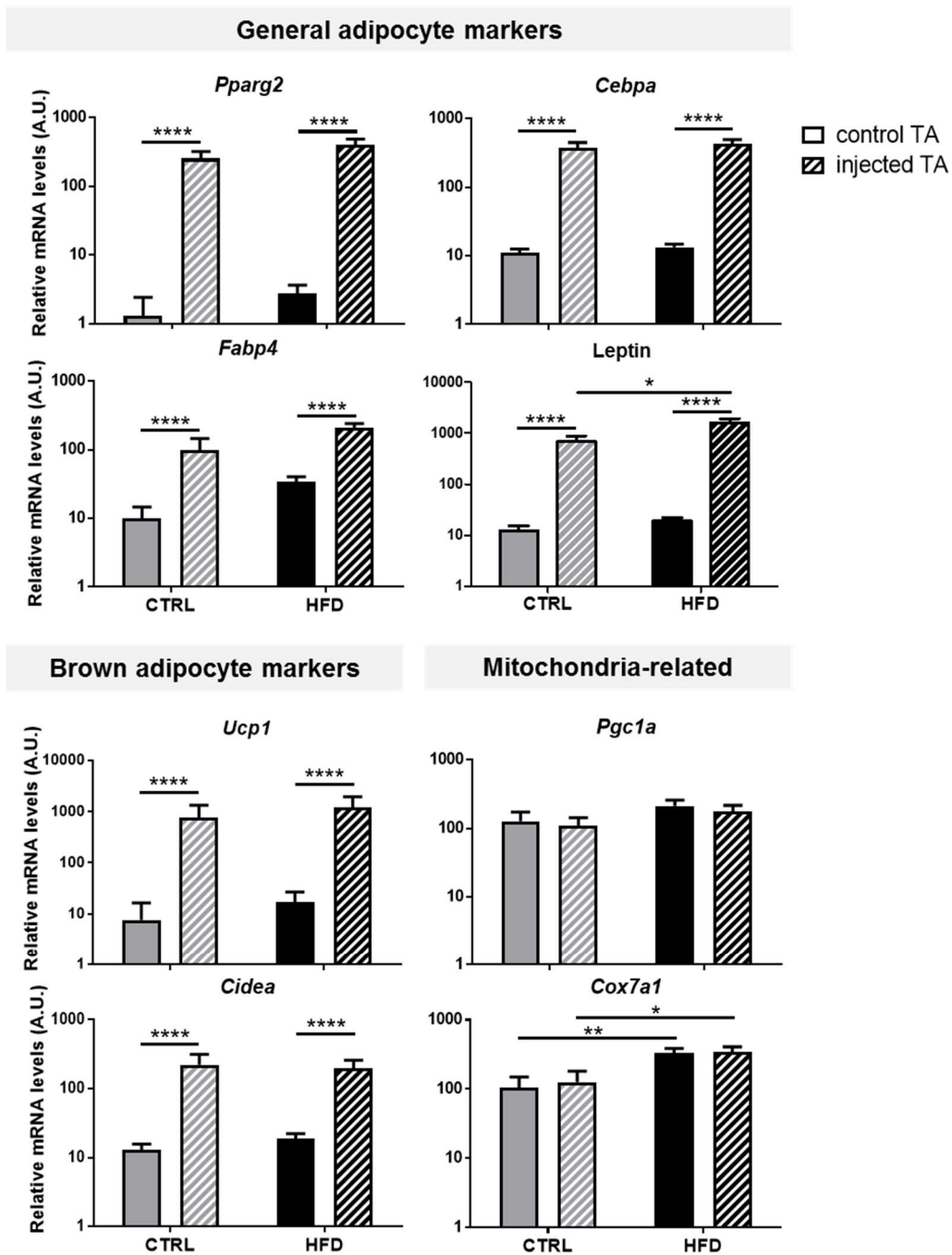


Figure 5.5: mRNA expression of leptin and *Cox7a1*, but not other general or brown adipocyte markers, is higher in adipocyte-infiltrated TA of HFD compared to CTRL mice. Control and glycerol-injected TA muscles were excised four weeks after intramuscular injection of glycerol, i.e., at week 16 of the high-fat diet study. Data are shown as mean and S.E.M. of relative mRNA levels (in A.U.) of general adipocyte markers, brown adipocyte markers and mitochondria-related genes normalized to 18S rRNA levels in HFD (n = 10) and CTRL mice (n = 8). * p < 0.05, ** p < 0.01, **** p < 0.0001, repeated-measures two-way ANOVA.

Effects of exercise and high-fat diet on FAPs

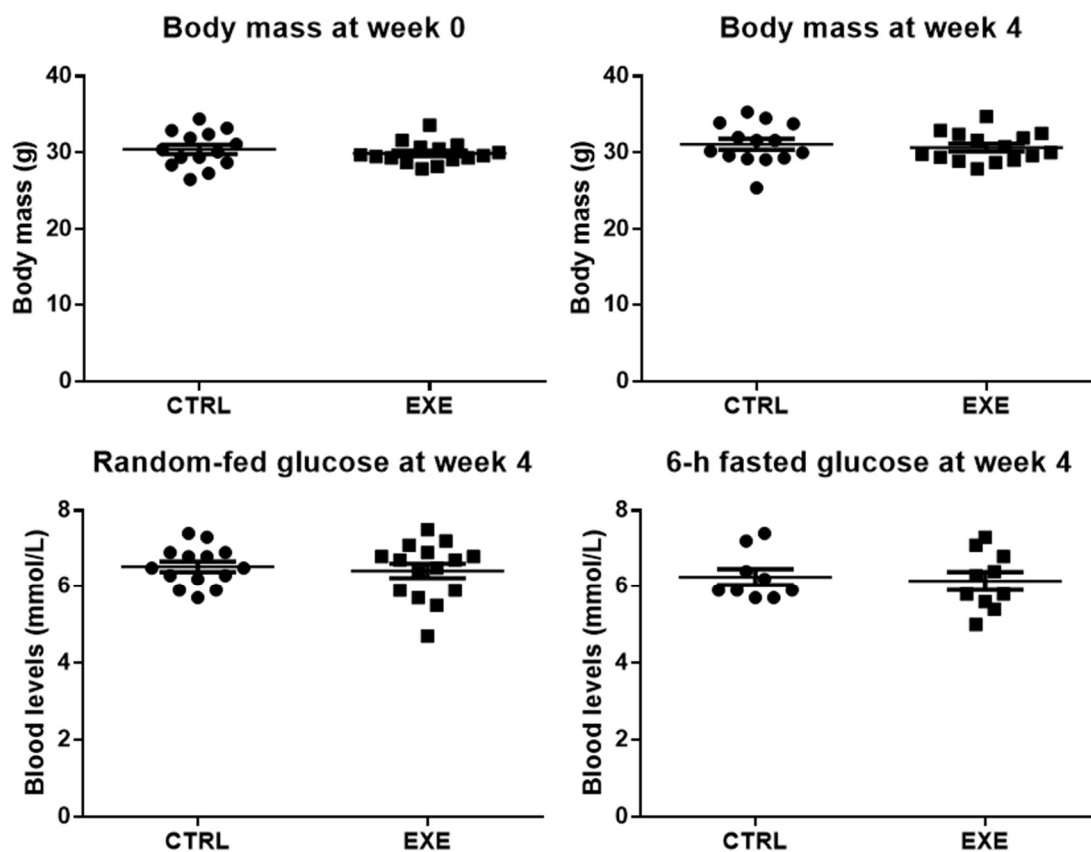
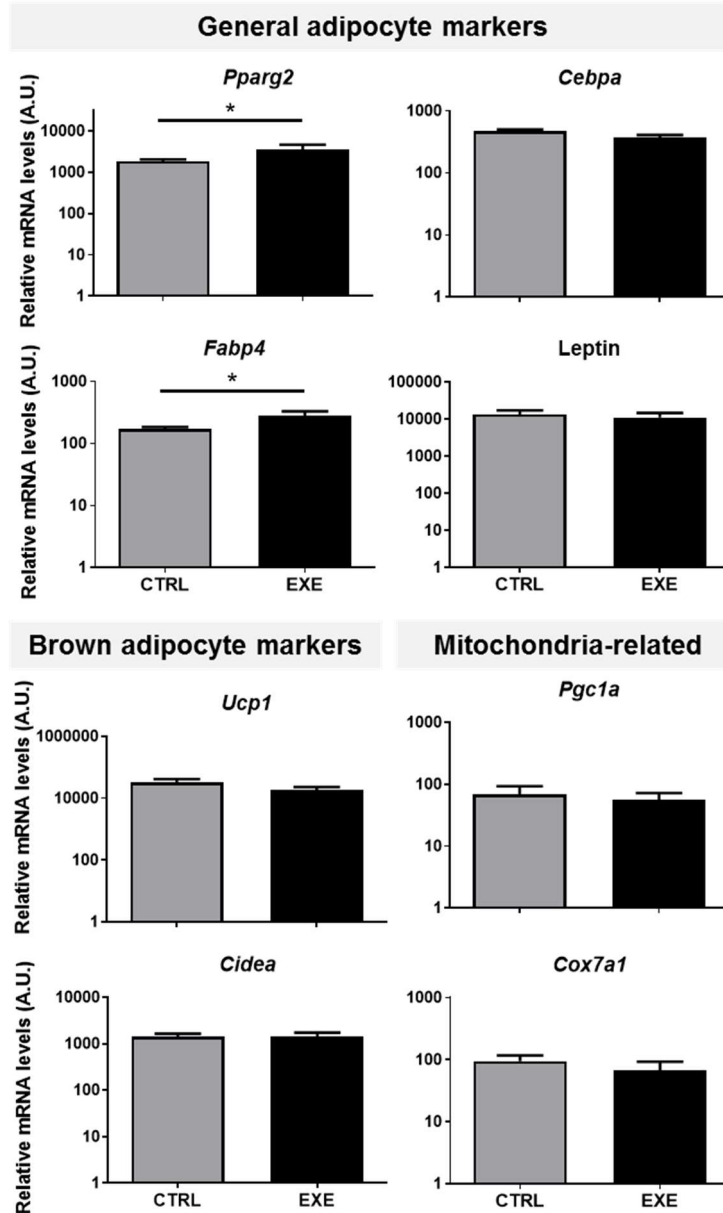


Figure 5.6: A four-week endurance exercise training intervention does not affect body mass and blood glucose levels in male Sv/129 mice. Data are shown as mean and S.E.M. of body mass and glucose levels of CTRL (n = 9 – 14) and EXE (n = 10 – 15) mice before and immediately after the four-week endurance training period. Unpaired Student's t-test was used to compare the groups.

A



B

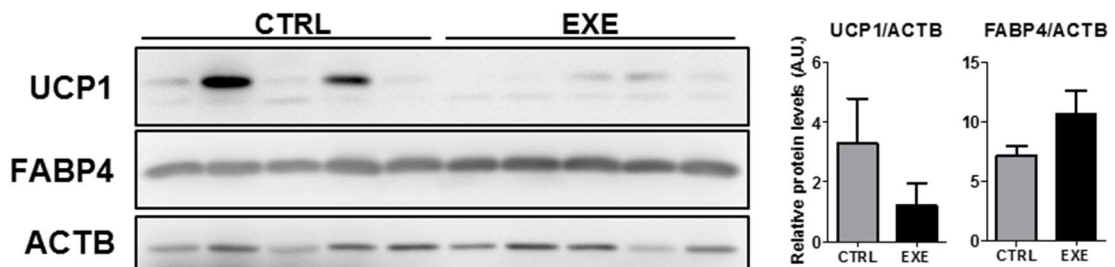


Figure 5.7: Expression of *Pparg2* and *Fabp4*, but not other general or brown adipocyte markers, is increased in ingWAT following a four-week endurance exercise training intervention. IngWAT was excised from CTRL and EXE mice between one and two days after the end of the four-week exercise training intervention. (A) Mean

Effects of exercise and high-fat diet on FAPs

and S.E.M. of relative mRNA levels (in A.U.) of general adipocyte markers, brown adipocyte markers and mitochondria-related genes normalized to 18S rRNA levels in ingWAT of CTRL (n = 5) and EXE (n = 5) mice after the four-week exercise training intervention. * p <0.05, unpaired Student's t-test. (B) Immunoblotting for UCP1 and FABP4 in ingWAT of CTRL and EXE mice following the four-week exercise training intervention. ACTB was used as a loading control. Graphs show mean and S.E.M. of relative protein levels measured by densitometry of UCP1 and FABP4 normalized to ACTB (in A.U.). Unpaired Student's t-test was used to compare groups.

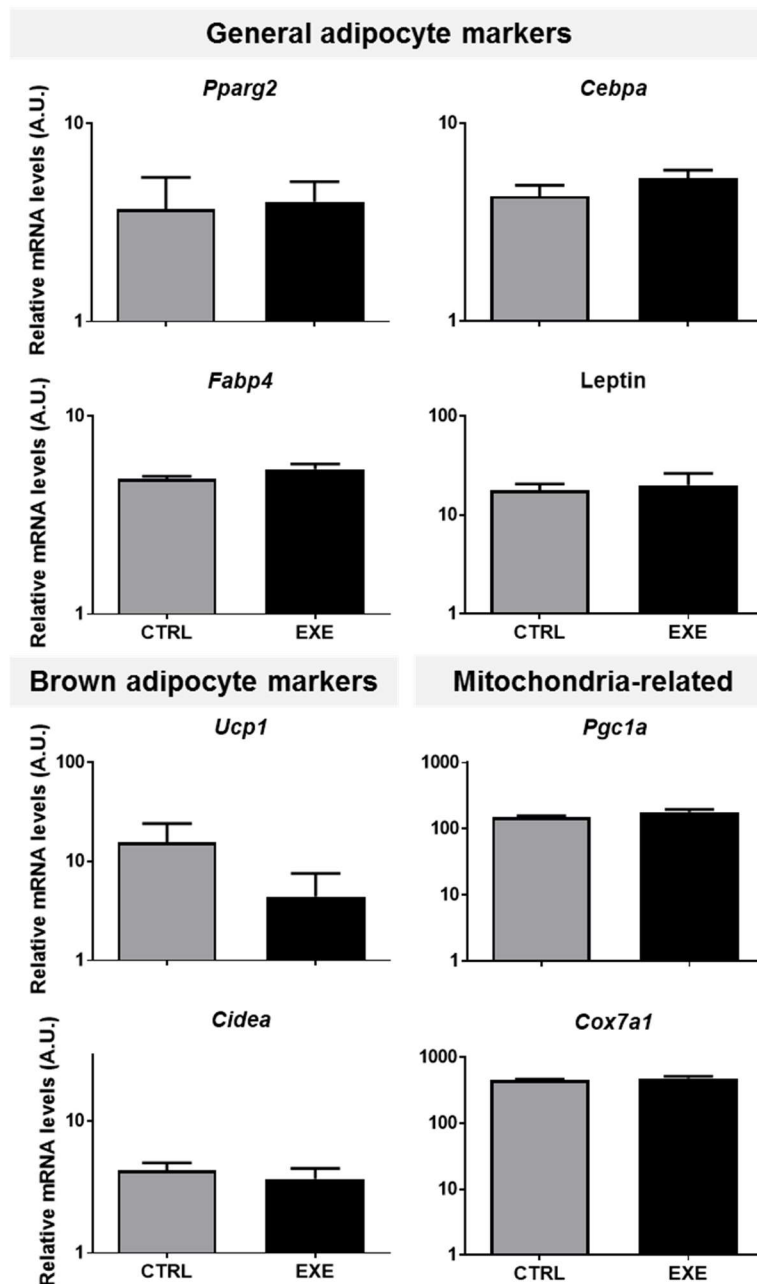


Figure 5.8: mRNA expression of *Pgc1a* and other genes highly expressed in white and/or brown adipocytes is not altered in the TA skeletal muscle following a four-week training intervention. TA skeletal muscle was excised from CTRL and EXE mice between one and two days after the end of the four-week exercise training intervention. Data are shown as mean and S.E.M. of relative mRNA levels (in A.U.) of general adipocyte markers, brown adipocyte markers and mitochondria-related genes normalized to 18S rRNA levels in CTRL (n = 5) and EXE (n = 5) mice. Unpaired Student's t-test was used to compare groups.

Effects of exercise and high-fat diet on FAPs

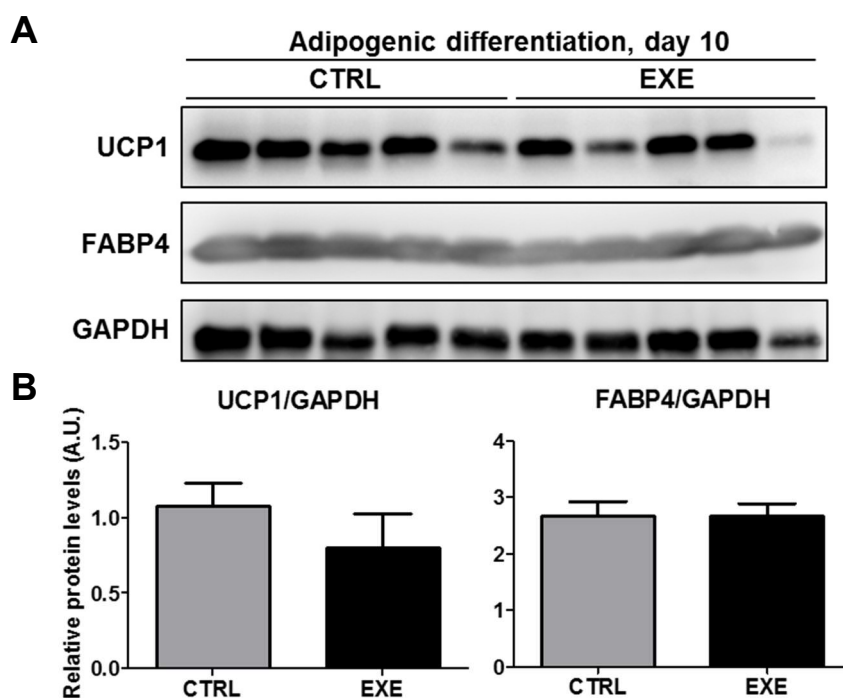


Figure 5.9: Exercise training does not affect the potential of FAPs to differentiate into UCP1-expressing adipocytes *in vitro*. FAPs were isolated from CTRL and EXE mice between one and three days after the end of the exercise training intervention, followed by *in vitro* expansion and differentiation. (A) Immunoblotting for UCP1 and FABP4 in FAPs isolated from CTRL and EXE mice following 10 days of brown adipogenic treatment *in vitro*. GAPDH was used as a loading control. (B) Mean and S.E.M. of relative UCP1 and FABP4 protein levels normalized to GAPDH levels measured by densitometry (n = 5 CTRL and 5 EXE mice). Unpaired Student's t-test was used to compare groups.

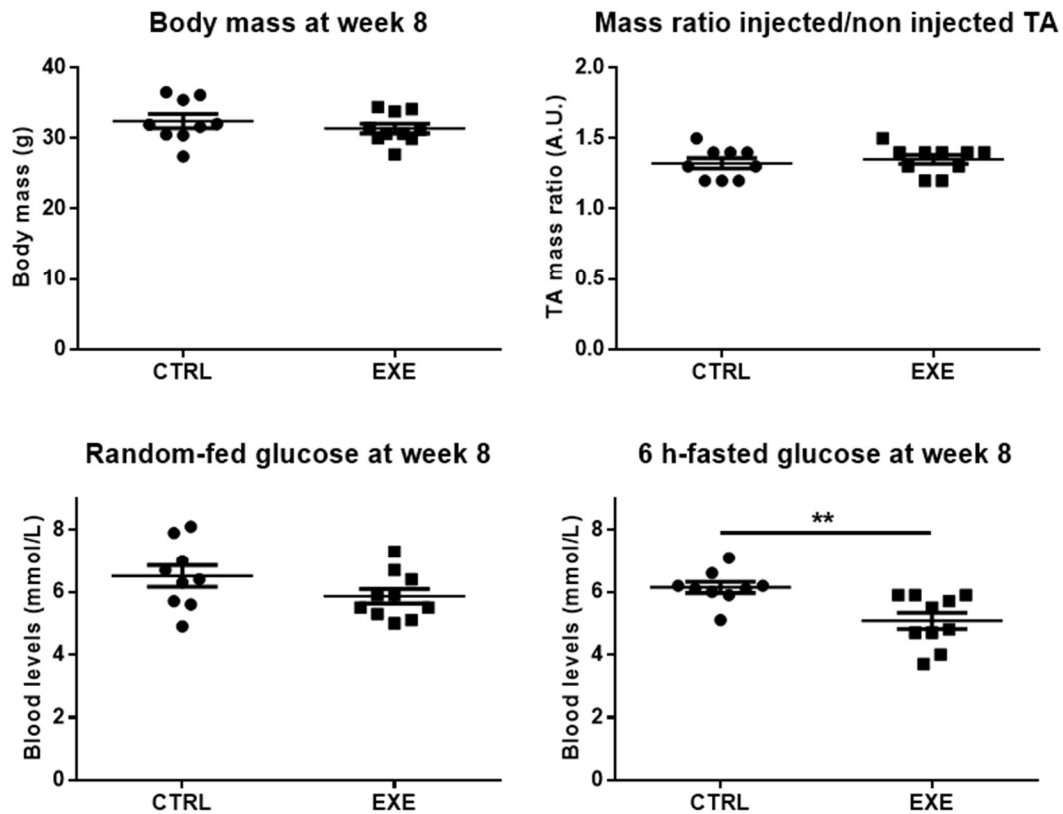


Figure 5.10: Fasting glucose-levels are decreased in exercise-trained compared to control mice, but body mass and skeletal muscle regeneration are unchanged after a four-week detraining period. (B) Mean and S.E.M of body mass, mass ratio between the glycerol-injected and the non-injected TA skeletal muscles, and blood glucose levels at random-fed state and after a 6-h fast in CTRL (n = 9) and EXE (n = 10) mice. ** p<0.01, unpaired Student's t-test.

Effects of exercise and high-fat diet on FAPs

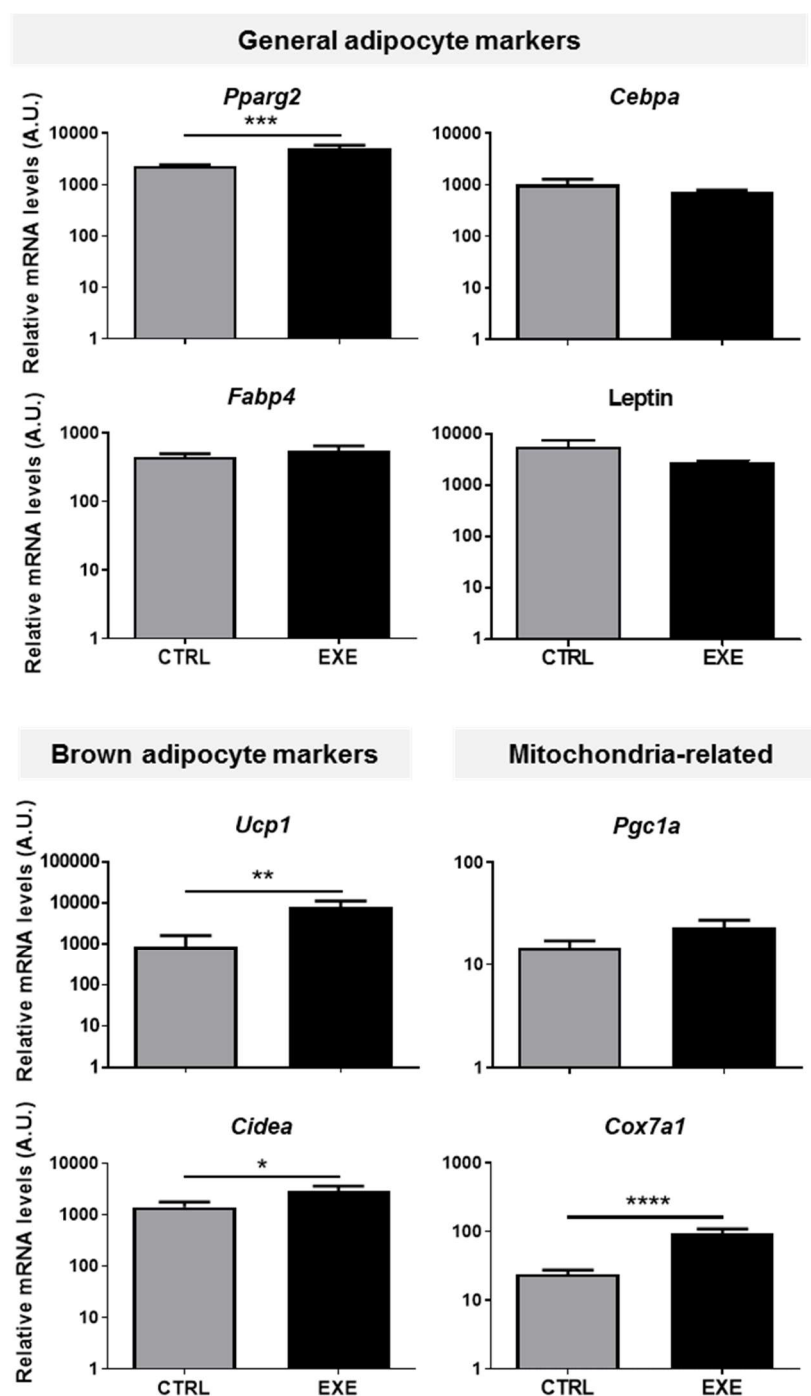


Figure 5.11: mRNA expression of *Ucp1* and other brown adipocyte markers is increased in ingWAT of exercise-trained mice after four weeks of detraining. IngWAT was excised from CTRL and EXE mice four weeks after the end of the training intervention (i.e., at experimental week eight). (A) Data are shown as mean and S.E.M. of relative mRNA levels (in A.U.) of general adipocyte markers, brown adipocyte markers and mitochondria-related genes normalized to 18S rRNA levels in CTRL (n = 6) and EXE (n = 7) mice. * p < 0.05, ** p < 0.01, *** p < 0.001, **** p < 0.0001, unpaired Student's t-test.

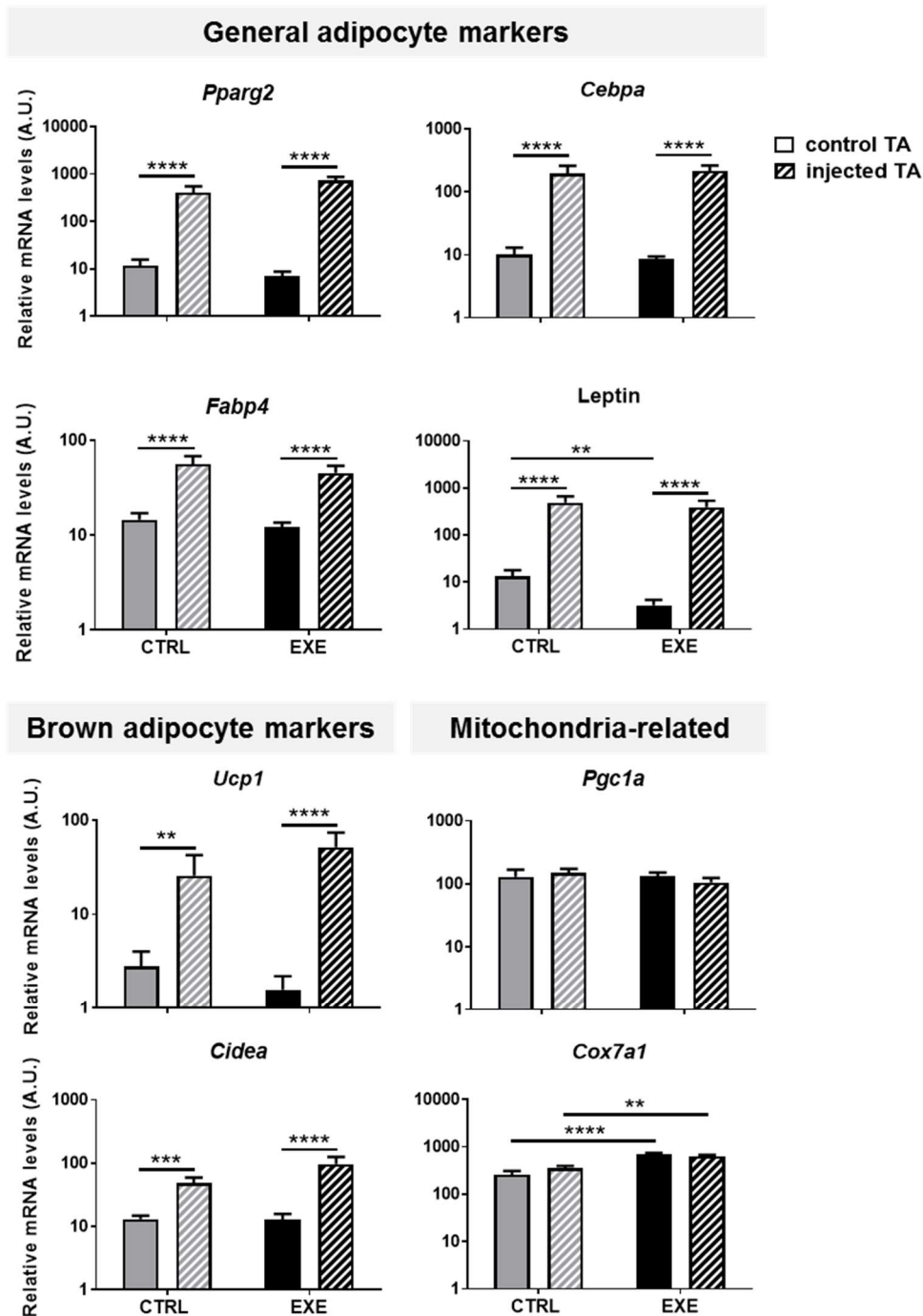


Figure 5.12: Expression of *Ucp1* and other general and brown adipocyte markers in fatty-infiltrated skeletal muscle in not altered in exercise-trained mice. Control and glycerol-injected TA skeletal muscles were excised four weeks after intramuscular glycerol injection, i.e. at experimental week eight. Data are shown as mean and S.E.M. of relative mRNA levels (in A.U.) of general adipocyte markers, brown adipocyte markers and mitochondria-related genes normalized to 18S rRNA levels in CTRL (n = 6) and EXE (n = 7) mice. ** p < 0.01, *** p < 0.001, **** p < 0.0001, repeated-measures two-way ANOVA.

Effects of exercise and high-fat diet on FAPs

6. Aging impairs the potential of FAPs to differentiate into brown-like adipocytes in an obesity-resistant mouse strain

6.1. Aging or ovariectomy does not impair skeletal muscle regeneration in Sv/129 female mice

A novel finding of this doctoral thesis is the difference in UCP1 expression in FAPs isolated from male and female mice after differentiation *in vitro*. The higher UCP1 protein expression in cells isolated from female compared to male mice despite expansion and differentiation in the same medium suggests that cell-autonomous factors, such as number of X chromosomes and epigenetic states, could underlie these differences in UCP1 expression. In addition, exposure of FAPs to different hormonal milieu before isolation could influence their capacity to differentiate into brown-like adipocytes *in vitro*. This would not be surprising, since estradiol and progesterone increase adipogenic differentiation and/or UCP1 expression *in vitro* [73], and ovariectomy decreases *Ucp1* mRNA expression in WAT [279]. This led us to the hypothesis that exposure of FAPs from female mice to higher levels of estradiol and progesterone could increase their potential to differentiate into brown-like adipocytes. In this case, FAPs from ovariectomized mice would display diminished UCP1 levels after differentiation.

In addition to the hormonal milieu, aging is known to affect stem cell function in several tissues (reviewed in [280]), including skeletal muscle [281-285]. Interestingly, Pisani et al. [167] have shown that aged female mice (18-months old) exhibit increased intramuscular adipocyte deposition in response to glycerol injections compared to their younger counterparts (3-month old), suggesting a possible impact of aging on FAP function.

To test the effects of aging and estrogen/progesterone deficiency on FAP differentiation into brown-like adipocytes, we investigated the *in vitro* and *in vivo* (glycerol-induced) differentiation of FAPs in young ovariectomized (OVX, three-months old) and aged (19-months old) female Sv129 mice. Young (three-months old) female Sv/129 mice were used as controls.

As shown in Figure 6.1, aging and ovariectomy did not affect skeletal muscle regeneration as measured by the mass ratio between the injected and the non-injected TA at week four post-injection. Furthermore, the ratio between TA mass and whole-body mass was also similar between the three groups, suggesting that aged mice were not sarcopenic. As

Aging impairs UCP1 expression in differentiated FAPs

expected from previous studies [286], body mass was higher in aged mice than in young and OVX mice. In other mouse strains, ovariectomy has been shown to increase body mass [287, 288] and fasting blood glucose [289]. In contrast, we did not observe differences in body mass between young and OVX mice. While blood glucose levels at random-fed state did not differ between groups, OVX mice displayed slightly lower blood glucose levels than young mice after a 6-h fast. These results suggest that Sv/129 female mice are not only resistant to high-fat diet-induced obesity, but also to the deleterious effects of ovariectomy on metabolism, at least in the short term.

6.2. Aging decreases the potential of FAPs to differentiate into brown-like adipocytes *in vitro*

The skeletal muscle satellite cell population seems to be reduced in aged [288] and ovariectomized [290] mice. The FAP response to these two conditions, however, remains unclear. Regarding adipocyte progenitors from other tissues, ovariectomy can impair the *ex vivo* proliferation [291] and increase the adipogenic differentiation rates [292] of ingWAT-derived stem cells. On the other hand, WAT preadipocytes isolated from aged rats [293, 294] and humans [295] proliferate and differentiate into adipocytes at lower rates than cells isolated from their younger counterparts *in vitro*. Thus, we tested whether the differentiation of skeletal muscle FAPs into brown-like adipocytes would also be affected by ovariectomy or aging. For this, we isolated FAPs from a fraction of the young (control), OVX and aged female Sv/129 mice described in section 6.1, followed by *in vitro* expansion and treatment with brown adipogenic medium for ten days. Interestingly, UCP1 expression in differentiated cells did not differ between the three groups (Figure 6.2A), suggesting that the cell-autonomous factors affecting adipogenic differentiation and UCP1 expression are not altered in OVX and aged mice.

The tendency for decreased UCP1 expression following differentiation in FAPs isolated from aged mice prompted us to investigate whether FAPs' capacity to differentiate into brown-like adipocyte was gradually decreasing in aged mice and would become significantly lower than in younger mice at later stages. For this, we isolated FAPs from mice at two months and 23 months of age and, after *in-vitro* expansion, treated them with the brown adipogenic medium for ten days. As shown in Figure 6.2B, FAPs isolated from 23-months old mice exhibit lower UCP1 expression following *in vitro* brown adipogenic differentiation compared to FAPs from young mice, despite no apparent impairments in differentiation, as assessed by microscopy (Figure 6.2C) and FABP4 protein levels.

6.3. Expression of *Ucp1* and other brown- and white-adipocyte markers in fatty-degenerated skeletal muscle is not altered in OVX and aged Sv/129 female mice

Skeletal muscle of ovariectomized rodents displays an altered lipid metabolism and augmented intramyocellular lipid accumulation [296], as well as impaired notexin-induced regeneration [297] and incomplete recovery from unloading-induced atrophy [298, 299]. Adipocyte UCP1 expression is also affected by sex-hormone deficiency: ovariectomy decreases UCP1 expression in BAT [300], and ovarian failure prevents the induction of UCP1 expression in gonadal WAT in response to CL316 treatment [301]. Skeletal muscle and adipose tissue metabolism are also altered in aged mice, which exhibit impaired browning of subcutaneous WAT [302] and increased adipocyte deposition in skeletal muscle in response to intramuscular glycerol injections [167]. Whether FAP differentiation into brown-like adipocytes *in vivo* during skeletal muscle fatty degeneration is decreased in ovariectomized and aged mice remains unclear. Thus, we investigated how these two conditions affect the expression of *Ucp1* and other brown- and white-adipocyte markers in fatty-infiltrated skeletal muscle. For this, TA skeletal muscles of a fraction of the young (control, 2-months old), OVX and aged (19-months old) Sv/129 female mice described in section 6.1 were injected with glycerol; the contralateral TAs were used as a control. Four weeks later, injected and control TA muscles were excised for analysis. The ingWAT depot was used as a control for the effects of ovariectomy and aging on subcutaneous WAT.

In ingWAT, expression of *Ucp1* and other genes highly-expressed in BAT – namely *Cidea*, *Pgc1a* and *Cox7a1* – was similar between young, OVX and aged mice. Aged mice displayed a slightly higher expression of *Fabp4* and lower expression of *Cebpa* compared to young mice (Figure 6.3). In the glycerol-injected TAs, no differences were observed between groups in the expression of genes highly expressed in brown adipocytes such as *Ucp1*, *Cidea* and *Cox7a1*, and the general/white adipocyte markers *Pparg2*, *Cebpa*, *Fabp4* and leptin. A slightly higher expression of *Pgc1a* was observed in the glycerol-injected TA of OVX mice compared with young and aged mice (Figure 6.4). These data suggest that *Ucp1* expression in subcutaneous WAT and in intramuscular adipocytes is not affected by the hormonal and microenvironment changes stemming from ovariectomy and aging in obesity-resistant, female Sv/129 mice. Furthermore, the similar expression of general or white adipocyte markers in fatty-infiltrated skeletal muscle indicates that, in Sv/129 mice, FAP microenvironment in OVX and aged (19-months old) mice is not more permissive to adipocyte deposition than in young mice, as had been shown in B6D2 mice [167].

Aging impairs UCP1 expression in differentiated FAPs

6.4. The response of intramuscular *Ucp1* expression to beta 3-adrenergic stimulus in fatty-infiltrated skeletal muscle is apparently preserved in aged Sv/129 female mice

While UCP1 expression following *in vitro* differentiation in FAPs from 19-months old female Sv/129 mice was not significantly different from FAPs isolated from young mice, cells isolated from 23-months old mice exhibited a nearly three-fold decrease in UCP1 expression following differentiation compared to cells isolated from young animals. Thus, we hypothesized that the differences in glycerol-induced fatty infiltration between young and 18-months old female B6D2 mice [167] could also be observed in Sv/129 female mice at later stages of life. To test this hypothesis, we compared the expression of brown and general adipocyte markers in fatty-infiltrated TAs from 2-months old and 23-months old Sv/129 female mice four weeks following intramuscular glycerol injections. Since aging has been related to a reduced response of *Ucp1* mRNA expression in BAT and WAT to treatment with the B3-adrenergic receptor agonist CL316 in rats [303], we took the opportunity to investigate how the response of intramuscular adipocytes to this stimulus is modulated by age. Thus, in this experiment, young and aged mice were treated with daily intraperitoneal injections of CL316 for five days before muscle excision (the young female Sv/129 mice used in the experiment shown in Figure 4.6B were used as the control, young group).

As illustrated in Figure 6.5, *Ucp1* mRNA expression was surprisingly higher in aged mice than in their young counterparts. The higher expression of general adipocyte markers in the glycerol-injected TA of aged mice suggests that intramuscular adipocyte deposition was stronger in this group. Thus, the enhanced *Ucp1* expression in the injected TA of aged mice could simply be the result of a higher number of intramuscular adipocytes, and not necessarily of upregulated *Ucp1* levels per adipocyte or of a higher percentage of brown-like adipocytes. An additional experiment including histological analysis of the fatty-infiltrated TAs would be necessary to compare the ratio between intramuscular brown-like and white adipocytes between young and aged mice. The contrast between the increased mRNA expression of general adipocyte markers in aged compared to young mice observed in this experiment and the unaltered mRNA levels observed in the experiment shown in section 6.3 might stem from the four-month difference in age between the two aged-mice groups (23 months in the present experiment and 19-months in the experiment described in section 6.3).

6.5. Discussion

The functionality and differentiation potential of mesenchymal stem cells from different tissues seems to be affected by ovariectomy and aging [191, 304]. Here, we show that the potential of skeletal muscle FAPs to differentiate into brown-like adipocytes *in vitro* is impaired in aged, but not ovariectomized, female Sv/129 mice.

The aging skeletal muscle milieu seems to impair satellite cell function [305, 306], but cell-autonomous factors are also emerging as important for the aging-related function decline in these cells [187, 307, 308]. The effects of aging on FAP function, on the other hand, are not clear. The decreased UCP1 expression in FAPs isolated from aged compared to young mice following differentiation *in vitro* suggests that aging also affects FAP function and plasticity, and that these alterations are not reversible by simply switching cell microenvironment. Interestingly, a decrease in the number of brown-like adipocytes in subcutaneous WAT was previously reported in aged mice [302]. Whether the capacity of WAT adipocyte progenitors to differentiate into brown-like adipocytes is also decreased in aging mice remains unclear. It is intriguing that the differences in UCP1 expression observed between FAPs from aged and young mice *in vitro* were not reflected on the *Ucp1* mRNA expression levels in fatty-infiltrated skeletal muscle of these two groups *in vivo*. This resembles the comparison between FAP-derived brown-like adipocytes from male and female mice, reported in Chapter 4 (Figure 4.13): although FAPs from females expressed significantly higher UCP1 levels than FAPs from males following differentiation *in vitro*, *Ucp1* mRNA levels in fatty-infiltrated skeletal muscle were similar in male and female mice. We speculate that the differences in brown adipogenic stimulus between the *in vivo* and *in vitro* experiments explain these contrasts. In fact, while brown adipogenesis was strongly stimulated *in vitro* by medium containing T3 and rosiglitazone, among other compounds known to promote the brown adipogenic fate, glycerol stimulates adipogenesis of FAPs, but does not provide any stimulus for brown adipogenesis. Thus, it cannot be ruled out that the intramuscular adipocytes from these different groups would respond differently to *in vivo* treatment with rosiglitazone, for example.

As shown in Chapter 4 (Figure 4.13), FAPs isolated from female mice express higher UCP1 levels following brown adipogenic differentiation *in vitro* compared to FAPs from male mice. This indicated that cell-autonomous factors or the exposure to different sex hormone levels before FAP isolation could influence UCP1 levels in FAPs differentiated *in vitro*. Indeed, sex hormones have been shown to regulate brown adipocyte differentiation and *Ucp1* expression *in vitro*. While adipocytes treated with testosterone exhibit fewer and smaller lipid droplets and lower *Ucp1* expression, treatment with progesterone or 17 β -estradiol

Aging impairs UCP1 expression in differentiated FAPs

increases the number and size of lipid droplets compared to control cells; progesterone was also shown to increase *Ucp1* mRNA levels at certain concentrations [73]. Additionally, these hormones also seem to differentially regulate the expression of a set of genes involved in mitochondrial biogenesis in brown adipocytes *in vitro* [309]. The present results show that FAPs from female Sv/129 mice retain their capacity to differentiate and express *Ucp1* mRNA *in vivo* and UCP1 protein *in vitro* following ovariectomy, suggesting that differences between sexes in UCP1 expression in FAP-derived adipocytes are explained either by cell-autonomous factors or by exposure to testosterone before isolation. It remains to be investigated whether the *in vivo* exposure of FAPs to testosterone in male mice leads to decreased UCP1 expression following differentiation *in vitro*. This hypothesis would be supported by a recent report showing that castration leads to increased expression of *Ucp1* in BAT and ingWAT in male mice [310].

We did not observe higher body mass in the OVX group compared to control mice, contrasting to previous results [287, 311]. The OVX mice also did not display increased blood glucose levels or decreased TA mass following intramuscular glycerol injections compared to control mice. This suggests that Sv/129 female mice could be resistant not only to obesity, but also to the deleterious effects of ovariectomy on metabolic parameters. Resistance to the effects of ovariectomy on body mass and glucose metabolism has been previously observed in rats artificially selected for high intrinsic aerobic fitness compared to rats selected for low intrinsic aerobic fitness [312]. Similarly, ovariectomy did not affect the expression of any evaluated gene in ingWAT and skeletal muscle following glycerol injection in the present study, with exception of increased *Pgc1a* mRNA expression in the injected TA. This suggests that ingWAT, FAPs and/or the skeletal muscle microenvironment are also not affected by ovariectomy in Sv/129 mice, at least in the short term. Understanding the mechanisms responsible for the differences between mouse strains resistant to ovariectomy or not could lead to the discovery of new targets to prevent the effects of sex-hormone deficiency on whole-body and adipocyte metabolism.

In contrast to 12-months old B6D2 mice [167], Sv/129 mice did not display increased intramuscular adipocyte deposition at 19 months of age, at least based on mRNA expression of adipocyte markers. In fact, except for the upregulation of *Fabp4* and the downregulation of *Cebpa* mRNA expression in ingWAT of aged mice compared with young mice, aging did not affect the mRNA expression of any of the brown- and white-adipocyte markers analyzed in ingWAT or fatty-infiltrated skeletal muscle. The decreased expression of *Cebpa* in ingWAT of aged mice resembles previous results showing that, in rats, aging downregulates *Cebpa* levels in WAT depots *in vivo* and in preadipocytes during *in vitro* differentiation. This decline in *Cebpa* was proposed as a cause for impaired preadipocyte

Aging impairs UCP1 expression in differentiated FAPs

function in aged rats [293]. However, this difference in *Cebpa* expression between young and aged mice was not observed in fatty-infiltrated skeletal muscle, which could be explained by intrinsic differences between skeletal muscle FAPs and WAT adipocyte precursors or by a differential impact of aging on the microenvironments in which these cells reside. Contrastingly, when 23-months old mice were compared to young mice, we observed an increase in mRNA expression of general adipocyte markers with aging, suggesting that aged-dependent alterations in skeletal muscle regeneration and fatty degeneration might occur at a later time point in Sv/129 female mice compared to other mouse backgrounds. The increased levels of *Ucp1* mRNA in 23-months old mice compared to 2-months old mice in response to glycerol-induced fatty degeneration followed by CL316 treatment could, therefore, simply reflect an augmented number of intramuscular adipocytes. Histological analysis of fatty-infiltrated skeletal muscle from these animals, including quantification of brown-like and white intramuscular adipocytes, would be needed to clarify whether the aged skeletal muscles differ from young skeletal muscles only in the amount of intramuscular adipocytes, or whether the phenotype (white/brown-like) of the intramuscular adipocytes is also altered.

In summary, our results show that the cell-intrinsic factors regulating UCP1 expression in FAP-derived adipocytes from female Sv/129 mice are altered in aged, but not in OVX mice. It remains to be elucidated whether other mouse strains are more prone to intramuscular adipocyte dysfunction in response to ovariectomy or aging. In this case, comparison between intramuscular adipocytes from these strains and Sv/129 mice could reveal molecular targets to improve intramuscular adipocyte function/browning during aging or estrogen deficiency.

Aging impairs UCP1 expression in differentiated FAPs

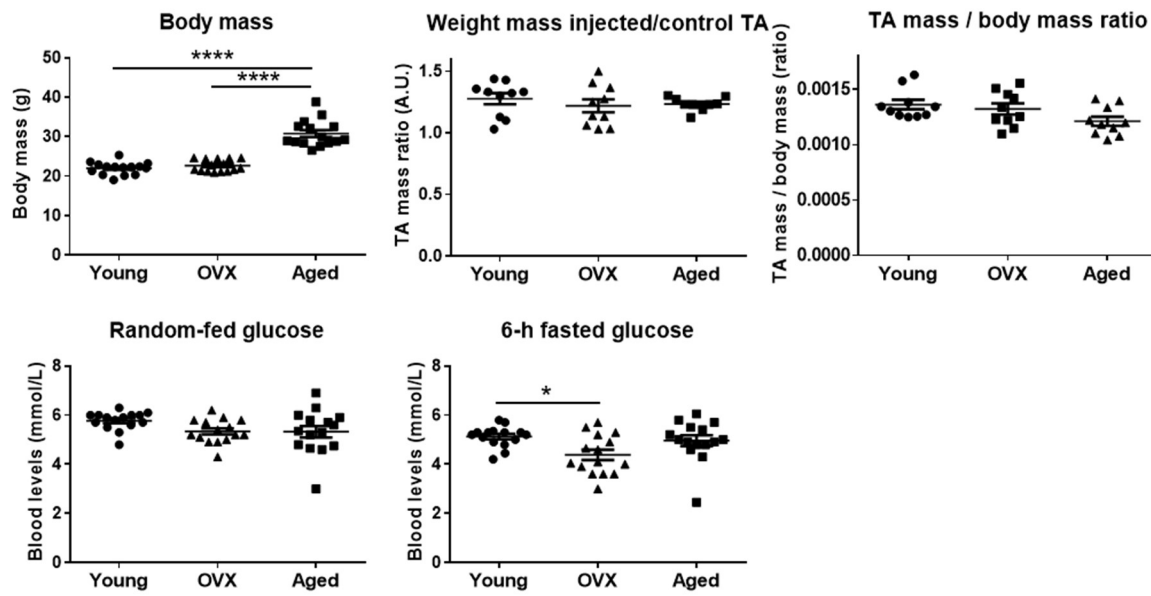


Figure 6.1: Aging and ovariectomy do not affect skeletal muscle regeneration in female Sv/129 mice. Data are shown as mean and S.E.M. of body mass, mass ratio between injected and control TA, ratio between TA and whole-body mass, and blood glucose levels at random-fed and fasted states in young (three-months old, $n = 10 - 15$), OVX (three-months old, ovariectomized at four weeks of age, $n = 10 - 15$) and aged (19-months old, $n = 10 - 15$) female Sv/129 mice. * $p < 0.05$, **** $p < 0.0001$, one-way ANOVA and Bonferroni post-hoc.

Aging impairs UCP1 expression in differentiated FAPs

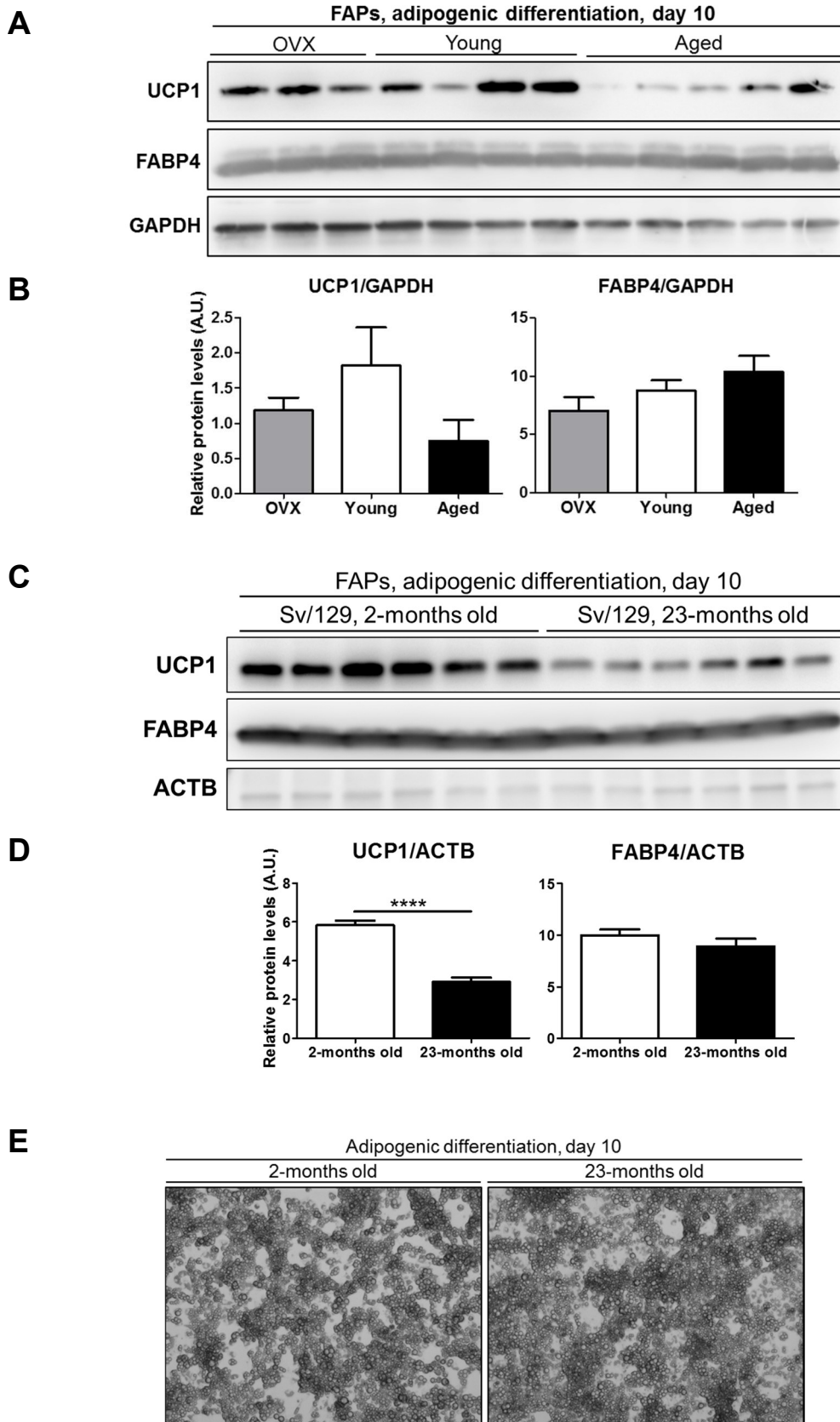


Figure 6.2: Aging, but not ovariectomy, decreases FAP potential to differentiate into brown-like adipocytes. (A-B) FAPs were isolated from skeletal muscle of young (three-

Aging impairs UCP1 expression in differentiated FAPs

months old, n = 4), OVX (three-months old, ovariectomized at four-weeks of age, n = 3) and aged (19-months old, n = 5) female Sv/129 mice, followed by *in vitro* expansion and differentiation. (A) Immunoblotting for UCP1 and FABP4 in FAPs isolated from young, OVX and aged mice following 10 days of brown adipogenic treatment *in vitro*. GAPDH was used as a loading control. (B) Mean and S.E.M. of relative UCP1 and FABP4 protein levels normalized to GAPDH levels measured by densitometry, one-way ANOVA was used to compare groups. (C-D) FAPs were isolated from skeletal muscle of young (two-months old, n = 6) and aged (23-months old, n = 6) female Sv/129 mice, followed by *in vitro* expansion and differentiation. (C) Immunoblotting for UCP1 and FABP4 in FAPs isolated from two-month old and 23-month old mice following 10 days of brown adipogenic treatment *in vitro*. ACTB was used as a loading control. (D) Mean and S.E.M. of relative UCP1 and FABP4 protein levels normalized to ACTB levels measured by densitometry. **** p < 0.0001, unpaired Student's t-test. (E) Representative images of FAPs isolated from Sv/129 female mice at two or 23 months of age at day 10 of the brown adipogenic differentiation treatment (100x magnification).

Aging impairs UCP1 expression in differentiated FAPs

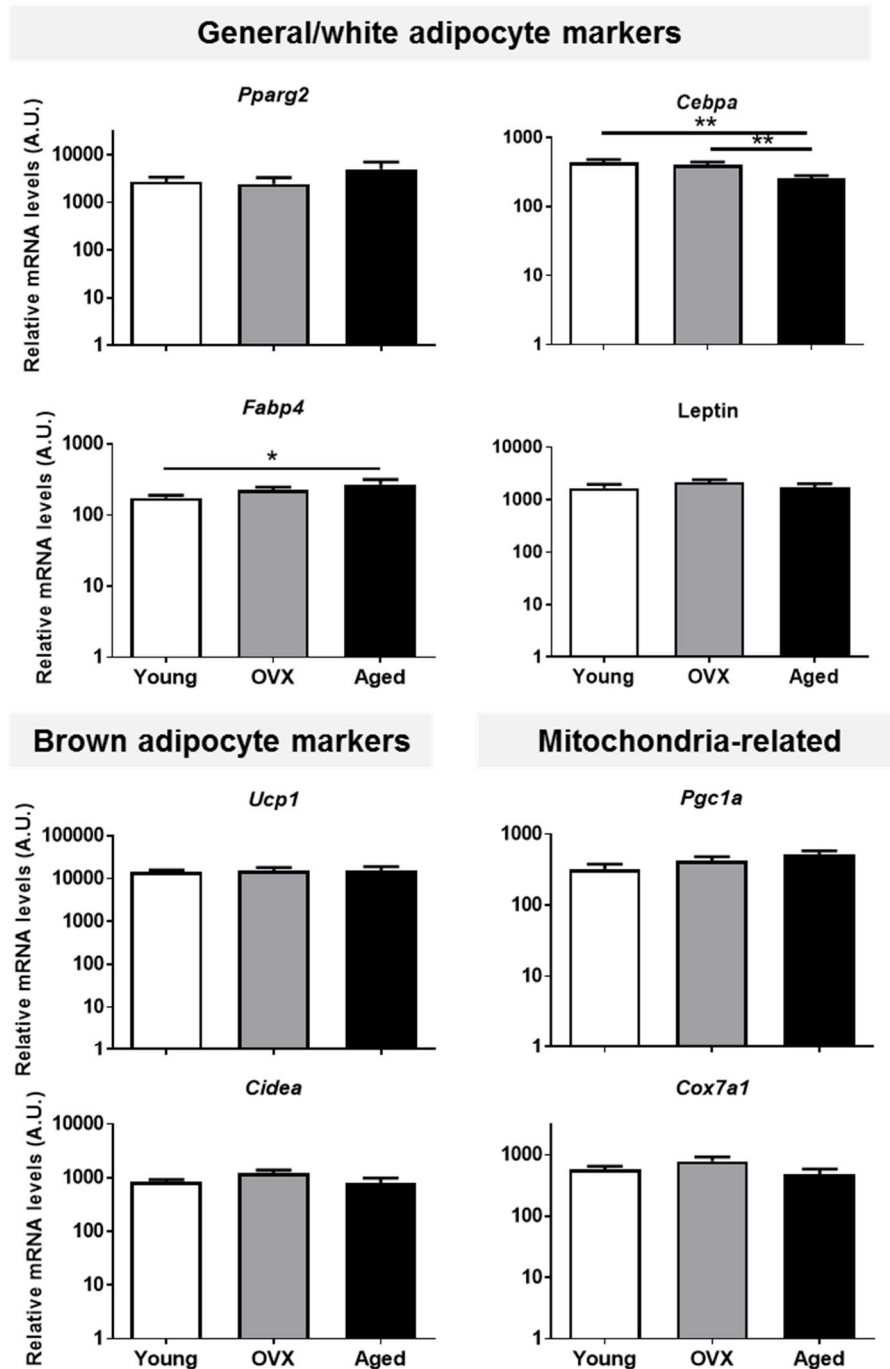


Figure 6.3: Aging and ovariectomy do not influence the expression of brown adipocyte markers in ingWAT of Sv/129 female mice. IngWAT was excised from young (three-months old, n = 8), OVX (three-months old, n = 8) and aged (19-months old, n = 8) Sv/129 mice four weeks following intramuscular injection of glycerol. Data are shown as mean and S.E.M. of relative mRNA levels (in A.U.) of general adipocyte markers, brown adipocyte markers and mitochondria-related genes normalized to expression levels of 18S rRNA. * p < 0.05, ** p < 0.01, one-way ANOVA and Bonferroni post hoc test.

Aging impairs UCP1 expression in differentiated FAPs

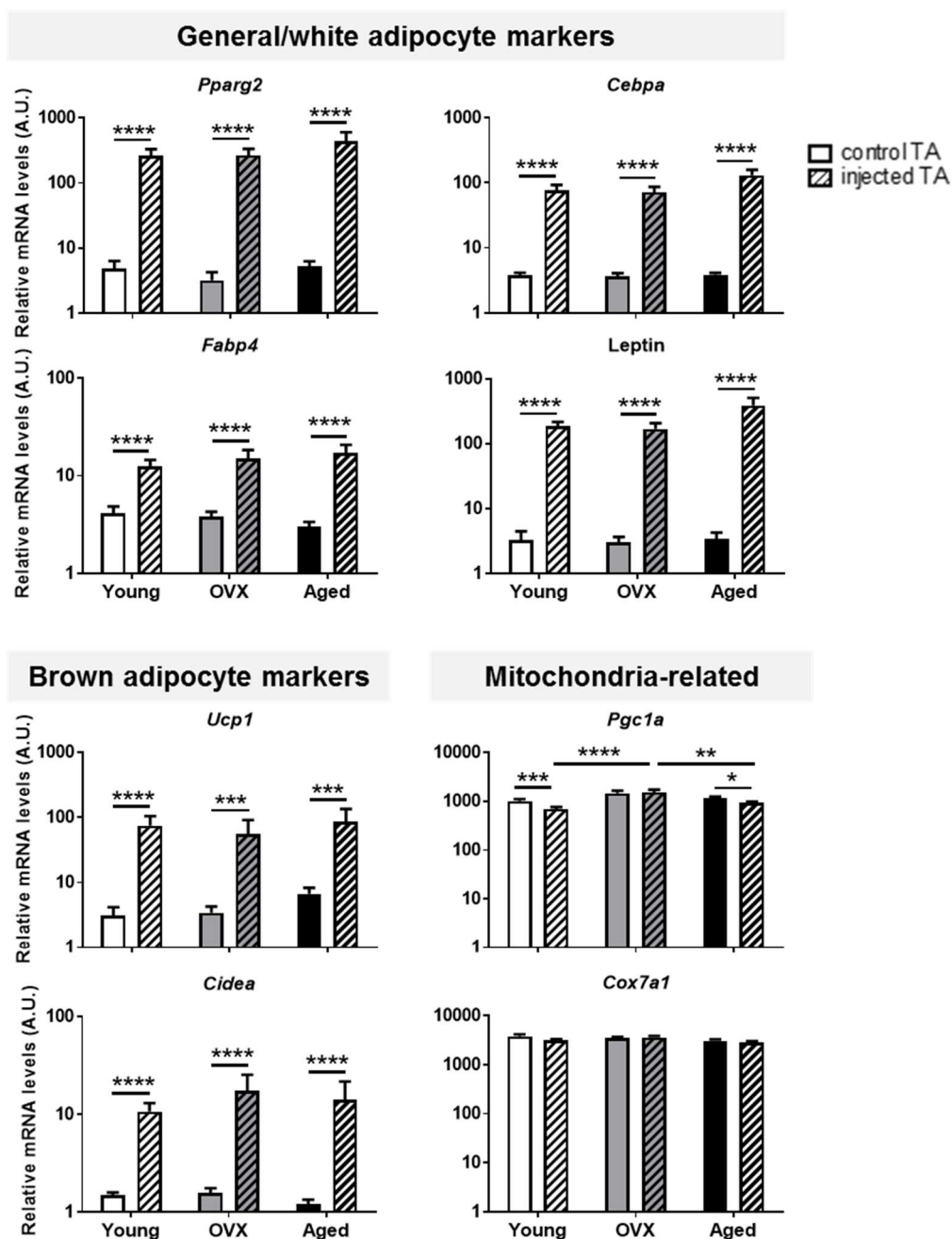


Figure 6.4.: Aging and ovariectomy do not influence the expression of most brown adipocyte markers in fatty-infiltrated skeletal muscle of Sv/129 female mice. Glycerol-injected and control TA skeletal muscles were excised from young (three-months old, n = 5), OVX (three-months old, n = 5) and aged (19-months old, n = 5) Sv/129 mice four weeks following intramuscular injection of glycerol. Data are shown as mean and S.E.M. of relative mRNA levels (in A.U.) of general adipocyte markers, brown adipocyte markers and mitochondria-related genes normalized to expression levels of 18S rRNA. * p < 0.05, ** p < 0.01, *** p < 0.001, **** p < 0.0001, two-way ANOVA and Bonferroni post hoc test.

Aging impairs UCP1 expression in differentiated FAPs

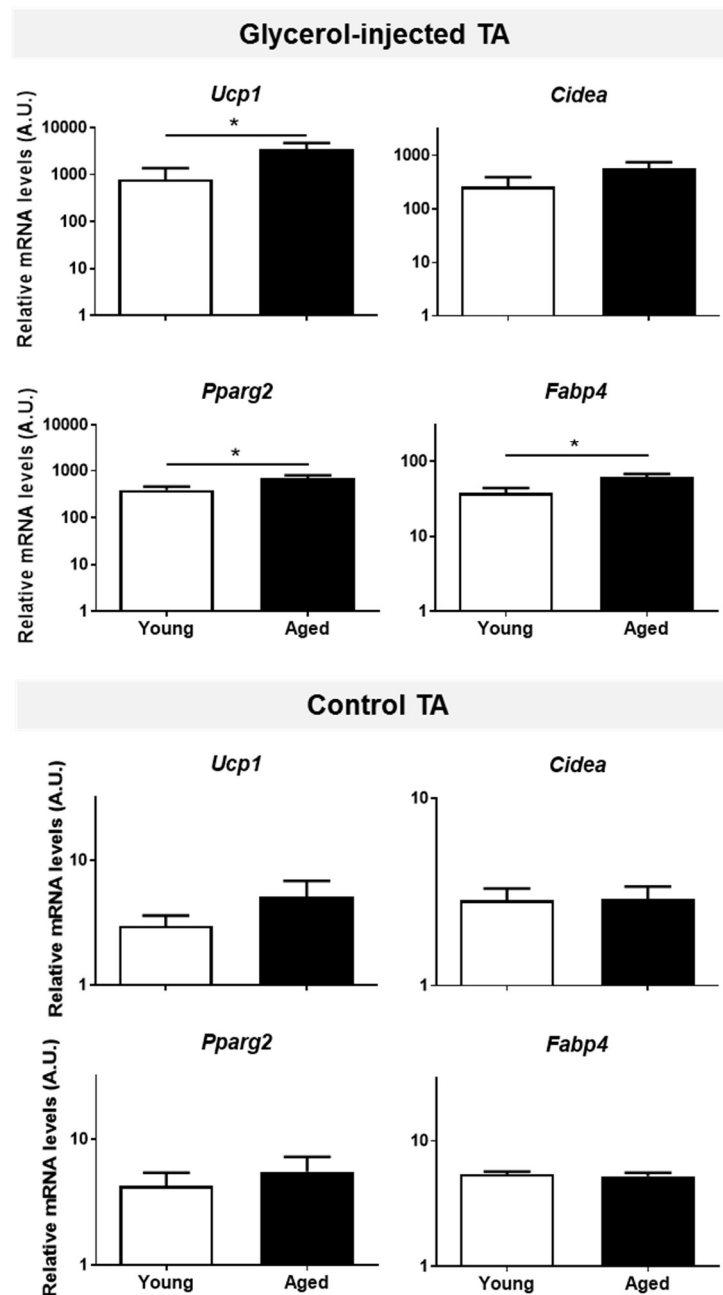


Figure 6.5: CL316-induced upregulation of *Ucp1* mRNA expression in fatty-infiltrated skeletal muscle is not impaired in aged female Sv/129 mice. Glycerol-injected and control TA skeletal muscles were excised from young (two-months old, n = 5) and aged (23-months old, n = 5) Sv/129 female mice at the end of a five-day daily treatment with CL316 started four weeks following intramuscular injection of glycerol. Data are shown as mean and S.E.M. of relative mRNA levels (in A.U.) of general and brown adipocyte markers normalized to expression levels of 18S rRNA. * p < 0.05, ** p < 0.01, *** p < 0.001, **** p < 0.0001, two-way ANOVA and Bonferroni post hoc test.

Aging impairs UCP1 expression in differentiated FAPs

7. Conclusions and Outlook

The deposition of intramuscular adipocytes can affect skeletal muscle metabolism and is associated with poor prognosis in several diseases. Currently, there is no treatment to eliminate adipocytes residing between myofibers, but shifting their phenotype towards that of metabolically, more active brown adipocytes could minimize their adverse effects on neighboring cells and on the tissue microenvironment. To achieve this, the ability of different precursor cells to acquire a brown adipocyte-like phenotype and the factors regulating their differentiation have to be better understood.

In Chapter 4 of this doctoral thesis, we show that primary skeletal muscle FAPs, but not MPs, are able to differentiate into brown-like, UCP1-positive adipocytes in response to treatment with a brown-adipogenic treatment. Similarly to brown and brite adipocytes from other adipose tissue depots, these cells display increased UCP1 levels when the thyroid hormone T3 is added to the induction and differentiation media. Resembling previous results from studies on adipocyte progenitors from skeletal muscle and from classical adipose tissue depots, cultured FAPs from obesity-resistant Sv/129 mice expressed higher UCP1 levels following differentiation than FAPs from obesity-prone C57Bl/6 mice; this difference was also observed *in vivo*, with Sv/129 mice displaying higher *Ucp1* mRNA expression in fatty-infiltrated muscles than C57Bl/6 mice. Interestingly, we observed that FAPs isolated from female mice reach a higher UCP1 expression level following brown adipogenic differentiation than FAPs isolated from male mice, identifying a novel factor regulating UCP1 expression in these cells. Since we could observe upregulation of *Ucp1* expression in skeletal muscle during fatty infiltration in Sv/129, but not C57Bl/6 mice, we chose Sv/129 mice as a model to further investigate the differentiation of FAPs into brown-like adipocytes.

The responsiveness of *Ucp1* expression in fatty-infiltrated skeletal muscle to B3-adrenergic receptor stimulation through CL316 injections, mirroring classical brown adipocytes (Chapter 4), prompted us to study how intramuscular FAPs and adipocytes respond to other factors known to affect the differentiation and/or activation of brown and brite adipocytes in other BAT and WAT depots, namely high-fat diet-feeding and exercise training. As described in Chapter 5, we observed that fatty-infiltrated skeletal muscle responds to high-fat diet feeding similarly to ingWAT, i.e., with an increase in leptin mRNA levels, but no regulation of *Ucp1* mRNA expression. Importantly, FAPs from HFD animals retained their ability to differentiate into UCP1-positive adipocytes, suggesting that, at least at the early stages of diet-induced metabolic disturbance, FAPs are still a plausible target

Conclusions and Outlook

for interventions aiming at intramuscular-adipocyte browning. Exercise-training status did not influence *Ucp1* expression in skeletal muscle during glycerol-induced fatty infiltration and UCP1 protein levels in FAPs differentiated into brown-like adipocytes *in vitro*. While this suggests that exercise training does not affect the capacity of FAPs to differentiate into UCP1-positive cells at the progenitor level, further experiments are needed to clarify whether exercise training can promote the transdifferentiation of intramuscular white adipocytes into brown or brite adipocytes. Interestingly, *Ucp1* expression in ingWAT of exercise-trained mice was higher than in untrained mice four weeks after the end of the training period, despite no differences immediately after it. Thus, the higher *Ucp1* mRNA expression in exercise-trained mice could result from indirect effects of endurance exercise training, such as diminished body insulation due to adipose tissue loss.

Additionally, we showed that aging, but not ovariectomy, decreases UCP1 expression in FAPs following brown adipogenic differentiation *in vitro*, though *Ucp1* mRNA levels in skeletal muscle during fatty infiltration *in vivo* were not decreased in ovariectomized or aged mice (Chapter 6). Together with the study on high-fat diet feeding (Chapter 5), the results from ovariectomized mice contribute to the notion that, at least in obesity-resistant Sv/129 mice, FAPs retain their ability to differentiate into UCP1-positive cells under different metabolic conditions that are commonly related to impaired skeletal muscle function. The results from the *in vitro* experiments using FAPs from aged mice, on the other hand, show that FAP function and plasticity can be affected by aging, similarly to what has been previously observed in other stem cell populations. Comparing the proteome of FAPs from young and aged mice could lead to the identification of targets to promote the brown-adipocyte phenotype in intramuscular adipocytes from aged mice. The confirmation of these results in human cells could suggest FAPs as a possible target to improve fatty-infiltrated skeletal muscle function in estrogen-deficient and/or older patients.

Intriguingly, the differences in UCP1 expression observed *in vitro* between FAPs isolated from male and female mice (Figure 4.13) and between FAPs isolated from young and aged mice (Figure 6.2) were not observed in *in vivo* experiments with glycerol-induced skeletal muscle fatty infiltration. We speculate that this could reflect the exposure of FAPs to stronger signals promoting the brown adipocyte phenotype *in vitro*, such as activation of thyroid hormone receptor and PPAR γ . If sex or aging affected these pathways, our *in vivo* model would be less sensitive to detect these differences. Furthermore, we assessed only mRNA levels of *Ucp1* in fatty infiltrated skeletal muscle, and cannot rule out that sex and age effects could have been detected at the protein level.

When comparing the response of fatty-infiltrated skeletal muscle of young and aged mice to treatment with the B3-adrenergic receptor agonist CL316, we observed higher mRNA expression of both brown and general adipocyte markers in the aged group. Thus, the higher *Ucp1* expression in the muscles from aged mice could merely result from increased adipogenesis. Since skeletal muscle from the two experimental groups seems to have been affected by adipocyte infiltration to different extents, histological analysis of fatty-infiltrated muscles and evaluation of the ratio between brown-like and white intramuscular adipocytes are needed to better understand the effects of aging on intramuscular brown adipocyte deposition *in vivo*. Furthermore, it would be interesting to investigate whether *Ucp1* expression in response to other potentially browning agents (for example, rosiglitazone) is affected by sex and aging *in vivo*.

The effect of FAP-derived brown-like adipocytes on myofiber function remains to be elucidated. While it is known that white adipocytes from classical and ectopic depots can impair myofiber metabolism, it is still not clear whether brown adipocytes could improve the fatty-infiltrated skeletal muscle microenvironment by secreting different adipokines and taking up excessive glucose from the circulation. Studies to address this matter could include *in vitro* treatment of myotubes with conditioned-medium from FAP-derived brown and white adipocytes, as well as co-culture of myotubes and FAP-derived brown and white adipocytes, and *in vivo* experiments assessing how fatty-infiltrated skeletal muscle function and metabolism are affected by intramuscular brown-like or white adipocytes. For example, based on the nearly ten-fold difference in *Ucp1* expression and on the increased number of UCP1-positive adipocytes observed in mice treated with CL316 compared to control mice (Figure 4.6), glucose uptake by fatty-infiltrated skeletal muscle in response to insulin could be assessed in these two groups. Additionally, myofibers could be isolated from fatty-infiltrated skeletal muscle of both groups for analysis of expression and phosphorylation of proteins involved in anabolic pathways (for example, mammalian target of rapamycin and p70-S6K).

Given the capacity for differentiation into brown-like adipocytes and the responsiveness to signals known to affect brown and white adipocytes, skeletal muscle FAPs could also be used as a model to understand the mechanisms behind the acquisition of a brown-adipocyte phenotype in adipogenic progenitors from other tissues. For this, direct comparisons between progenitors from WAT, BAT and skeletal muscle regarding differentiation, UCP1 expression levels and functional characterization would be needed. Furthermore, we observed that FAPs become senescent considerably early following isolation and differentiate poorly when trypsinized and replated, a feature also observed in cells isolated from WAT or BAT under the culture conditions used in our experiments. Thus,

Conclusions and Outlook

the establishment of culture conditions prolonging the maintenance of FAP stemness and proliferation before senescence, or the production of a FAP immortalized cell line could be of great value to further dissect FAP function and differentiation.

Future studies shall test whether the results presented here are also valid for human FAPs. The few studies on human skeletal muscle FAPs have shown that these cells acquire a white-adipocyte phenotype following adipogenic differentiation. However, these studies include experiments with FAPs passaged before differentiation, sorted following *ex vivo* expansion and/or differentiated with lower concentrations of T3. Thus, these differences in cell culture methods compared to our experiments could have contributed to the low or absent levels of *Ucp1* expression observed in other studies. Confirming the ability of human FAPs to differentiate into brown-like adipocytes would open room for the development of new therapies aiming at improved skeletal muscle health through increased brown adipogenesis at the expense of white adipogenesis.

Finally, since intramuscular adipocyte deposition is rare in mice, we used an artificial model of skeletal muscle injury and fatty degeneration to study FAP adipogenic differentiation *in vivo*, through which we were able to show that intramuscular *Ucp1* expression increases with adipocyte deposition in an obesity-resistant mouse strain. Additional experiments should analyze whether FAPs retain their ability to differentiate into brown-like adipocytes in human skeletal muscle affected by fatty-infiltration due to sarcopenia, atrophy, obesity, tendon tears and other clinical conditions.

8. References

1. Ng, M., et al., *Global, regional, and national prevalence of overweight and obesity in children and adults during 1980-2013: a systematic analysis for the Global Burden of Disease Study 2013*. Lancet, 2014. **384**(9945): p. 766-81.
2. Collaboration, N.C.D.R.F., *Trends in adult body-mass index in 200 countries from 1975 to 2014: a pooled analysis of 1698 population-based measurement studies with 19.2 million participants*. Lancet, 2016. **387**(10026): p. 1377-96.
3. Mescher, A.L. and L.C. Junqueira, *Junqueira's basic histology text & atlas*. 13th ed. 2013, New York, N.Y.: McGraw-Hill Education. Online-Ressource.
4. Mauriege, P., et al., *Regional variation in adipose tissue lipolysis in lean and obese men*. J Lipid Res, 1991. **32**(10): p. 1625-33.
5. Soronen, J., et al., *Adipose tissue gene expression analysis reveals changes in inflammatory, mitochondrial respiratory and lipid metabolic pathways in obese insulin-resistant subjects*. BMC Med Genomics, 2012. **5**: p. 9.
6. Skurk, T., et al., *Relationship between adipocyte size and adipokine expression and secretion*. J Clin Endocrinol Metab, 2007. **92**(3): p. 1023-33.
7. Hotamisligil, G.S., N.S. Shargill, and B.M. Spiegelman, *Adipose expression of tumor necrosis factor-alpha: direct role in obesity-linked insulin resistance*. Science, 1993. **259**(5091): p. 87-91.
8. Fain, J.N., et al., *Resistin release by human adipose tissue explants in primary culture*. Biochem Biophys Res Commun, 2003. **300**(3): p. 674-8.
9. Maachi, M., et al., *Systemic low-grade inflammation is related to both circulating and adipose tissue TNFalpha, leptin and IL-6 levels in obese women*. Int J Obes Relat Metab Disord, 2004. **28**(8): p. 993-7.
10. Almind, K., et al., *Ectopic brown adipose tissue in muscle provides a mechanism for differences in risk of metabolic syndrome in mice*. Proc Natl Acad Sci U S A, 2007. **104**(7): p. 2366-71.
11. Stanford, K.I., et al., *A novel role for subcutaneous adipose tissue in exercise-induced improvements in glucose homeostasis*. Diabetes, 2015. **64**(6): p. 2002-14.
12. Chaurasia, B., et al., *Adipocyte Ceramides Regulate Subcutaneous Adipose Browning, Inflammation, and Metabolism*. Cell Metab, 2016. **24**(6): p. 820-834.
13. Jue, T., et al., *Direct observation of glycogen synthesis in human muscle with ¹³C NMR*. Proc Natl Acad Sci U S A, 1989. **86**(12): p. 4489-91.
14. Shulman, G.I., et al., *Quantitation of muscle glycogen synthesis in normal subjects and subjects with non-insulin-dependent diabetes by ¹³C nuclear magnetic resonance spectroscopy*. N Engl J Med, 1990. **322**(4): p. 223-8.
15. Barbatelli, G., et al., *The emergence of cold-induced brown adipocytes in mouse white fat depots is determined predominantly by white to brown adipocyte transdifferentiation*. Am J Physiol Endocrinol Metab, 2010. **298**(6): p. E1244-53.
16. Rosenwald, M., et al., *Bi-directional interconversion of brite and white adipocytes*. Nat Cell Biol, 2013. **15**(6): p. 659-67.
17. Himms-Hagen, J., et al., *Multilocular fat cells in WAT of CL-316243-treated rats derive directly from white adipocytes*. Am J Physiol Cell Physiol, 2000. **279**(3): p. C670-81.
18. Nakamura, Y., et al., *FABP3 and brown adipocyte-characteristic mitochondrial fatty acid oxidation enzymes are induced in beige cells in a different pathway from UCP1*. Biochem Biophys Res Commun, 2013. **441**(1): p. 42-6.
19. Guerra, C., et al., *Emergence of brown adipocytes in white fat in mice is under genetic control. Effects on body weight and adiposity*. J Clin Invest, 1998. **102**(2): p. 412-20.

References

20. Gallagher, D., et al., *Adipose tissue distribution is different in type 2 diabetes*. Am J Clin Nutr, 2009. **89**(3): p. 807-14.
21. Marcus, R.L., et al., *Intramuscular adipose tissue, sarcopenia, and mobility function in older individuals*. J Aging Res, 2012. **2012**: p. 629637.
22. Shaw, H.B., *A Contribution to the Study of the Morphology of Adipose Tissue*. J Anat Physiol, 1901. **36**(Pt 1): p. 1-13.
23. Akabas, S.R., *Textbook of obesity biological, psychological and cultural influences*. 2012, Chichester: Wiley-Blackwell. 479 S.
24. Leblanc, J., *Subcutaneous fat and skin temperature*. Can J Biochem Physiol, 1954. **32**(4): p. 354-8.
25. Baker, P.T. and F. Daniels, Jr., *Relationship between skinfold thickness and body cooling for two hours at 15 degrees C*. J Appl Physiol, 1956. **8**(4): p. 409-16.
26. Sjostrom, L. and P. Bjorntorp, *Body composition and adipose cellularity in human obesity*. Acta Med Scand, 1974. **195**(3): p. 201-11.
27. Jeffery, E., et al., *Rapid depot-specific activation of adipocyte precursor cells at the onset of obesity*. Nat Cell Biol, 2015. **17**(4): p. 376-85.
28. Jeffery, E., et al., *The Adipose Tissue Microenvironment Regulates Depot-Specific Adipogenesis in Obesity*. Cell Metab, 2016. **24**(1): p. 142-50.
29. Waki, H. and P. Tontonoz, *Endocrine functions of adipose tissue*. Annu Rev Pathol, 2007. **2**: p. 31-56.
30. Mitchell, J.B., et al., *Immunophenotype of human adipose-derived cells: temporal changes in stromal-associated and stem cell-associated markers*. Stem Cells, 2006. **24**(2): p. 376-85.
31. Cinti, S., et al., *Immunohistochemical localization of leptin and uncoupling protein in white and brown adipose tissue*. Endocrinology, 1997. **138**(2): p. 797-804.
32. Tauchi-Sato, K., et al., *The surface of lipid droplets is a phospholipid monolayer with a unique Fatty Acid composition*. J Biol Chem, 2002. **277**(46): p. 44507-12.
33. Greenberg, A.S., et al., *Perilipin, a major hormonally regulated adipocyte-specific phosphoprotein associated with the periphery of lipid storage droplets*. J Biol Chem, 1991. **266**(17): p. 11341-6.
34. Puri, V., et al., *Fat-specific protein 27, a novel lipid droplet protein that enhances triglyceride storage*. J Biol Chem, 2007. **282**(47): p. 34213-8.
35. Nishino, N., et al., *FSP27 contributes to efficient energy storage in murine white adipocytes by promoting the formation of unilocular lipid droplets*. J Clin Invest, 2008. **118**(8): p. 2808-21.
36. Granneman, J.G., et al., *Analysis of lipolytic protein trafficking and interactions in adipocytes*. J Biol Chem, 2007. **282**(8): p. 5726-35.
37. Yu, J., et al., *Lipid droplet remodeling and interaction with mitochondria in mouse brown adipose tissue during cold treatment*. Biochim Biophys Acta, 2015. **1853**(5): p. 918-28.
38. Cinti, S., *Transdifferentiation properties of adipocytes in the adipose organ*. Am J Physiol Endocrinol Metab, 2009. **297**(5): p. E977-86.
39. Green, A. and E.A. Newsholme, *Sensitivity of glucose uptake and lipolysis of white adipocytes of the rat to insulin and effects of some metabolites*. Biochem J, 1979. **180**(2): p. 365-70.
40. Dimitriadis, G., et al., *Insulin effects in muscle and adipose tissue*. Diabetes Res Clin Pract, 2011. **93** Suppl 1: p. S52-9.
41. Duncan, R.E., et al., *Regulation of lipolysis in adipocytes*. Annu Rev Nutr, 2007. **27**: p. 79-101.
42. Hassan, M., N. Latif, and M. Yacoub, *Adipose tissue: friend or foe?* Nat Rev Cardiol, 2012. **9**(12): p. 689-702.
43. Vitali, A., et al., *The adipose organ of obesity-prone C57BL/6J mice is composed of mixed white and brown adipocytes*. J Lipid Res, 2012. **53**(4): p. 619-29.

44. Murano, I., C. Zingaretti, and S. Cinti, *The adipose organ of SV129 mice contains a prevalence of brown adipocytes and shows plasticity after cold exposure*. *Adipocytes*, 2005. **1**(2): p. 121-130.
45. Frontini, A. and S. Cinti, *Distribution and development of brown adipocytes in the murine and human adipose organ*. *Cell Metab*, 2010. **11**(4): p. 253-6.
46. Tanko, L.B., et al., *Peripheral adiposity exhibits an independent dominant antiatherogenic effect in elderly women*. *Circulation*, 2003. **107**(12): p. 1626-31.
47. Porter, S.A., et al., *Abdominal subcutaneous adipose tissue: a protective fat depot?* *Diabetes Care*, 2009. **32**(6): p. 1068-75.
48. Lemieux, S., et al., *Seven-year changes in body fat and visceral adipose tissue in women. Association with indexes of plasma glucose-insulin homeostasis*. *Diabetes Care*, 1996. **19**(9): p. 983-91.
49. Parlee, S.D., et al., *Quantifying size and number of adipocytes in adipose tissue*. *Methods Enzymol*, 2014. **537**: p. 93-122.
50. Joe, A.W., et al., *Depot-specific differences in adipogenic progenitor abundance and proliferative response to high-fat diet*. *Stem Cells*, 2009. **27**(10): p. 2563-70.
51. Cannon, B. and J. Nedergaard, *Brown adipose tissue: function and physiological significance*. *Physiol Rev*, 2004. **84**(1): p. 277-359.
52. Hillman, N.H., S.G. Kallapur, and A.H. Jobe, *Physiology of transition from intrauterine to extrauterine life*. *Clin Perinatol*, 2012. **39**(4): p. 769-83.
53. Nedergaard, J., T. Bengtsson, and B. Cannon, *Unexpected evidence for active brown adipose tissue in adult humans*. *Am J Physiol Endocrinol Metab*, 2007. **293**(2): p. E444-52.
54. Cypess, A.M., et al., *Identification and importance of brown adipose tissue in adult humans*. *N Engl J Med*, 2009. **360**(15): p. 1509-17.
55. Virtanen, K.A., et al., *Functional brown adipose tissue in healthy adults*. *N Engl J Med*, 2009. **360**(15): p. 1518-25.
56. van den Beukel, J.C., et al., *Women have more potential to induce browning of perirenal adipose tissue than men*. *Obesity (Silver Spring)*, 2015. **23**(8): p. 1671-9.
57. Cypess, A.M., et al., *Cold but not sympathomimetics activates human brown adipose tissue in vivo*. *Proc Natl Acad Sci U S A*, 2012. **109**(25): p. 10001-5.
58. van Marken Lichtenbelt, W.D., et al., *Cold-activated brown adipose tissue in healthy men*. *N Engl J Med*, 2009. **360**(15): p. 1500-8.
59. Nnodim, J.O. and J.D. Lever, *Neural and vascular provisions of rat interscapular brown adipose tissue*. *Am J Anat*, 1988. **182**(3): p. 283-93.
60. Asano, A., et al., *Adrenergic activation of vascular endothelial growth factor mRNA expression in rat brown adipose tissue: implication in cold-induced angiogenesis*. *Biochem J*, 1997. **328 (Pt 1)**: p. 179-83.
61. Wang, H., et al., *Unique regulation of adipose triglyceride lipase (ATGL) by perilipin 5, a lipid droplet-associated protein*. *J Biol Chem*, 2011. **286**(18): p. 15707-15.
62. Puri, V., et al., *Cidea is associated with lipid droplets and insulin sensitivity in humans*. *Proc Natl Acad Sci U S A*, 2008. **105**(22): p. 7833-8.
63. Barneda, D., et al., *The brown adipocyte protein CIDEA promotes lipid droplet fusion via a phosphatidic acid-binding amphipathic helix*. *Elife*, 2015. **4**: p. e07485.
64. Villarroya, F., et al., *Brown adipose tissue as a secretory organ*. *Nat Rev Endocrinol*, 2017. **13**(1): p. 26-35.
65. Young, J.B., et al., *Effect of diet and cold exposure on norepinephrine turnover in brown adipose tissue of the rat*. *J Clin Invest*, 1982. **69**(5): p. 1061-71.
66. Grujic, D., et al., *Beta3-adrenergic receptors on white and brown adipocytes mediate beta3-selective agonist-induced effects on energy expenditure, insulin secretion, and food intake. A study using transgenic and gene knockout mice*. *J Biol Chem*, 1997. **272**(28): p. 17686-93.

References

67. Granneman, J.G., *Norepinephrine infusions increase adenylate cyclase responsiveness in brown adipose tissue*. J Pharmacol Exp Ther, 1988. **245**(3): p. 1075-80.
68. Gallardo-Montejano, V.I., et al., *Nuclear Perilipin 5 integrates lipid droplet lipolysis with PGC-1alpha/SIRT1-dependent transcriptional regulation of mitochondrial function*. Nat Commun, 2016. **7**: p. 12723.
69. Stralfors, P., P. Bjorgell, and P. Befrage, *Hormonal regulation of hormone-sensitive lipase in intact adipocytes: identification of phosphorylated sites and effects on the phosphorylation by lipolytic hormones and insulin*. Proc Natl Acad Sci U S A, 1984. **81**(11): p. 3317-21.
70. Anthonsen, M.W., et al., *Identification of novel phosphorylation sites in hormone-sensitive lipase that are phosphorylated in response to isoproterenol and govern activation properties in vitro*. J Biol Chem, 1998. **273**(1): p. 215-21.
71. Cao, W., et al., *p38 mitogen-activated protein kinase is the central regulator of cyclic AMP-dependent transcription of the brown fat uncoupling protein 1 gene*. Mol Cell Biol, 2004. **24**(7): p. 3057-67.
72. Seamon, K.B., W. Padgett, and J.W. Daly, *Forskolin: unique diterpene activator of adenylate cyclase in membranes and in intact cells*. Proc Natl Acad Sci U S A, 1981. **78**(6): p. 3363-7.
73. Rodriguez, A.M., et al., *Opposite actions of testosterone and progesterone on UCP1 mRNA expression in cultured brown adipocytes*. Cell Mol Life Sci, 2002. **59**(10): p. 1714-23.
74. Rehnmark, S., et al., *Alpha- and beta-adrenergic induction of the expression of the uncoupling protein thermogenin in brown adipocytes differentiated in culture*. J Biol Chem, 1990. **265**(27): p. 16464-71.
75. Chen, H.Y., et al., *Synergism between cAMP and PPARgamma Signalling in the Initiation of UCP1 Gene Expression in HIB1B Brown Adipocytes*. PPAR Res, 2013. **2013**: p. 476049.
76. Li, Y., et al., *Taking control over intracellular fatty acid levels is essential for the analysis of thermogenic function in cultured primary brown and brite/beige adipocytes*. EMBO Rep, 2014. **15**(10): p. 1069-76.
77. Cypess, A.M., et al., *Activation of human brown adipose tissue by a beta3-adrenergic receptor agonist*. Cell Metab, 2015. **21**(1): p. 33-8.
78. Hefco, E., et al., *Effect of acute exposure to cold on the activity of the hypothalamic-pituitary-thyroid system*. Endocrinology, 1975. **97**(5): p. 1185-95.
79. Bianco, A.C. and J.E. Silva, *Nuclear 3,5,3'-triiodothyronine (T3) in brown adipose tissue: receptor occupancy and sources of T3 as determined by in vivo techniques*. Endocrinology, 1987. **120**(1): p. 55-62.
80. Rabelo, R., et al., *Delineation of thyroid hormone-responsive sequences within a critical enhancer in the rat uncoupling protein gene*. Endocrinology, 1995. **136**(3): p. 1003-13.
81. Bianco, A.C., X.Y. Sheng, and J.E. Silva, *Triiodothyronine amplifies norepinephrine stimulation of uncoupling protein gene transcription by a mechanism not requiring protein synthesis*. J Biol Chem, 1988. **263**(34): p. 18168-75.
82. de Jesus, L.A., et al., *The type 2 iodothyronine deiodinase is essential for adaptive thermogenesis in brown adipose tissue*. J Clin Invest, 2001. **108**(9): p. 1379-85.
83. Bukowiecki, L.J., A. Geloën, and A.J. Collet, *Proliferation and differentiation of brown adipocytes from interstitial cells during cold acclimation*. Am J Physiol, 1986. **250**(6 Pt 1): p. C880-7.
84. Cousin, B., et al., *Cellular changes during cold acclimation in adipose tissues*. J Cell Physiol, 1996. **167**(2): p. 285-9.
85. Matthias, A., et al., *Thermogenic responses in brown fat cells are fully UCP1-dependent. UCP2 or UCP3 do not substitute for UCP1 in adrenergically or fatty acid-induced thermogenesis*. J Biol Chem, 2000. **275**(33): p. 25073-81.

86. Ricquier, D. and J.C. Kader, *Mitochondrial protein alteration in active brown fat: a sodium dodecyl sulfate-polyacrylamide gel electrophoretic study*. *Biochem Biophys Res Commun*, 1976. **73**(3): p. 577-83.
87. Lodish, H., *Molecular cell biology*. 4th ed. 2000, Basingstoke: Freeman. 1084 S.
88. Bouillaud, F., et al., *The possible proton translocating activity of the mitochondrial uncoupling protein of brown adipose tissue. Reconstitution studies in liposomes*. *FEBS Lett*, 1983. **164**(2): p. 272-6.
89. Fedorenko, A., P.V. Lishko, and Y. Kirichok, *Mechanism of fatty-acid-dependent UCP1 uncoupling in brown fat mitochondria*. *Cell*, 2012. **151**(2): p. 400-13.
90. Crichton, P.G., Y. Lee, and E.R. Kunji, *The molecular features of uncoupling protein 1 support a conventional mitochondrial carrier-like mechanism*. *Biochimie*, 2017. **134**: p. 35-50.
91. Li, Y., T. Fromme, and M. Klingenspor, *Meaningful respirometric measurements of UCP1-mediated thermogenesis*. *Biochimie*, 2017. **134**: p. 56-61.
92. Shabalina, I.G., et al., *Native UCP1 displays simple competitive kinetics between the regulators purine nucleotides and fatty acids*. *J Biol Chem*, 2004. **279**(37): p. 38236-48.
93. Rim, J.S. and L.P. Kozak, *Regulatory motifs for CREB-binding protein and Nfe2l2 transcription factors in the upstream enhancer of the mitochondrial uncoupling protein 1 gene*. *J Biol Chem*, 2002. **277**(37): p. 34589-600.
94. Alvarez, R., et al., *Both retinoic-acid-receptor- and retinoid-X-receptor-dependent signalling pathways mediate the induction of the brown-adipose-tissue-uncoupling-protein-1 gene by retinoids*. *Biochem J*, 2000. **345 Pt 1**: p. 91-7.
95. Alvarez, R., et al., *A novel regulatory pathway of brown fat thermogenesis. Retinoic acid is a transcriptional activator of the mitochondrial uncoupling protein gene*. *J Biol Chem*, 1995. **270**(10): p. 5666-73.
96. Barbera, M.J., et al., *Peroxisome proliferator-activated receptor alpha activates transcription of the brown fat uncoupling protein-1 gene. A link between regulation of the thermogenic and lipid oxidation pathways in the brown fat cell*. *J Biol Chem*, 2001. **276**(2): p. 1486-93.
97. Yubero, P., et al., *CCAAT/enhancer binding proteins alpha and beta are transcriptional activators of the brown fat uncoupling protein gene promoter*. *Biochem Biophys Res Commun*, 1994. **198**(2): p. 653-9.
98. Cousin, B., et al., *Occurrence of brown adipocytes in rat white adipose tissue: molecular and morphological characterization*. *J Cell Sci*, 1992. **103 (Pt 4)**: p. 931-42.
99. Giralt, M. and F. Villarroya, *White, brown, beige/brite: different adipose cells for different functions?* *Endocrinology*, 2013. **154**(9): p. 2992-3000.
100. Seale, P., et al., *PRDM16 controls a brown fat/skeletal muscle switch*. *Nature*, 2008. **454**(7207): p. 961-7.
101. Wu, M.V., et al., *Thermogenic capacity is antagonistically regulated in classical brown and white subcutaneous fat depots by high fat diet and endurance training in rats: impact on whole-body energy expenditure*. *J Biol Chem*, 2014. **289**(49): p. 34129-40.
102. Knudsen, J.G., et al., *Role of IL-6 in exercise training- and cold-induced UCP1 expression in subcutaneous white adipose tissue*. *PLoS One*, 2014. **9**(1): p. e84910.
103. Stanford, K.I., R.J. Middelbeek, and L.J. Goodyear, *Exercise Effects on White Adipose Tissue: Beiging and Metabolic Adaptations*. *Diabetes*, 2015. **64**(7): p. 2361-8.
104. Bostrom, P., et al., *A PGC1-alpha-dependent myokine that drives brown-fat-like development of white fat and thermogenesis*. *Nature*, 2012. **481**(7382): p. 463-8.
105. Rao, R.R., et al., *Meteorin-like is a hormone that regulates immune-adipose interactions to increase beige fat thermogenesis*. *Cell*, 2014. **157**(6): p. 1279-91.

References

106. Ohno, H., et al., *PPARgamma agonists induce a white-to-brown fat conversion through stabilization of PRDM16 protein*. Cell Metab, 2012. **15**(3): p. 395-404.
107. Fisher, F.M., et al., *FGF21 regulates PGC-1alpha and browning of white adipose tissues in adaptive thermogenesis*. Genes Dev, 2012. **26**(3): p. 271-81.
108. Bordicchia, M., et al., *Cardiac natriuretic peptides act via p38 MAPK to induce the brown fat thermogenic program in mouse and human adipocytes*. J Clin Invest, 2012. **122**(3): p. 1022-36.
109. Carriere, A., et al., *Browning of white adipose cells by intermediate metabolites: an adaptive mechanism to alleviate redox pressure*. Diabetes, 2014. **63**(10): p. 3253-65.
110. Schulz, T.J., et al., *Identification of inducible brown adipocyte progenitors residing in skeletal muscle and white fat*. Proc Natl Acad Sci U S A, 2011. **108**(1): p. 143-8.
111. Tseng, Y.H., et al., *New role of bone morphogenetic protein 7 in brown adipogenesis and energy expenditure*. Nature, 2008. **454**(7207): p. 1000-4.
112. Modica, S., et al., *Bmp4 Promotes a Brown to White-like Adipocyte Shift*. Cell Rep, 2016. **16**(8): p. 2243-58.
113. Shan, B., et al., *The metabolic ER stress sensor IRE1alpha suppresses alternative activation of macrophages and impairs energy expenditure in obesity*. Nat Immunol, 2017. **18**(5): p. 519-529.
114. Cannon, B. and J. Nedergaard, *Cultures of adipose precursor cells from brown adipose tissue and of clonal brown-adipocyte-like cell lines*. Methods Mol Biol, 2001. **155**: p. 213-24.
115. Aune, U.L., L. Ruiz, and S. Kajimura, *Isolation and differentiation of stromal vascular cells to beige/brite cells*. J Vis Exp, 2013(73).
116. Timmons, J.A., et al., *Myogenic gene expression signature establishes that brown and white adipocytes originate from distinct cell lineages*. Proc Natl Acad Sci U S A, 2007. **104**(11): p. 4401-6.
117. Sanchez-Gurmaches, J. and D.A. Guertin, *Adipocytes arise from multiple lineages that are heterogeneously and dynamically distributed*. Nat Commun, 2014. **5**: p. 4099.
118. Berry, R. and M.S. Rodeheffer, *Characterization of the adipocyte cellular lineage in vivo*. Nat Cell Biol, 2013. **15**(3): p. 302-8.
119. Lee, Y.H., et al., *In vivo identification of bipotential adipocyte progenitors recruited by beta3-adrenoceptor activation and high-fat feeding*. Cell Metab, 2012. **15**(4): p. 480-91.
120. Rodeheffer, M.S., K. Birsoy, and J.M. Friedman, *Identification of white adipocyte progenitor cells in vivo*. Cell, 2008. **135**(2): p. 240-9.
121. Long, J.Z., et al., *A smooth muscle-like origin for beige adipocytes*. Cell Metab, 2014. **19**(5): p. 810-20.
122. Iwayama, T., et al., *PDGFRalpha signaling drives adipose tissue fibrosis by targeting progenitor cell plasticity*. Genes Dev, 2015. **29**(11): p. 1106-19.
123. Silva, K.R., et al., *Stromal-vascular fraction content and adipose stem cell behavior are altered in morbid obese and post bariatric surgery ex-obese women*. Stem Cell Res Ther, 2015. **6**: p. 72.
124. Carey, A.L., et al., *Reduced UCP-1 content in in vitro differentiated beige/brite adipocytes derived from preadipocytes of human subcutaneous white adipose tissues in obesity*. PLoS One, 2014. **9**(3): p. e91997.
125. Rosen, E.D. and O.A. MacDougald, *Adipocyte differentiation from the inside out*. Nat Rev Mol Cell Biol, 2006. **7**(12): p. 885-96.
126. Bowers, R.R., et al., *Stable stem cell commitment to the adipocyte lineage by inhibition of DNA methylation: role of the BMP-4 gene*. Proc Natl Acad Sci U S A, 2006. **103**(35): p. 13022-7.
127. Gupta, R.K., et al., *Transcriptional control of preadipocyte determination by Zfp423*. Nature, 2010. **464**(7288): p. 619-23.

128. Smas, C.M. and H.S. Sul, *Pref-1, a protein containing EGF-like repeats, inhibits adipocyte differentiation*. Cell, 1993. **73**(4): p. 725-34.
129. Smas, C.M., et al., *Transcriptional repression of pref-1 by glucocorticoids promotes 3T3-L1 adipocyte differentiation*. J Biol Chem, 1999. **274**(18): p. 12632-41.
130. Li, D., et al., *Kruppel-like factor-6 promotes preadipocyte differentiation through histone deacetylase 3-dependent repression of DLK1*. J Biol Chem, 2005. **280**(29): p. 26941-52.
131. Tang, Q.Q. and M.D. Lane, *Adipogenesis: from stem cell to adipocyte*. Annu Rev Biochem, 2012. **81**: p. 715-36.
132. Scott, M.A., et al., *Current methods of adipogenic differentiation of mesenchymal stem cells*. Stem Cells Dev, 2011. **20**(10): p. 1793-804.
133. Kim, S.P., et al., *Transcriptional activation of peroxisome proliferator-activated receptor-gamma requires activation of both protein kinase A and Akt during adipocyte differentiation*. Biochem Biophys Res Commun, 2010. **399**(1): p. 55-9.
134. Zhang, J.W., et al., *Role of CREB in transcriptional regulation of CCAAT/enhancer-binding protein beta gene during adipogenesis*. J Biol Chem, 2004. **279**(6): p. 4471-8.
135. Tang, Q.Q., J.W. Zhang, and M. Daniel Lane, *Sequential gene promoter interactions of C/EBPbeta, C/EBPalpha, and PPARgamma during adipogenesis*. Biochem Biophys Res Commun, 2004. **319**(1): p. 235-9.
136. Hamm, J.K., B.H. Park, and S.R. Farmer, *A role for C/EBPbeta in regulating peroxisome proliferator-activated receptor gamma activity during adipogenesis in 3T3-L1 preadipocytes*. J Biol Chem, 2001. **276**(21): p. 18464-71.
137. Seale, P., et al., *Transcriptional control of brown fat determination by PRDM16*. Cell Metab, 2007. **6**(1): p. 38-54.
138. Kajimura, S., et al., *Regulation of the brown and white fat gene programs through a PRDM16/CtBP transcriptional complex*. Genes Dev, 2008. **22**(10): p. 1397-409.
139. Rosen, E.D., et al., *Transcriptional regulation of adipogenesis*. Genes Dev, 2000. **14**(11): p. 1293-307.
140. Imai, T., et al., *Peroxisome proliferator-activated receptor gamma is required in mature white and brown adipocytes for their survival in the mouse*. Proc Natl Acad Sci U S A, 2004. **101**(13): p. 4543-7.
141. Janssen, I., et al., *Skeletal muscle mass and distribution in 468 men and women aged 18-88 yr*. J Appl Physiol (1985), 2000. **89**(1): p. 81-8.
142. Baar, K. and K. Esser, *Phosphorylation of p70(S6k) correlates with increased skeletal muscle mass following resistance exercise*. Am J Physiol, 1999. **276**(1 Pt 1): p. C120-7.
143. Ogasawara, R., et al., *The role of mTOR signalling in the regulation of skeletal muscle mass in a rodent model of resistance exercise*. Sci Rep, 2016. **6**: p. 31142.
144. Lang, S.M., et al., *Delayed recovery of skeletal muscle mass following hindlimb immobilization in mTOR heterozygous mice*. PLoS One, 2012. **7**(6): p. e38910.
145. Wilmet, E., et al., *Longitudinal study of the bone mineral content and of soft tissue composition after spinal cord section*. Paraplegia, 1995. **33**(11): p. 674-7.
146. Castro, M.J., et al., *Influence of complete spinal cord injury on skeletal muscle cross-sectional area within the first 6 months of injury*. Eur J Appl Physiol Occup Physiol, 1999. **80**(4): p. 373-8.
147. Akima, H., et al., *Effect of short-duration spaceflight on thigh and leg muscle volume*. Med Sci Sports Exerc, 2000. **32**(10): p. 1743-7.
148. Contreras, O., et al., *Connective tissue cells expressing fibro/adipogenic progenitor markers increase under chronic damage: relevance in fibroblast-myofibroblast differentiation and skeletal muscle fibrosis*. Cell Tissue Res, 2016. **364**(3): p. 647-60.

References

149. Adams, G.R., B.M. Hather, and G.A. Dudley, *Effect of short-term unweighting on human skeletal muscle strength and size*. *Aviat Space Environ Med*, 1994. **65**(12): p. 1116-21.
150. de Boer, M.D., et al., *The temporal responses of protein synthesis, gene expression and cell signalling in human quadriceps muscle and patellar tendon to disuse*. *J Physiol*, 2007. **585**(Pt 1): p. 241-51.
151. Berg, H.E., et al., *Effects of lower limb unloading on skeletal muscle mass and function in humans*. *J Appl Physiol* (1985), 1991. **70**(4): p. 1882-5.
152. Pagano, A.F., et al., *Muscle Regeneration with Intermuscular Adipose Tissue (IMAT) Accumulation Is Modulated by Mechanical Constraints*. *PLoS One*, 2015. **10**(12): p. e0144230.
153. Alkner, B.A. and P.A. Tesch, *Knee extensor and plantar flexor muscle size and function following 90 days of bed rest with or without resistance exercise*. *Eur J Appl Physiol*, 2004. **93**(3): p. 294-305.
154. Convertino, V.A., D.F. Doerr, and S.L. Stein, *Changes in size and compliance of the calf after 30 days of simulated microgravity*. *J Appl Physiol* (1985), 1989. **66**(3): p. 1509-12.
155. Berg, H.E., et al., *Hip, thigh and calf muscle atrophy and bone loss after 5-week bedrest inactivity*. *Eur J Appl Physiol*, 2007. **99**(3): p. 283-9.
156. Berg, H.E., L. Larsson, and P.A. Tesch, *Lower limb skeletal muscle function after 6 wk of bed rest*. *J Appl Physiol* (1985), 1997. **82**(1): p. 182-8.
157. Metter, E.J., et al., *Age-associated loss of power and strength in the upper extremities in women and men*. *J Gerontol A Biol Sci Med Sci*, 1997. **52**(5): p. B267-76.
158. Walston, J.D., *Sarcopenia in older adults*. *Curr Opin Rheumatol*, 2012. **24**(6): p. 623-7.
159. Exeter, D. and D.A. Connell, *Skeletal muscle: functional anatomy and pathophysiology*. *Semin Musculoskelet Radiol*, 2010. **14**(2): p. 97-105.
160. Schiaffino, S. and C. Reggiani, *Fiber types in mammalian skeletal muscles*. *Physiol Rev*, 2011. **91**(4): p. 1447-531.
161. Pedersen, B.K., *Muscles and their myokines*. *J Exp Biol*, 2011. **214**(Pt 2): p. 337-46.
162. Steinhardt, R.A., G. Bi, and J.M. Alderton, *Cell membrane resealing by a vesicular mechanism similar to neurotransmitter release*. *Science*, 1994. **263**(5145): p. 390-3.
163. Kanda, K., et al., *Eccentric exercise-induced delayed-onset muscle soreness and changes in markers of muscle damage and inflammation*. *Exerc Immunol Rev*, 2013. **19**: p. 72-85.
164. Joe, A.W., et al., *Muscle injury activates resident fibro/adipogenic progenitors that facilitate myogenesis*. *Nat Cell Biol*, 2010. **12**(2): p. 153-63.
165. Uezumi, A., et al., *Fibrosis and adipogenesis originate from a common mesenchymal progenitor in skeletal muscle*. *J Cell Sci*, 2011. **124**(Pt 21): p. 3654-64.
166. Lukjanenko, L., et al., *Genomic profiling reveals that transient adipogenic activation is a hallmark of mouse models of skeletal muscle regeneration*. *PLoS One*, 2013. **8**(8): p. e71084.
167. Pisani, D.F., et al., *Mouse model of skeletal muscle adiposity: a glycerol treatment approach*. *Biochem Biophys Res Commun*, 2010. **396**(3): p. 767-73.
168. Hardy, D., et al., *Comparative Study of Injury Models for Studying Muscle Regeneration in Mice*. *PLoS One*, 2016. **11**(1): p. e0147198.
169. Yin, H., F. Price, and M.A. Rudnicki, *Satellite cells and the muscle stem cell niche*. *Physiol Rev*, 2013. **93**(1): p. 23-67.
170. Garry, G.A., M.L. Antony, and D.J. Garry, *Cardiotoxin Induced Injury and Skeletal Muscle Regeneration*. *Methods Mol Biol*, 2016. **1460**: p. 61-71.

171. Brown, L.A., et al., *Diet-induced obesity alters anabolic signalling in mice at the onset of skeletal muscle regeneration*. *Acta Physiol (Oxf)*, 2015. **215**(1): p. 46-57.
172. Mahdy, M.A., K. Warita, and Y.Z. Hosaka, *Early ultrastructural events of skeletal muscle damage following cardiotoxin-induced injury and glycerol-induced injury*. *Micron*, 2016. **91**: p. 29-40.
173. Mauro, A., *Satellite cell of skeletal muscle fibers*. *J Biophys Biochem Cytol*, 1961. **9**: p. 493-5.
174. Snow, M.H., *Myogenic cell formation in regenerating rat skeletal muscle injured by mincing. I. A fine structural study*. *Anat Rec*, 1977. **188**(2): p. 181-99.
175. Snow, M.H., *Myogenic cell formation in regenerating rat skeletal muscle injured by mincing. II. An autoradiographic study*. *Anat Rec*, 1977. **188**(2): p. 201-17.
176. Kuang, S., et al., *Asymmetric self-renewal and commitment of satellite stem cells in muscle*. *Cell*, 2007. **129**(5): p. 999-1010.
177. Seale, P., et al., *Pax7 is required for the specification of myogenic satellite cells*. *Cell*, 2000. **102**(6): p. 777-86.
178. Blanco-Bose, W.E., et al., *Purification of mouse primary myoblasts based on alpha 7 integrin expression*. *Exp Cell Res*, 2001. **265**(2): p. 212-20.
179. Maesner, C.C., A.E. Almada, and A.J. Wagers, *Established cell surface markers efficiently isolate highly overlapping populations of skeletal muscle satellite cells by fluorescence-activated cell sorting*. *Skelet Muscle*, 2016. **6**: p. 35.
180. Kuang, S., et al., *Distinct roles for Pax7 and Pax3 in adult regenerative myogenesis*. *J Cell Biol*, 2006. **172**(1): p. 103-13.
181. von Maltzahn, J., et al., *Pax7 is critical for the normal function of satellite cells in adult skeletal muscle*. *Proc Natl Acad Sci U S A*, 2013. **110**(41): p. 16474-9.
182. Egner, I.M., J.C. Bruusgaard, and K. Gundersen, *Satellite cell depletion prevents fiber hypertrophy in skeletal muscle*. *Development*, 2016. **143**(16): p. 2898-906.
183. Jackson, J.R., et al., *Reduced voluntary running performance is associated with impaired coordination as a result of muscle satellite cell depletion in adult mice*. *Skelet Muscle*, 2015. **5**: p. 41.
184. Le Grand, F., et al., *Wnt7a activates the planar cell polarity pathway to drive the symmetric expansion of satellite stem cells*. *Cell Stem Cell*, 2009. **4**(6): p. 535-47.
185. Cooper, R.N., et al., *In vivo satellite cell activation via Myf5 and MyoD in regenerating mouse skeletal muscle*. *J Cell Sci*, 1999. **112 (Pt 17)**: p. 2895-901.
186. Asakura, A., M. Komaki, and M. Rudnicki, *Muscle satellite cells are multipotential stem cells that exhibit myogenic, osteogenic, and adipogenic differentiation*. *Differentiation*, 2001. **68**(4-5): p. 245-53.
187. Bernet, J.D., et al., *p38 MAPK signaling underlies a cell-autonomous loss of stem cell self-renewal in skeletal muscle of aged mice*. *Nat Med*, 2014. **20**(3): p. 265-71.
188. Lee, S.R., et al., *Effects of chronic high-fat feeding on skeletal muscle mass and function in middle-aged mice*. *Aging Clin Exp Res*, 2015. **27**(4): p. 403-11.
189. Joannis, S., et al., *Exercise conditioning in old mice improves skeletal muscle regeneration*. *FASEB J*, 2016. **30**(9): p. 3256-68.
190. D'Souza, D.M., et al., *Diet-induced obesity impairs muscle satellite cell activation and muscle repair through alterations in hepatocyte growth factor signaling*. *Physiol Rep*, 2015. **3**(8).
191. Kitajima, Y. and Y. Ono, *Estrogens maintain skeletal muscle and satellite cell functions*. *J Endocrinol*, 2016. **229**(3): p. 267-75.
192. Yin, H., et al., *MicroRNA-133 controls brown adipose determination in skeletal muscle satellite cells by targeting Prdm16*. *Cell Metab*, 2013. **17**(2): p. 210-24.
193. Shefer, G., M. Wleklinski-Lee, and Z. Yablonka-Reuveni, *Skeletal muscle satellite cells can spontaneously enter an alternative mesenchymal pathway*. *J Cell Sci*, 2004. **117**(Pt 22): p. 5393-404.

References

194. Starkey, J.D., et al., *Skeletal muscle satellite cells are committed to myogenesis and do not spontaneously adopt nonmyogenic fates*. *J Histochem Cytochem*, 2011. **59**(1): p. 33-46.
195. Uezumi, A., et al., *Mesenchymal progenitors distinct from satellite cells contribute to ectopic fat cell formation in skeletal muscle*. *Nat Cell Biol*, 2010. **12**(2): p. 143-52.
196. Pisani, D.F., et al., *Hierarchization of myogenic and adipogenic progenitors within human skeletal muscle*. *Stem Cells*, 2010. **28**(12): p. 2182-94.
197. Uezumi, A., et al., *Identification and characterization of PDGFRalpha+ mesenchymal progenitors in human skeletal muscle*. *Cell Death Dis*, 2014. **5**: p. e1186.
198. Agle, C.C., et al., *Human skeletal muscle fibroblasts, but not myogenic cells, readily undergo adipogenic differentiation*. *J Cell Sci*, 2013. **126**(Pt 24): p. 5610-25.
199. Agle, C.C., et al., *Isolation and quantitative immunocytochemical characterization of primary myogenic cells and fibroblasts from human skeletal muscle*. *J Vis Exp*, 2015(95): p. 52049.
200. Arrighi, N., et al., *Characterization of adipocytes derived from fibro/adipogenic progenitors resident in human skeletal muscle*. *Cell Death Dis*, 2015. **6**: p. e1733.
201. Farup, J., et al., *Interactions between muscle stem cells, mesenchymal-derived cells and immune cells in muscle homeostasis, regeneration and disease*. *Cell Death Dis*, 2015. **6**: p. e1830.
202. Heredia, J.E., et al., *Type 2 innate signals stimulate fibro/adipogenic progenitors to facilitate muscle regeneration*. *Cell*, 2013. **153**(2): p. 376-88.
203. Dong, Y., et al., *Glucocorticoids increase adipocytes in muscle by affecting IL-4 regulated FAP activity*. *FASEB J*, 2014. **28**(9): p. 4123-32.
204. Lemos, D.R., et al., *Nilotinib reduces muscle fibrosis in chronic muscle injury by promoting TNF-mediated apoptosis of fibro/adipogenic progenitors*. *Nat Med*, 2015. **21**(7): p. 786-94.
205. Fiore, D., et al., *Pharmacological blockage of fibro/adipogenic progenitor expansion and suppression of regenerative fibrogenesis is associated with impaired skeletal muscle regeneration*. *Stem Cell Res*, 2016. **17**(1): p. 161-9.
206. Lemos, D.R., et al., *Functionally convergent white adipogenic progenitors of different lineages participate in a diffused system supporting tissue regeneration*. *Stem Cells*, 2012. **30**(6): p. 1152-62.
207. De Lisio, M., et al., *Substrate and strain alter the muscle-derived mesenchymal stem cell secretome to promote myogenesis*. *Stem Cell Res Ther*, 2014. **5**(3): p. 74.
208. Valero, M.C., et al., *Eccentric exercise facilitates mesenchymal stem cell appearance in skeletal muscle*. *PLoS One*, 2012. **7**(1): p. e29760.
209. Zou, K., et al., *Mesenchymal stem cells augment the adaptive response to eccentric exercise*. *Med Sci Sports Exerc*, 2015. **47**(2): p. 315-25.
210. Uezumi, A., M. Ikemoto-Uezumi, and K. Tsuchida, *Roles of nonmyogenic mesenchymal progenitors in pathogenesis and regeneration of skeletal muscle*. *Front Physiol*, 2014. **5**: p. 68.
211. Phelps, M., P. Stuelsatz, and Z. Yablonka-Reuveni, *Expression profile and overexpression outcome indicate a role for betaKlotho in skeletal muscle fibro/adipogenesis*. *FEBS J*, 2016. **283**(9): p. 1653-68.
212. Buford, T.W., et al., *Active muscle regeneration following eccentric contraction-induced injury is similar between healthy young and older adults*. *J Appl Physiol* (1985), 2014. **116**(11): p. 1481-90.
213. Manini, T.M., et al., *Reduced physical activity increases intermuscular adipose tissue in healthy young adults*. *Am J Clin Nutr*, 2007. **85**(2): p. 377-84.
214. Goodpaster, B.H., F.L. Thaete, and D.E. Kelley, *Thigh adipose tissue distribution is associated with insulin resistance in obesity and in type 2 diabetes mellitus*. *Am J Clin Nutr*, 2000. **71**(4): p. 885-92.

215. Fischmann, A., et al., *Quantitative MRI and loss of free ambulation in Duchenne muscular dystrophy*. J Neurol, 2013. **260**(4): p. 969-74.
216. Maddocks, M., et al., *Skeletal muscle adiposity is associated with physical activity, exercise capacity and fibre shift in COPD*. Eur Respir J, 2014. **44**(5): p. 1188-98.
217. Gladstone, J.N., et al., *Fatty infiltration and atrophy of the rotator cuff do not improve after rotator cuff repair and correlate with poor functional outcome*. Am J Sports Med, 2007. **35**(5): p. 719-28.
218. Lee, S., et al., *Relationships between insulin sensitivity, skeletal muscle mass and muscle quality in obese adolescent boys*. Eur J Clin Nutr, 2012. **66**(12): p. 1366-8.
219. Choi, S.J., et al., *Intramyocellular Lipid and Impaired Myofiber Contraction in Normal Weight and Obese Older Adults*. J Gerontol A Biol Sci Med Sci, 2016. **71**(4): p. 557-64.
220. Baum, T., et al., *Association of Quadriceps Muscle Fat With Isometric Strength Measurements in Healthy Males Using Chemical Shift Encoding-Based Water-Fat Magnetic Resonance Imaging*. J Comput Assist Tomogr, 2016. **40**(3): p. 447-51.
221. Skurk, T., C. Alberti-Huber, and H. Hauner, *Effect of conditioned media from mature human adipocytes on insulin-stimulated Akt/PKB phosphorylation in human skeletal muscle cells: role of BMI and fat cell size*. Horm Metab Res, 2009. **41**(3): p. 190-6.
222. Dietze, D., et al., *Impairment of insulin signaling in human skeletal muscle cells by co-culture with human adipocytes*. Diabetes, 2002. **51**(8): p. 2369-76.
223. Seyoum, B., A. Fite, and A.B. Abou-Samra, *Effects of 3T3 adipocytes on interleukin-6 expression and insulin signaling in L6 skeletal muscle cells*. Biochem Biophys Res Commun, 2011. **410**(1): p. 13-8.
224. Pellegrinelli, V., et al., *Human adipocytes induce inflammation and atrophy in muscle cells during obesity*. Diabetes, 2015. **64**(9): p. 3121-34.
225. Mogi, M., et al., *Diabetic mice exhibited a peculiar alteration in body composition with exaggerated ectopic fat deposition after muscle injury due to anomalous cell differentiation*. J Cachexia Sarcopenia Muscle, 2016. **7**(2): p. 213-24.
226. Biltz, N.K. and G.A. Meyer, *A novel method for the quantification of fatty infiltration in skeletal muscle*. Skelet Muscle, 2017. **7**: p. 1.
227. Mahdy, M.A., et al., *Comparative study of muscle regeneration following cardiotoxin and glycerol injury*. Ann Anat, 2015. **202**: p. 18-27.
228. Liu, W., et al., *Intramuscular adipose is derived from a non-Pax3 lineage and required for efficient regeneration of skeletal muscles*. Dev Biol, 2012. **361**(1): p. 27-38.
229. Li, Y., et al., *Intrinsic differences in BRITE adipogenesis of primary adipocytes from two different mouse strains*. Biochim Biophys Acta, 2014. **1841**(9): p. 1345-52.
230. Crisan, M., et al., *A reservoir of brown adipocyte progenitors in human skeletal muscle*. Stem Cells, 2008. **26**(9): p. 2425-33.
231. Vogeser, M., et al., *Fasting serum insulin and the homeostasis model of insulin resistance (HOMA-IR) in the monitoring of lifestyle interventions in obese persons*. Clin Biochem, 2007. **40**(13-14): p. 964-8.
232. Galimov, A., et al., *MicroRNA-29a in Adult Muscle Stem Cells Controls Skeletal Muscle Regeneration During Injury and Exercise Downstream of Fibroblast Growth Factor-2*. Stem Cells, 2016. **34**(3): p. 768-80.
233. Laemmli, U.K., *Cleavage of structural proteins during the assembly of the head of bacteriophage T4*. Nature, 1970. **227**(5259): p. 680-5.
234. Yoshida, T., et al., *beta 3-Adrenergic agonist induces a functionally active uncoupling protein in fat and slow-twitch muscle fibers*. Am J Physiol, 1998. **274**(3 Pt 1): p. E469-75.
235. Nagase, I., et al., *Expression of uncoupling protein in skeletal muscle and white fat of obese mice treated with thermogenic beta 3-adrenergic agonist*. J Clin Invest, 1996. **97**(12): p. 2898-904.

References

236. Jacobsson, A., et al., *The uncoupling protein thermogenin during acclimation: indications for pretranslational control*. Am J Physiol, 1994. **267**(4 Pt 2): p. R999-1007.
237. Rosell, M., et al., *Brown and white adipose tissues: intrinsic differences in gene expression and response to cold exposure in mice*. Am J Physiol Endocrinol Metab, 2014. **306**(8): p. E945-64.
238. Ricquier, D., et al., *Expression of uncoupling protein mRNA in thermogenic or weakly thermogenic brown adipose tissue. Evidence for a rapid beta-adrenoreceptor-mediated and transcriptionally regulated step during activation of thermogenesis*. J Biol Chem, 1986. **261**(30): p. 13905-10.
239. Mita, T., et al., *FABP4 is secreted from adipocytes by adenyl cyclase-PKA- and guanylyl cyclase-PKG-dependent lipolytic mechanisms*. Obesity (Silver Spring), 2015. **23**(2): p. 359-67.
240. Bianco, A.C. and J.E. Silva, *Intracellular conversion of thyroxine to triiodothyronine is required for the optimal thermogenic function of brown adipose tissue*. J Clin Invest, 1987. **79**(1): p. 295-300.
241. Christoffolete, M.A., et al., *Mice with targeted disruption of the Dio2 gene have cold-induced overexpression of the uncoupling protein 1 gene but fail to increase brown adipose tissue lipogenesis and adaptive thermogenesis*. Diabetes, 2004. **53**(3): p. 577-84.
242. Guerra, C., et al., *Triiodothyronine induces the transcription of the uncoupling protein gene and stabilizes its mRNA in fetal rat brown adipocyte primary cultures*. J Biol Chem, 1996. **271**(4): p. 2076-81.
243. Lee, J.Y., et al., *Triiodothyronine induces UCP-1 expression and mitochondrial biogenesis in human adipocytes*. Am J Physiol Cell Physiol, 2012. **302**(2): p. C463-72.
244. Rodriguez-Cuenca, S., et al., *Sex-dependent thermogenesis, differences in mitochondrial morphology and function, and adrenergic response in brown adipose tissue*. J Biol Chem, 2002. **277**(45): p. 42958-63.
245. Frontini, A., et al., *Thymus uncoupling protein 1 is exclusive to typical brown adipocytes and is not found in thymocytes*. J Histochem Cytochem, 2007. **55**(2): p. 183-9.
246. Rousset, S., et al., *Uncoupling protein 2, but not uncoupling protein 1, is expressed in the female mouse reproductive tract*. J Biol Chem, 2003. **278**(46): p. 45843-7.
247. Garcia-Cazarin, M.L., J.L. Gamboa, and F.H. Andrade, *Rat diaphragm mitochondria have lower intrinsic respiratory rates than mitochondria in limb muscles*. Am J Physiol Regul Integr Comp Physiol, 2011. **300**(6): p. R1311-5.
248. Nibbelink, M., et al., *Brown fat UCP1 is specifically expressed in uterine longitudinal smooth muscle cells*. J Biol Chem, 2001. **276**(50): p. 47291-5.
249. Boettcher, M., et al., *Intermuscular adipose tissue (IMAT): association with other adipose tissue compartments and insulin sensitivity*. J Magn Reson Imaging, 2009. **29**(6): p. 1340-5.
250. De Coppi, P., et al., *Rosiglitazone modifies the adipogenic potential of human muscle satellite cells*. Diabetologia, 2006. **49**(8): p. 1962-73.
251. Stuelsatz, P., A. Shearer, and Z. Yablonka-Reuveni, *Ancestral Myf5 gene activity in periocular connective tissue identifies a subset of fibro/adipogenic progenitors but does not connote a myogenic origin*. Dev Biol, 2014. **385**(2): p. 366-79.
252. Laurens, C., et al., *Adipogenic progenitors from obese human skeletal muscle give rise to functional white adipocytes that contribute to insulin resistance*. Int J Obes (Lond), 2016. **40**(3): p. 497-506.
253. Lau, A.M., Y.H. Tseng, and T.J. Schulz, *Adipogenic fate commitment of muscle-derived progenitor cells: isolation, culture, and differentiation*. Methods Mol Biol, 2014. **1213**: p. 229-43.

254. Wrutniak-Cabello, C., F. Casas, and G. Cabello, *Thyroid hormone action in mitochondria*. J Mol Endocrinol, 2001. **26**(1): p. 67-77.
255. Collins, S., et al., *Strain-specific response to beta 3-adrenergic receptor agonist treatment of diet-induced obesity in mice*. Endocrinology, 1997. **138**(1): p. 405-13.
256. Garcia-Ruiz, E., et al., *The intake of high-fat diets induces the acquisition of brown adipocyte gene expression features in white adipose tissue*. Int J Obes (Lond), 2015. **39**(11): p. 1619-29.
257. Fromme, T. and M. Klingenspor, *Uncoupling protein 1 expression and high-fat diets*. Am J Physiol Regul Integr Comp Physiol, 2011. **300**(1): p. R1-8.
258. Russell, A.P., et al., *Brown adipocyte progenitor population is modified in obese and diabetic skeletal muscle*. Int J Obes (Lond), 2012. **36**(1): p. 155-8.
259. De Matteis, R., et al., *Exercise as a new physiological stimulus for brown adipose tissue activity*. Nutr Metab Cardiovasc Dis, 2013. **23**(6): p. 582-90.
260. Scarpace, P.J., S. Yenice, and N. Tumer, *Influence of exercise training and age on uncoupling protein mRNA expression in brown adipose tissue*. Pharmacol Biochem Behav, 1994. **49**(4): p. 1057-9.
261. Ringholm, S., et al., *PGC-1alpha is required for exercise- and exercise training-induced UCP1 up-regulation in mouse white adipose tissue*. PLoS One, 2013. **8**(5): p. e64123.
262. Zeve, D., et al., *Exercise-Induced Skeletal Muscle Adaptations Alter the Activity of Adipose Progenitor Cells*. PLoS One, 2016. **11**(3): p. e0152129.
263. Xu, X., et al., *Exercise ameliorates high-fat diet-induced metabolic and vascular dysfunction, and increases adipocyte progenitor cell population in brown adipose tissue*. Am J Physiol Regul Integr Comp Physiol, 2011. **300**(5): p. R1115-25.
264. Gao, M., Y. Ma, and D. Liu, *High-fat diet-induced adiposity, adipose inflammation, hepatic steatosis and hyperinsulinemia in outbred CD-1 mice*. PLoS One, 2015. **10**(3): p. e0119784.
265. Vieira, V.J., et al., *Effects of exercise and low-fat diet on adipose tissue inflammation and metabolic complications in obese mice*. Am J Physiol Endocrinol Metab, 2009. **296**(5): p. E1164-71.
266. Gollisch, K.S., et al., *Effects of exercise training on subcutaneous and visceral adipose tissue in normal- and high-fat diet-fed rats*. Am J Physiol Endocrinol Metab, 2009. **297**(2): p. E495-504.
267. Jain, S.S., et al., *High-fat diet-induced mitochondrial biogenesis is regulated by mitochondrial-derived reactive oxygen species activation of CaMKII*. Diabetes, 2014. **63**(6): p. 1907-13.
268. Hancock, C.R., et al., *High-fat diets cause insulin resistance despite an increase in muscle mitochondria*. Proc Natl Acad Sci U S A, 2008. **105**(22): p. 7815-20.
269. Turner, N., et al., *Excess lipid availability increases mitochondrial fatty acid oxidative capacity in muscle: evidence against a role for reduced fatty acid oxidation in lipid-induced insulin resistance in rodents*. Diabetes, 2007. **56**(8): p. 2085-92.
270. Cummins, T.D., et al., *Metabolic remodeling of white adipose tissue in obesity*. Am J Physiol Endocrinol Metab, 2014. **307**(3): p. E262-77.
271. Isakson, P., et al., *Impaired preadipocyte differentiation in human abdominal obesity: role of Wnt, tumor necrosis factor-alpha, and inflammation*. Diabetes, 2009. **58**(7): p. 1550-7.
272. van Harmelen, V., et al., *Effect of BMI and age on adipose tissue cellularity and differentiation capacity in women*. Int J Obes Relat Metab Disord, 2003. **27**(8): p. 889-95.
273. Lira, F.S., et al., *Endurance training induces depot-specific changes in IL-10/TNF-alpha ratio in rat adipose tissue*. Cytokine, 2009. **45**(2): p. 80-5.
274. Kliewer, S.A., et al., *Fatty acids and eicosanoids regulate gene expression through direct interactions with peroxisome proliferator-activated receptors alpha and gamma*. Proc Natl Acad Sci U S A, 1997. **94**(9): p. 4318-23.

References

275. Lee, J.E. and K. Ge, *Transcriptional and epigenetic regulation of PPARgamma expression during adipogenesis*. Cell Biosci, 2014. **4**: p. 29.
276. Clarke, S.L., C.E. Robinson, and J.M. Gimble, *CAAT/enhancer binding proteins directly modulate transcription from the peroxisome proliferator-activated receptor gamma 2 promoter*. Biochem Biophys Res Commun, 1997. **240**(1): p. 99-103.
277. Schachtrup, C., et al., *Functional analysis of peroxisome-proliferator-responsive element motifs in genes of fatty acid-binding proteins*. Biochem J, 2004. **382**(Pt 1): p. 239-45.
278. Bukowiecki, L., et al., *Mechanism of enhanced lipolysis in adipose tissue of exercise-trained rats*. Am J Physiol, 1980. **239**(6): p. E422-9.
279. Camporez, J.P., et al., *Cellular mechanism by which estradiol protects female ovariectomized mice from high-fat diet-induced hepatic and muscle insulin resistance*. Endocrinology, 2013. **154**(3): p. 1021-8.
280. Signer, R.A. and S.J. Morrison, *Mechanisms that regulate stem cell aging and life span*. Cell Stem Cell, 2013. **12**(2): p. 152-65.
281. Stearns-Reider, K.M., et al., *Aging of the skeletal muscle extracellular matrix drives a stem cell fibrogenic conversion*. Aging Cell, 2017.
282. Brack, A.S., H. Bildsoe, and S.M. Hughes, *Evidence that satellite cell decrement contributes to preferential decline in nuclear number from large fibres during murine age-related muscle atrophy*. J Cell Sci, 2005. **118**(Pt 20): p. 4813-21.
283. Kuswanto, W., et al., *Poor Repair of Skeletal Muscle in Aging Mice Reflects a Defect in Local, Interleukin-33-Dependent Accumulation of Regulatory T Cells*. Immunity, 2016. **44**(2): p. 355-67.
284. Shefer, G., et al., *Reduced satellite cell numbers and myogenic capacity in aging can be alleviated by endurance exercise*. PLoS One, 2010. **5**(10): p. e13307.
285. Liu, L., et al., *Chromatin modifications as determinants of muscle stem cell quiescence and chronological aging*. Cell Rep, 2013. **4**(1): p. 189-204.
286. Houtkooper, R.H., et al., *The metabolic footprint of aging in mice*. Sci Rep, 2011. **1**: p. 134.
287. Pallier, E., R. Aubert, and D. Lemonnier, *Effect of diet and ovariectomy on adipose tissue cellularity in mice*. Reprod Nutr Dev, 1980. **20**(3A): p. 631-6.
288. Day, K., et al., *The depletion of skeletal muscle satellite cells with age is concomitant with reduced capacity of single progenitors to produce reserve progeny*. Dev Biol, 2010. **340**(2): p. 330-43.
289. Tawfik, S.H., et al., *Similar and additive effects of ovariectomy and diabetes on insulin resistance and lipid metabolism*. Biochem Res Int, 2015. **2015**: p. 567945.
290. Frechette, D.M., et al., *Diminished satellite cells and elevated adipogenic gene expression in muscle as caused by ovariectomy are averted by low-magnitude mechanical signals*. J Appl Physiol (1985), 2015. **119**(1): p. 27-36.
291. Wang, L., et al., *Osteogenic differentiation potential of adipose-derived stem cells from ovariectomized mice*. Cell Prolif, 2017. **50**(2).
292. Fu, Y., et al., *Adipogenic differentiation potential of adipose-derived mesenchymal stem cells from ovariectomized mice*. Cell Prolif, 2014. **47**(6): p. 604-14.
293. Karagiannides, I., et al., *Altered expression of C/EBP family members results in decreased adipogenesis with aging*. Am J Physiol Regul Integr Comp Physiol, 2001. **280**(6): p. R1772-80.
294. Kirkland, J.L., C.H. Hollenberg, and W.S. Gillon, *Age, anatomic site, and the replication and differentiation of adipocyte precursors*. Am J Physiol, 1990. **258**(2 Pt 1): p. C206-10.
295. Caso, G., et al., *Peripheral fat loss and decline in adipogenesis in older humans*. Metabolism, 2013. **62**(3): p. 337-40.
296. Jackson, K.C., et al., *Ectopic lipid deposition and the metabolic profile of skeletal muscle in ovariectomized mice*. Am J Physiol Regul Integr Comp Physiol, 2013. **304**(3): p. R206-17.

297. Velders, M., et al., *Selective estrogen receptor-beta activation stimulates skeletal muscle growth and regeneration*. FASEB J, 2012. **26**(5): p. 1909-20.
298. Sitnick, M., et al., *Ovariectomy prevents the recovery of atrophied gastrocnemius skeletal muscle mass*. J Appl Physiol (1985), 2006. **100**(1): p. 286-93.
299. McClung, J.M., et al., *Estrogen status and skeletal muscle recovery from disuse atrophy*. J Appl Physiol (1985), 2006. **100**(6): p. 2012-23.
300. Pedersen, S.B., et al., *Regulation of UCP1, UCP2, and UCP3 mRNA expression in brown adipose tissue, white adipose tissue, and skeletal muscle in rats by estrogen*. Biochem Biophys Res Commun, 2001. **288**(1): p. 191-7.
301. Kim, S.N., et al., *Sex differences in sympathetic innervation and browning of white adipose tissue of mice*. Biol Sex Differ, 2016. **7**: p. 67.
302. Rogers, N.H., et al., *Aging leads to a programmed loss of brown adipocytes in murine subcutaneous white adipose tissue*. Aging Cell, 2012. **11**(6): p. 1074-83.
303. Kumar, M.V., R.L. Moore, and P.J. Scarpace, *Beta3-adrenergic regulation of leptin, food intake, and adiposity is impaired with age*. Pflugers Arch, 1999. **438**(5): p. 681-8.
304. Gao, B., et al., *Dose-dependent effect of estrogen suppresses the osteo-adipogenic transdifferentiation of osteoblasts via canonical Wnt signaling pathway*. PLoS One, 2014. **9**(6): p. e99137.
305. Conboy, I.M., et al., *Rejuvenation of aged progenitor cells by exposure to a young systemic environment*. Nature, 2005. **433**(7027): p. 760-4.
306. Brack, A.S., et al., *Increased Wnt signaling during aging alters muscle stem cell fate and increases fibrosis*. Science, 2007. **317**(5839): p. 807-10.
307. Cosgrove, B.D., et al., *Rejuvenation of the muscle stem cell population restores strength to injured aged muscles*. Nat Med, 2014. **20**(3): p. 255-64.
308. Sousa-Victor, P., et al., *Geriatric muscle stem cells switch reversible quiescence into senescence*. Nature, 2014. **506**(7488): p. 316-21.
309. Rodriguez-Cuenca, S., et al., *Expression of mitochondrial biogenesis-signaling factors in brown adipocytes is influenced specifically by 17beta-estradiol, testosterone, and progesterone*. Am J Physiol Endocrinol Metab, 2007. **292**(1): p. E340-6.
310. Hashimoto, O., et al., *Castration induced browning in subcutaneous white adipose tissue in male mice*. Biochem Biophys Res Commun, 2016. **478**(4): p. 1746-50.
311. do Valle Gomes-Gatto, C., et al., *Estrogen deficiency in ovariectomized rats: can resistance training re-establish angiogenesis in visceral adipose tissue?* Clinics (Sao Paulo), 2016. **71**(9): p. 528-36.
312. Vieira-Potter, V.J., et al., *Female rats selectively bred for high intrinsic aerobic fitness are protected from ovariectomy-associated metabolic dysfunction*. Am J Physiol Regul Integr Comp Physiol, 2015. **308**(6): p. R530-42.

References

Curriculum vitae

TATIANE GORSKI

Wehntalerstrasse 416

8046 Zürich

Switzerland

tatiane.gorski@usz.ch

Born on 15.09.1987 in São Leopoldo (Brazil)

Education

- | | |
|----------------|--|
| 2013 - Current | Doctoral studies in Health Sciences and Technology
Doctoral program: Molecular and Translational Biomedicine
Swiss Federal Institute of Technology Zurich, Switzerland |
| 2010 - 2012 | Master of Science in Sport Science (Minor: Molecular Life Sciences)
University of Bern, Switzerland |
| 2005 - 2010 | Bachelor of Science in Sport Science (with distinction)
Federal University of Rio Grande do Sul, Brazil |

Professional Experience

- | | |
|----------------|---|
| 2013 – current | Doctoral student, Krützfeldt lab
Division of Endocrinology, Diabetology and Clinical Nutrition
University Hospital Zurich, Zurich (Switzerland) |
| 2012 | Prescription of exercise for overweight and obese patients
Nutramedi (Obesity Clinic), Porto Alegre (Brazil) |
| 2011 – 2012 | Research Intern
Swiss Health and Performance Lab, Bern (Switzerland) |

Curriculum vitae

- 2009 Internship (physical activity for cancer patients)
Department for Pediatric Oncology
Hospital de Clínicas de Porto Alegre, Porto Alegre (Brazil)
- 2008 Internship (exercise for cardiac prevention and rehabilitation)
Exercise Medicine Center
Hospital Mãe de Deus, Porto Alegre (Brazil)
- 2007 Tutor for Exercise Physiology
Federal University of Rio Grande do Sul, Porto Alegre (Brazil)

Scholarships and Awards

Best presentation at the Annual Meeting of the Swiss Society of Endocrinology and Diabetes (category: student), Bern (Switzerland), 2015

Young Investigator Award – 2nd Prize at the 4th Annual Conference of the Swiss Society of Sport Science (category: natural sciences), Magglingen (Switzerland), 2012

Master Grant of the University of Bern – Bern (Switzerland), 2010 – 2012

Erasmus Mundus Scholarship – Project Euro Brazilian Windows, Porto (Portugal), 2009 – 2010.

Young Researcher Scholarship of the Federal University of Rio Grande do Sul, Porto Alegre (Brazil), 2007 – 2008

Distinction at the 19th Young Researchers' Congress of the Federal University of Rio Grande do Sul, Porto Alegre (Brazil), 2007

Publications

Scientific peer reviewed journals

Gorski T, Rosser T, Hoppeler H, Vogt M. Relative Age Effect in Young Swiss Alpine Skiers From 2004 to 2011. *Int J Sports Physiol Perform* 2016;11(4):455-63.

Alberton CL, Pinto SS, **Gorski T**, Antunes AH, Finatto P, Cadore EL, Bergamin M, Krueger LF. Rating of perceived exertion in maximal incremental tests during head-out water-based aerobic exercises. *J Sports Sci* 2016;34(18):1691-8

Gorski T, Rosser T, Hoppeler H, Vogt M. An anthropometric and physical profile of young Swiss alpine skiers between 2004 and 2011. *Int J Sports Physiol Perform* 2014;9(1):108-116

Figueiredo P, Ross S, **Gorski T**, Vilas Boas JP, Fernandes R. Kinematic and electromyographic changes during 200 m front crawl at race pace. *Int J Sports Med* 2013;34(1):49-55

Gorski T, Cadore EL, Pinto SS, Da Silva EM, Correa CS, Beltrami FG, Kruel LFM. Use of nonsteroidal anti-inflammatory drugs (NSAIDs) in triathletes: prevalence, level of awareness, and reasons for use. *Br J Sports Med* 2011;45(2):85-90

Presentations, Posters and Abstracts

Gorski T et al.. Fibro/adipogenic progenitors from skeletal muscle differentiate into thyroid-hormone responsive brown-like adipocytes. Endocrine Society's 98th Annual Meeting and Expo, Boston, 2016

Gorski T et al.. Fibro/adipogenic progenitors from skeletal muscle differentiate into brown-like adipocytes. Annual Meeting of the Swiss Society of Endocrinology and Diabetes, Bern, 2015

Gorski T et al.. Normalization of physical tests' results can attenuate the relative age effect in young Swiss alpine skiers. 17th Annual Congress of the European College of Sports Science. Bruges, 2012

Gorski T et al.. Does the relative age play a role in performance and selection of Swiss skiers? 4th Annual Conference of the Swiss Society of Sport Science. Magglingen, 2012

Gorski T et al.. Influence of exercise order on the acute hormonal responses to concurrent training. 16th Annual Congress of the European College of Sports Science. Liverpool, 2011

Reviewer for Scientific Journals

2010 – current European Journal of Applied Physiology

2015 – current BMJ Open